AMERICAN UNIVERSITY OF BEIRUT


THE STUDY OF A NOVEL PS-BASED

DEGRADATION SYSTEM: MIL-88-A AS A

HETEROGENEOUS ACTIVATOR, APPLICATION ON

NAPROXEN AND COMPARISON WITH $H_2O_2$ USING A

NEWLY DEVELOPED ANALYTICAL TECHNIQUE


by
RIME NAZIH EL ASMAR


A thesis
submitted in partial fulfillment of the requirements
for the degree of Master of Science
to the Department of Chemistry
of the Faculty of Arts and Sciences
at the American University of Beirut


Beirut, Lebanon
July 2019

AMERICAN UNIVERSITY OF BEIRUT


THE STUDY OF A NOVEL PS-BASED DEGRADATION SYSTEM:
MIL-88-A AS A HETEROGENEOUS ACTIVATOR, APPLICATION
ON NAPROXEN AND COMPARISON WITH H2O2 USING A
NEWLY DEVELOPED ANALYTICAL TECHNIQUE

By
RIME NAZIH EL ASMAR


Approved by:

_____          Advisor
Dr. Antoine Ghauch, Associate Professor
Department of Chemistry

_____          Member of Committee
Dr. Tarek Ghaddar, Professor
Department of Chemistry

_____          Member of Committee
Dr. Digambara Patra, Associate Professor
Department of Chemistry


Date of thesis defense: July 25, 2019

# AMERICAN UNIVERSITY OF BEIRUT

## THESIS, DISSERTATION, PROJECT RELEASE FORM

Student Name:

| El Asmar | Rime | Nazih |
|---|---|---|
| Last | First | Middle |

☑ Master's Thesis          ◯ Master's Project          ◯ Doctoral
Dissertation

☐    I authorize the American University of Beirut to: (a) reproduce hard or electronic copies of my thesis, dissertation, or project; (b) include such copies in the archives and digital repositories of the University; and (c) make freely available such copies to third parties for research or educational purposes.

☑    I authorize the American University of Beirut, to: (a) reproduce hard or electronic copies of it; (b) include such copies in the archives and digital repositories of the University; and (c) make freely available such copies to third parties for research or educational purposes
After:
       **One ---- year from the date of submission of my thesis, dissertation, or project.**
       **Two ✓ years from the date of submission of my thesis, dissertation, or project.**
       **Three ---- years from the date of submission of my thesis, dissertation, or project.**

_____          July 30, 2019

Signature                                    Date

# ACKNOWLEDGMENTS

# AN ABSTRACT OF THE THESIS OF

Rime Nazih El Asmar     for          Master of Science
                                     Major: Chemistry

Title: The study of a novel PS-based degradation system: MIL-88-A as a heterogeneous activator, application on Naproxen and comparison with $H_2O_2$ using a newly developed analytical technique

The thesis work is divided into two parts:

In the first section, MIL-88-A, an iron based MOF ($Fe^{3+}$/Fumaric acid), was synthesized in aqueous medium without the use of an organic solvent, then characterized and tested as a heterogeneous persulfate activator for the elimination of naproxen. A solution containing naproxen simulating the waste water effluent of a production facility was placed in continuously stirred reactors and spiked with MIL-88-A/sodium persulfate mix. The system was optimized in terms of MIL-88-A and persulfate dosages where 65-70% degradation of $[Naproxen]_0 = 50$  mg $L^{-1}$ occurred in a period of two hours in conditions of $[MIL\text{-}88\text{-}A]_0 = 25$ mg $L^{-1}$ and $[PS]_0 = 5$ mM spiked at t = 60 min. MIL-88-A was proved to be recyclable for at least 4 cycles and the introduction of UV-A irradiation to the system enhanced degradation to reach complete removal of naproxen within two hours reaction time . The effect of various factors on the system was studied. Chlorides and phosphates had no effect on the activation/degradation process. On the other hand, bicarbonates exhibited a strong inhibition effect and degradation process was optimal at acidic conditions (pH = 4). The system was also tested against another oxidant, $H_2O_2$, and the results showed that PS has higher efficiency in naproxen degradation.

In the second section, for the sake of comparing MIL-88-A/PS and MIL-88-A/$H_2O_2$ systems, $[H_2O_2]$ quantification method was developed by simple modifications to an HPLC-DAD setup. The modifications included the use of acidified potassium iodide solution as a mobile phase and a series of capillary columns instead of the reverse phase column usually used. The method's LDR ranged from 0.01-150 nm with LOD and LOQ $8.29 \times 10^{-4}$ mM and $2.76 \times 10^{-3}$ mM respectively. The method was proven to be cost effective where the cost per analysis ranged between 0.8 and 1.8 USD cents depending on the concentration of the sample tested. Validation of the proposed method was based on statistical comparison applied to a commonly used titrimetric method. Finally the method was tested in different water matrices (spring, seawater, media containing high concentrations of: chlorides, bicarbonates, humic acids and micro pollutants) which showed high regression coefficients and sensitivity in all calibration curves using different matrices.

Keyword: AOPs, Naproxen, MIL-88-A, persulfate, hydrogen peroxide, HPLC

# CONTENTS

# CHAPTER I

# INTRODUCTION

## A. PPCPs as emerging contaminants

Pharmaceuticals and personal care products (PPCPs) are a group of contaminants that include but are not limited to antibiotics, hormones, antimicrobial agents, cosmetics, fragrances, etc. The continuous discharge of PPCPs into waste water lead to their presence in trace amounts in both surface and ground water. This issue became the research focus of many laboratories due to the threats such contaminants carry to the environment and the potential dangers to public health [1–3].

PPCPs enter the environment through several ways and usually end up as trace contaminants. Their presence is mainly attributed to the direct disposal of expired pharmaceuticals to landfills and/or indirectly to waste water treatment plants (WWTPs) [4,5], in addition to the effluents from the pharmaceutical industries and hospitals [6]. Pharmaceutical industries form a point source pollution of which high concentration of PPCPs enter the environment.

In most cases, these PPCPs are of two components: excipients and active pharmaceutical ingredients (AIPs). The  presence of APIs in waste water plants had been reported, in different counties over the world, in the levels of ng $L^{-1}$ to µg $L^{-1}$ [1], such as USA [7], UK [8], Spain [9], Finland [10], and Japan [11]. One main category of these pharmaceuticals is the nonsteroidal anti-inflammatory drugs (NSAIDs) such as acetylsalicylic acid, diclofenac, ibuprofen, ketoprofen, and naproxen [2]. Their low cost, over the counter availability, in addition to their relatively minor side-effects made
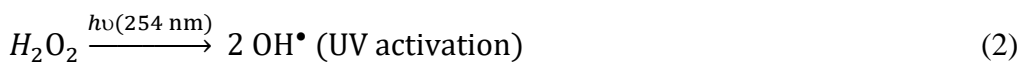
them among the most widely used pharmaceuticals. Consequently, considerable amount of these APIs and their metabolites reach groundwater, and even surface and drinking water [3,12].
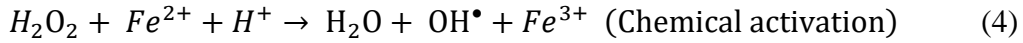
## B. Advanced oxidation processes

AOPs are based on activating oxidants to produce, directly or indirectly, hydroxyl radicals that are able to oxidize organic contaminants in the medium [13]. Common AOPs include ozonation, UV-based processes (UV/$H_2O_2$, UV/$H_2O_2$/$O_3$, etc.) and Fenton reaction ($Fe^{2+}$/$H_2O_2$) are currently applied in industrial WWTPs [14–16].

## C. Hydrogen peroxide ($H_2O_2$) based AOPs

$H_2O_2$ is one of the most commonly used oxidants in AOPs. It has a relatively high oxidation/reduction potential of 1.8 V [17]. Several radicals are produced upon the activation of $H_2O_2$ of which hydroxyl radicals ($OH^\bullet$) are the most dominant ones [18]. $OH^\bullet$'s have a high oxidation/reduction potential of 2.7 in acidic media and 1.8 in neutral ones [19] which make them excellent oxidants in AOPs applied for the degradation of numerous organic contaminants [20,21]. $H_2O_2$ is activated by ozonation [22] (eq. 1), photo-irradiation [22] (eq. 2), ultra-sonication [22] (eq. 3), or by chemical activation [15] (eq. 4).

$$H_2O_2 + 2O_3 \rightarrow 2\,OH^\bullet + 3O_2 \ \text{(Ozonation)} \tag{1}$$

$$H_2O_2 \xrightarrow{h\upsilon(254\,\text{nm})} 2\,OH^\bullet \ \text{(UV activation)} \tag{2}$$

$$H_2O_2 \xrightarrow{ultrasonication} 2\,OH^\bullet \ \text{(ultrasonication activation)} \tag{3}$$

$$H_2O_2 + Fe^{2+} + H^+ \rightarrow H_2O + OH^\bullet + Fe^{3+} \quad \text{(Chemical activation)} \qquad (4)$$

## D. Persulfate based AOPs

PS ($S_2O_8^{2-}$) ($E_0 = 2.1$ V) is one of the oxidants used in AOPs which upon its

activation generates sulfate radicals ($SO_4^{-\bullet}$) ($E_0 = 2.6$ V) [23]. Sulfate radicals hold a

strong oxidation potential under a wider pH range than hydroxyl radicals [24], produce

less disinfection byproducts [25], and is also considered to be non-selective and thus

degrade a wider range of contaminants [23]. PS is activated by physical methods such

as UV-irradiation (eq.5), ultra-sonication (eq.6), heating (eq.7), or by chemical

activation techniques such as homogeneous metal catalysis (eq.8) and heterogeneous

photocatalysis [20].

$$S_2O_8^{2-} \xrightarrow{h\upsilon} 2\ SO_4^{-\bullet} \quad \text{(UV activation)} \qquad\qquad\qquad (5)$$

$$S_2O_8^{2-} \xrightarrow{ultrasonication} 2\ SO_4^{-\bullet} \quad \text{(ultrasonication activation)} \qquad (6)$$

$$S_2O_8^{2-} \rightarrow 2\ SO_4^{-\bullet} \quad \text{(Thermal activation) with } 30^o\ C\ < T < 99^o \qquad (7)$$

$$S_2O_8^{2-} + Fe^{2+} \rightarrow SO_4^{2-} + SO_4^{-\bullet} + Fe^{3+} \quad \text{(Chemical activation)} \qquad (8)$$
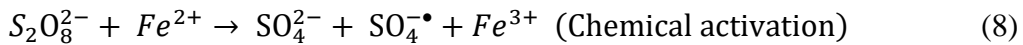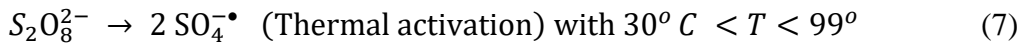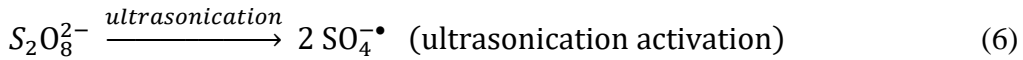
## E. Metal organic frameworks as iron-based catalyst for AOPs

Iron-based catalysts are vastly studied and applied due to the abundance and low

cost, non-toxic nature, and high efficiency of iron. Nonetheless, iron catalysts are rarely

reusable. For this reason, it is important to develop iron-based catalysts for the

activation of PS that are heterogeneous and can be reclaimed. The applicability of

entrapping iron using metal organic frameworks (MOFs) to be used as a heterogeneous

catalyst for the activation of PS is being explored recently for the use in water treatment.

MOFs are a novel class of porous materials, synthesized from a metal salt, providing metal ions, and organic ligands. MOFs exhibit special structural properties, such as high surface area, thermal stability, porosity, variability in pore structure, abundance of open metal sites and photosensitivity [26]. Such properties render it vastly studied for use in various applications [26,27]. Such applications include $CO_2$ capture [28,29] storage of hydrogen [30], adsorption of harmful gases, hydrocarbons, water vapor and alcohols [27,31,32]. MOFs are also researched and developed for use in drug delivery [33,34], magnetism [35], polymerization [36], catalysis [37], and many other applications.

MOFs are mainly stable in water when they are a combination of Ti, Zr, Fe, Al and/or Cr with carboxylate-based ligands [38]. Water-stable MOFs have been recently investigated for their adsorptive properties towards hazardous organic compounds in waste water [26,39–43]. Other than adsorption, MOFs, mostly Fe-based MOFs, were proven to have an effective photocatalytic activity for the removal of organic contaminants. Such activity can be direct through transforming energy from the MOF into the compound or indirect through a homogeneous mediator such as PS or $H_2O_2$ [44–48].

## F. Objectives

The aim of this research is to synthesize an iron-based MOF using an environmentally friendly method. For the best of our knowledge, MIL-88-A is the only

iron based MOF found in literature that can be easily synthesized using water. It was also used in several AOPs studies and showed promising results [49–51]. However, the existing studies were conducted using relatively high concentration of MOF [50,51] and were all performed only for the degradation of dyes [39,52] and in presence of photo-irradiation [50,51]. This research is conducted on the degradation of naproxen using a MIL-88-A/persulfate system with an evaluation the effect of different parameters on the performance of the system. The system was also tested using $H_2O_2$ for which a new analytical technique for the quantification of $[H_2O_2]$ was developed to serve the purpose of comparing MIL-88-A/PS versus MIL-88-A/$H_2O_2$ activated systems.

# BIBLIOGRAPHY

[1]    J.-L. Liu, M.-H. Wong, Pharmaceuticals and personal care products (PPCPs): a

       review on environmental contamination in China, Environ. Int. 59 (2013) 208–224.

[2]    J.L. Tambosi, L.Y. Yamanaka, H.J. JosÃ\copyright, R. de F.P.M. Moreira, H.F.

       SchrÃ\Pder, Recent research data on the removal of pharmaceuticals from sewage

       treatment plants (STP), QuÃ\-Mica Nov. 33 (2010) 411–420.

[3]    T. Heberer, Occurrence, fate, and removal of pharmaceutical residues in the aquatic

       environment: A review of recent research data, Toxicol. Lett. (2002).

       doi:10.1016/S0378-4274(02)00041-3.

[4]    K.E. Arnold, A.R. Brown, G.T. Ankley, J.P. Sumpter, Medicating the environment:

       assessing risks of pharmaceuticals to wildlife and ecosystems, Philos. Trans. R. Soc.

       B Biol. Sci. 369 (2014).

[5]    C.G. Daughton, T.A. Ternes, Pharmaceuticals and personal care products in the

       environment: Agents of subtle change?, Environ. Health Perspect. (1999).

       doi:10.1007/s11113-013-9316-3.

[6]    J. Rivera-Utrilla, M. Sánchez-Polo, M.Á. Ferro-García, G. Prados-Joya, R. Ocampo-

       Pérez, Pharmaceuticals as emerging contaminants and their removal from water. A

       review, Chemosphere. 93 (2013) 1268–1287.

       doi:http://dx.doi.org/10.1016/j.chemosphere.2013.07.059.

[7]    G.R. Boyd, J.M. Palmeri, S. Zhang, D.A. Grimm, Pharmaceuticals and personal care

       products (PPCPs) and endocrine disrupting chemicals (EDCs) in stormwater canals

       and Bayou St. John in New Orleans, Louisiana, USA, Sci. Total Environ. (2004).

doi:10.1016/j.scitotenv.2004.03.018.

[8]     D. Ashton, M. Hilton, K. V. Thomas, Investigating the environmental transport of human pharmaceuticals to streams in the United Kingdom, Sci. Total Environ. (2004). doi:10.1016/j.scitotenv.2004.04.062.

[9]     M. Carballa, F. Omil, J.M. Lema, M. Llompart, C. García-Jares, I. Rodríguez, M. Gómez, T. Ternes, Behavior of pharmaceuticals, cosmetics and hormones in a sewage treatment plant, Water Res. (2004). doi:10.1016/j.watres.2004.03.029.

[10]    N. Lindqvist, T. Tuhkanen, L. Kronberg, Occurrence of acidic pharmaceuticals in raw and treated sewages and in receiving waters, Water Res. (2005). doi:10.1016/j.watres.2005.04.003.

[11]    N. Nakada, T. Tanishima, H. Shinohara, K. Kiri, H. Takada, Pharmaceutical chemicals and endocrine disrupters in municipal wastewater in Tokyo and their removal during activated sludge treatment, Water Res. (2006). doi:10.1016/j.watres.2006.06.039.

[12]    T.A. Ternes, M. Meisenheimer, D. McDowell, F. Sacher, H.J. Brauch, B. Haist-Gulde, G. Preuss, U. Wilme, N. Zulei-Seibert, Removal of pharmaceuticals during drinking water treatment, Environ. Sci. Technol. (2002). doi:10.1021/es015757k.

[13]    P.R. Gogate, A.B. Pandit, A review of imperative technologies for wastewater treatment I: oxidation technologies at ambient conditions, Adv. Environ. Res. 8 (2004) 501–551. doi:http://dx.doi.org/10.1016/S1093-0191(03)00032-7.

[14]    C. Wei, F. Zhang, Y. Hu, C. Feng, H. Wu, Ozonation in water treatment: The generation, basic properties of ozone and its practical application, Rev. Chem. Eng. (2017). doi:10.1515/revce-2016-0008.

[15]    S.O. Ganiyu, M. Zhou, C.A. Martínez-Huitle, Heterogeneous electro-Fenton and photoelectro-Fenton processes: A critical review of fundamental principles and application for water/wastewater treatment, Appl. Catal. B Environ. (2018). doi:10.1016/j.apcatb.2018.04.044.

[16]    B.A. Wols, C.H.M. Hofman-Caris, Review of photochemical reaction constants of organic micropollutants required for UV advanced oxidation processes in water, Water Res. (2012). doi:10.1016/j.watres.2012.03.036.

[17]    S.G. Huling, B.E. Pivetz, In-Situ Chemical Oxidation, EPA Eng. Issue. (2006) 1–60. doi:EPA/600/R-06/072.

[18]    L. Chen, X. Li, J. Zhang, J. Fang, Y. Huang, P. Wang, J. Ma, Production of Hydroxyl Radical via the Activation of Hydrogen Peroxide by Hydroxylamine, Environ. Sci. Technol. 49 (2015) 10373–10379. doi:10.1021/acs.est.5b00483.

[19]    G. V. Buxton, C.L. Greenstock, W.P. Helman, A.B. Ross, Critical Review of rate constants for reactions of hydrated electrons, hydrogen atoms and hydroxyl radicals (???OH/???O??? in Aqueous Solution, J. Phys. Chem. Ref. Data. 17 (1988) 513–886. doi:10.1063/1.555805.

[20]    M. Passananti, F. Temussi, M.R. Iesce, L. Previtera, G. Mailhot, D. Vione, M. Brigante, Photoenhanced transformation of nicotine in aquatic environments: Involvement of naturally occurring radical sources, Water Res. 55 (2014) 106–114. doi:10.1016/j.watres.2014.02.016.

[21]    J.L. Wang, L.J. Xu, Advanced oxidation processes for wastewater treatment: Formation of hydroxyl radical and application, Crit. Rev. Environ. Sci. Technol. 42 (2012) 251–325. doi:10.1080/10643389.2010.507698.

[22]    A.D. Bokare, W. Choi, Review of iron-free Fenton-like systems for activating H2O2 in advanced oxidation processes., J. Hazard. Mater. (2014). doi:10.1016/j.jhazmat.2014.04.054.

[23]    L.W. Matzek, K.E. Carter, Activated persulfate for organic chemical degradation: A review, Chemosphere. (2016). doi:10.1016/j.chemosphere.2016.02.055.

[24]    W. Da Oh, Z. Dong, T.T. Lim, Generation of sulfate radical through heterogeneous catalysis for organic contaminants removal: Current development, challenges and prospects, Appl. Catal. B Environ. (2016). doi:10.1016/j.apcatb.2016.04.003.

[25]    S. Luo, Z. Wei, D.D. Dionysiou, R. Spinney, W.P. Hu, L. Chai, Z. Yang, T. Ye, R. Xiao, Mechanistic insight into reactivity of sulfate radical with aromatic contaminants through single-electron transfer pathway, Chem. Eng. J. (2017). doi:10.1016/j.cej.2017.06.179.

[26]    N.A. Khan, Z. Hasan, S.H. Jhung, Adsorptive removal of hazardous materials using metal-organic frameworks (MOFs): A review, J. Hazard. Mater. (2013). doi:10.1016/j.jhazmat.2012.11.011.

[27]    D. Britt, D. Tranchemontagne, O.M. Yaghi, Metal-organic frameworks with high capacity and selectivity for harmful gases, Proc. Natl. Acad. Sci. (2008). doi:10.1073/pnas.0804900105.

[28]    J.R. Li, Y. Ma, M.C. McCarthy, J. Sculley, J. Yu, H.K. Jeong, P.B. Balbuena, H.C. Zhou, Carbon dioxide capture-related gas adsorption and separation in metal-organic frameworks, Coord. Chem. Rev. (2011). doi:10.1016/j.ccr.2011.02.012.

[29]    K. Sumida, D.L. Rogow, J.A. Mason, T.M. McDonald, E.D. Bloch, Z.R. Herm, T.H. Bae, J.R. Long, Carbon dioxide capture in metal-organic frameworks, Chem. Rev.

(2012). doi:10.1021/cr2003272.

[30] L.J. Murray, M. Dincă, J.R. Long, Hydrogen storage in metal–organic frameworks, Chem. Soc. Rev. (2009). doi:10.1109/JPHOTOV.2018.2868021.

[31] H. Wu, Q. Gong, D.H. Olson, J. Li, Commensurate adsorption of hydrocarbons and alcohols in microporous metal organic frameworks, Chem. Rev. (2012). doi:10.1021/cr200216x.

[32] H. Jasuja, J. Zang, D.S. Sholl, K.S. Walton, Rational tuning of water vapor and $CO_2$ adsorption in highly stable Zr-based MOFs, J. Phys. Chem. C. (2012). doi:10.1021/jp308657x.

[33] P. Horcajada, R. Gref, T. Baati, P.K. Allan, G. Maurin, P. Couvreur, G. Férey, R.E. Morris, C. Serre, Metal-organic frameworks in biomedicine, Chem. Rev. (2012). doi:10.1021/cr200256v.

[34] A.C. McKinlay, R.E. Morris, P. Horcajada, G. Férey, R. Gref, P. Couvreur, C. Serre, BioMOFs: Metal-organic frameworks for biological and medical applications, Angew. Chemie - Int. Ed. (2010). doi:10.1002/anie.201000048.

[35] M. Kurmoo, Magnetic metal-organic frameworks, Chem. Soc. Rev. (2009). doi:10.1039/b804757j.

[36] T. Uemura, N. Yanai, S. Kitagawa, Polymerization reactions in porous coordination polymers, Chem. Soc. Rev. (2009). doi:10.1039/b802583p.

[37] J. Lee, O.K. Farha, J. Roberts, K.A. Scheidt, S.T. Nguyen, J.T. Hupp, Metal-organic framework materials as catalysts, Chem. Soc. Rev. (2009). doi:10.1039/b807080f.

[38] S. Yuan, L. Feng, K. Wang, J. Pang, M. Bosch, C. Lollar, Y. Sun, J. Qin, X. Yang, P. Zhang, Q. Wang, L. Zou, Y. Zhang, L. Zhang, Y. Fang, J. Li, H.C. Zhou, Stable

Metal–Organic Frameworks: Design, Synthesis, and Applications, Adv. Mater. (2018). doi:10.1002/adma.201704303.

[39] E. Haque, J.E. Lee, I.T. Jang, Y.K. Hwang, J.S. Chang, J. Jegal, S.H. Jhung, Adsorptive removal of methyl orange from aqueous solution with metal-organic frameworks, porous chromium-benzenedicarboxylates, J. Hazard. Mater. (2010). doi:10.1016/j.jhazmat.2010.05.047.

[40] F. Leng, W. Wang, X.J. Zhao, X.L. Hu, Y.F. Li, Adsorption interaction between a metal-organic framework of chromium-benzenedicarboxylates and uranine in aqueous solution, Colloids Surfaces A Physicochem. Eng. Asp. (2014). doi:10.1016/j.colsurfa.2013.08.074.

[41] C. Chen, M. Zhang, Q. Guan, W. Li, Kinetic and thermodynamic studies on the adsorption of xylenol orange onto MIL-101(Cr), Chem. Eng. J. (2012). doi:10.1016/j.cej.2011.12.021.

[42] Z. Hasan, J. Jeon, S.H. Jhung, Adsorptive removal of naproxen and clofibric acid from water using metal-organic frameworks, J. Hazard. Mater. (2012). doi:10.1016/j.jhazmat.2012.01.005.

[43] E.Y. Park, Z. Hasan, N.A. Khan, S.H. Jhung, Adsorptive removal of bisphenol-A from water with a metal-organic framework, a porous chromium-benzenedicarboxylate., J. Nanosci. Nanotechnol. (2013).

[44] J.J. Du, Y.P. Yuan, J.X. Sun, F.M. Peng, X. Jiang, L.G. Qiu, A.J. Xie, Y.H. Shen, J.F. Zhu, New photocatalysts based on MIL-53 metal-organic frameworks for the decolorization of methylene blue dye, J. Hazard. Mater. (2011). doi:10.1016/j.jhazmat.2011.04.029.

[45]    H. Hu, H. Zhang, Y. Chen, Y. Chen, L. Zhuang, H. Ou, Enhanced photocatalysis degradation of organophosphorus flame retardant using MIL-101(Fe)/persulfate: Effect of irradiation wavelength and real water matrixes, Chem. Eng. J. 368 (2019) 273–284. doi:10.1016/j.cej.2019.02.190.

[46]    H. Lv, H. Zhao, T. Cao, L. Qian, Y. Wang, G. Zhao, Efficient degradation of high concentration azo-dye wastewater by heterogeneous Fenton process with iron-based metal-organic framework, J. Mol. Catal. A Chem. (2015). doi:10.1016/j.molcata.2015.02.007.

[47]    M.J. Duan, Z. yu Guan, Y.W. Ma, J.Q. Wan, Y. Wang, Y.F. Qu, A novel catalyst of MIL-101(Fe) doped with Co and Cu as persulfate activator: synthesis, characterization, and catalytic performance, Chem. Pap. (2018). doi:10.1007/s11696-017-0276-7.

[48]    J. Tang, J. Wang, Fe-based metal organic framework/graphene oxide composite as an efficient catalyst for Fenton-like degradation of methyl orange, RSC Adv. (2017). doi:10.1039/c7ra10145g.

[49]    K.Y.A. Lin, F.K. Hsu, Magnetic iron/carbon nanorods derived from a metal organic framework as an efficient heterogeneous catalyst for the chemical oxidation process in water, RSC Adv. (2015). doi:10.1039/c5ra06043e.

[50]    J. Wang, J. Wan, Y. Ma, Y. Wang, M. Pu, Z. Guan, Metal-organic frameworks MIL-88A with suitable synthesis conditions and optimal dosage for effective catalytic degradation of Orange G through persulfate activation, RSC Adv. (2016). doi:10.1039/C6RA24429G.

[51]    K.Y. Andrew Lin, H.A. Chang, C.J. Hsu, Iron-based metal organic framework, MIL-

88A, as a heterogeneous persulfate catalyst for decolorization of Rhodamine B in water, RSC Adv. (2015). doi:10.1039/c5ra01447f.

[52]   M. Sarker, S. Shin, J.H. Jeong, S.H. Jhung, Mesoporous metal-organic framework PCN-222(Fe): Promising adsorbent for removal of big anionic and cationic dyes from water, Chem. Eng. J. 371 (2019) 252–259. doi:10.1016/J.CEJ.2019.04.039.

# CHAPTER II

PROJECT 1

## A. MIL-88-A for the Degradation of Naproxen through Persulfate Activation

As mentioned in the introduction, traditional waste water treatment has been proven to be insufficient for the elimination of organic contaminants that are highly stable and resistant to biodegradation. Thus coming up with an advanced technology became crucial. MOF/PS based AOPs is one of the novel technologies in which the catalyst is heterogeneous and in many cases is reusable.

Among these contaminants is naproxen which its degradation was studied in a system of PS activated by an iron-based MOF, MIL-88-A. MIL-88-A was synthesized hydrothermally and characterized using available characterization techniques. The system was optimized and tested for its recyclability, matrix variations, and efficiency against other oxidant ($H_2O_2$). Effect of UV-A irradiation on the system was also studied.

The results of this project are presented in the form of a paper to be submitted to Industrial and Environmental Chemistry Research.

# A. Iron-Based Metal Organic Framework MIL-88-A for the Degradation of Naproxen in Water through Persulfate Activation

American University of Beirut, Faculty of Arts and Sciences, Department of Chemistry

P.O. Box 11-0236 Riad El Solh – 1107-2020 Beirut – Lebanon

Rime El Asmar, Abbas Baalbaki, Zahraa Abou Khalil, Antoine Ghauch*

Metal Organic Frameworks (MOFs) are a relatively new class of porous 3d material that is being researched for its possible applications in environmental remediation and waste water treatment. It has also been investigated for the use in catalysis and AOP. The challenges of applying MOF-based catalysis lies in its stability, reusability, and environmentally friendly synthesis process. MIL-88-A, an iron based MOF ($Fe^{3+}$/Fumaric acid), can be synthesized in aqueous medium which is an advantage over other MOFs that require hazardous organic solvents. In this paper, MIL-88-A was synthesized, characterized, and used as a catalyst for the degradation of naproxen using AOPs. A solution containing naproxen simulating the waste water effluent of a pharmaceutical production facility was placed in continuously stirred reactors and spiked with MIL-88-A/sodium persulfate. The system was optimized and tested for its recyclability and matrix variations (salinity, phosphates, pH, and bicarbonates). The system was tested against another oxidant, $H_2O_2$ and finally under UV-A irradiation to remove any residual naproxen. Results showed that MIL-88-A is an activator of persulfate where 65-70% degradation of $[Naproxen]_0 = 50$ mg $L^{-1}$ occurred in a period
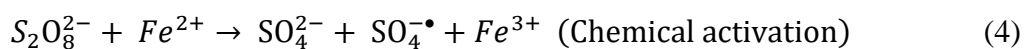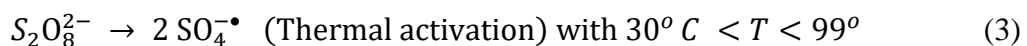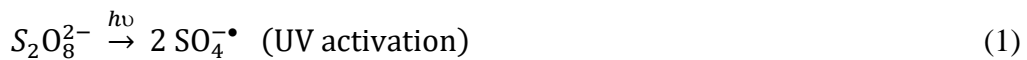
of two hours. MIL-88-A was proved to be recyclable for at least 4 cycles. Salinity and phosphate had no effect on the degradation; however, bicarbonates exhibited a strong inhibition. The activation/degradation process was optimal at acidic conditions (pH = 4). PS was shown to be superior oxidant over $H_2O_2$ when using MIL-88-A. And lastly, UV-A lead to complete degradation within two hours of reaction time implying that the proposed system is successful for the elimination of organic pollutants from water.

## 1. Introduction

Pharmaceuticals and personal care products (PPCPs) are a group of contaminants that include but are not limited to antibiotics, hormones, antimicrobial agents, cosmetics, fragrances, etc. The continuous discharge of PPCPs into waste water lead to their presence in trace amounts in both surface and ground water. This issue became the research focus of many laboratories due to the threats such contaminants carry to the environment and the potential dangers to public health [1–3]. PPCPs enter the environment through several ways and usually end up as trace contaminants. Their presence is mainly attributed to the direct disposal of expired pharmaceuticals to landfills and/or indirectly to waste water treatment plants (WWTPs) [4,5], in addition to the effluents from the pharmaceutical industries and hospitals [6]. Pharmaceutical industries form a point source pollution of which high concentration of PPCPs enter the environment, this paper address treatment at these sources and thus it deals with realistically high concentration. In most cases, these PPCPs are of two components: excipients and active pharmaceutical ingredients (AIPs). The presence of APIs in waste water plants had been reported, in different counties over the world, in the levels of ng $L^{-1}$ to µg $L^{-1}$ [1], such as USA [7], UK [8], Spain [9], Finland [10], and Japan [11]. One main category of these pharmaceuticals is the nonsteroidal anti-inflammatory drugs (NSAIDs) such as acetylsalicylic acid, diclofenac, ibuprofen, ketoprofen, and naproxen [2]. Their low cost, over the counter availability, in addition to their relatively minor side-effects made them among the most widely used pharmaceuticals. Consequently, considerable amount of these APIs and their metabolites reach groundwater, and

even surface and drinking water [3,12]. Traditional waste water treatment has been proven to be insufficient for the elimination of these compounds due to their high chemical stability and resistance to biodegradation [2]. Alternative methods such as advanced oxidation processes (AOPs) are the currently studied solutions for the effective elimination of pharmaceuticals in water. AOPs are based on activating oxidants to produce, directly or indirectly, hydroxyl radicals that are able to oxidize organic contaminants in the medium [13]. Common AOPs include ozonation, UV-based processes (UV/$H_2O_2$, UV/$H_2O_2$/$O_3$, etc.) and Fenton reaction ($Fe^{2+}$/$H_2O_2$) currently applied in industrial WWTPs [14–16]. AOPs that are in the research and development phase include electrochemical-based, ultrasonic-based, Persulfate (PS)-based, and photocatalytic-based processes. PS ($S_2O_8^{2-}$) ($E_0$ = 2.1 V) is one of the oxidants used in AOPs which upon its activation generates sulfate radicals ($SO_4^-$·) ($E_0$ = 2.6 V) [17]. Sulfate radicals hold a strong oxidation potential under a wider pH range than hydroxyl radicals [18], produce less disinfection byproducts [19], and is also considered to be non-selective and thus degrade a wider range of contaminants [17]. PS is activated by physical methods such as UV-irradiation (eq.1), ultra-sonication (eq.2), heating (eq.3), or by chemical activation techniques such as homogeneous metal catalysis (eq.4) and heterogeneous photocatalysis [20].

$$S_2O_8^{2-} \xrightarrow{h\upsilon} 2\ SO_4^{-\bullet} \ \text{(UV activation)} \tag{1}$$

$$S_2O_8^{2-} \xrightarrow{ultrasonication} 2\ SO_4^{-\bullet} \ \text{(ultrasonication activation)} \tag{2}$$

$$S_2O_8^{2-} \rightarrow 2\ SO_4^{-\bullet} \ \text{(Thermal activation) with } 30^o\ C\ < T < 99^o \tag{3}$$

$$S_2O_8^{2-} + Fe^{2+} \rightarrow SO_4^{2-} + SO_4^{-\bullet} + Fe^{3+} \ \text{(Chemical activation)} \tag{4}$$

Iron-based catalysts are vastly studied and applied due to the abundance and low cost, non-toxic nature, and high efficiency of iron. Nonetheless, iron catalysts are rarely reusable. For this reason, it is important to develop iron-based catalysts for the activation of PS that are heterogeneous and can be reclaimed. The applicability of entrapping iron using metal organic frameworks (MOFs) to be used as a heterogeneous catalyst for the activation of PS is explored in this paper. MOFs are a novel class of porous materials, synthesized from a metal salt, providing metal ions, and organic ligands. MOFs exhibit special structural properties, such as high surface area, thermal stability, porosity, variability in pore structure, abundance of open metal sites and photosensitivity [20]. Such properties render it vastly studied for use in various applications [20,21]. Such applications include $CO_2$ capture [22,23] storage of hydrogen [24], adsorption of harmful gases, hydrocarbons, water vapor and alcohols [21,25,26]. MOFs are also researched and developed for use in drug delivery [27,28], magnetism [29], polymerization [30], catalysis [31], and many other applications.

MOFs are mainly stable in water when they are a combination of Ti, Zr, Fe, Al and/or Cr with carboxylate-based ligands [32]. Water-stable MOFs have been recently investigated for their adsorptive properties towards hazardous organic compounds in waste water [20,33–37].

The studies on the removal of contaminants via adsorption using water stable MOFs are summarized in Table 1. Most of the MOFs in these studies are synthesized using organic solvents with moderate to high toxicity [38]. Using MOFs that can be synthesized using water as a solvent  are a more sustainable option and

recommended according to the first, third and fifth principles of the 12 principles of green chemistry which are summarized in Table 1S [39].

Moreover, MOFs, most of the time, should be subjected to functionalization and post synthetic treatment for an efficient adsorption to take place increasing the entire synthesis process time, cost, and labor demands. Adsorption in these studies are mostly attributed to hydrogen bonding or electronic interactions between the functional groups of the MOFs and the adsorbed compound, which renders the process to be selective and not efficient for a wide range of contaminants. Furthermore, the majority of the conducted studies lack recyclability and desorption analysis which doesn't provide a sustainable solution for the effective degradation and/or removal of contaminants. Such techniques are not considered effective especially that relatively high concentrations of MOFs are being used, where the adsorption capacity in these studies ranged between 16 and 1450 mg/g (Table 1).

Table 1: Adsorption of organic and inorganic compounds on different MOFs

| MOFs | Adsorbed Compound | Reference | Adsorption Capacity (mg/g) | Drawbacks |
|---|---|---|---|---|
| MIL-101-Cr | Methyl orange (MO) | [33] | 114 | Use of Hydrofluoric |
| | Uranine | [34] | 126 | acid (HF) in |
| | Xylon orange (XO) | [35] | 311 | synthesis which is |
| | | | | highly toxic and |
| | Clofibric acid | [36] | 315 | corrosive [43,44] |
| | Naproxen | | 119 | Chromium is toxic, |
| | | | | especially in its |
| MIL-101-Cr | Bisphenol A | [40] | 156 | hexavalent state |
| functionalized | MO | [33] | 194 | [45] |
| | Clofibric acid | [41] | 347 | Functionalization |
| | Hg (II) | [42] | 51.27 | and post synthetic |

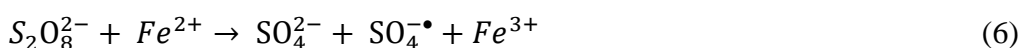| | | | | steps are highly demanding |
|---|---|---|---|---|
| MIL-235 | MO<br>Methylene blue (MB) | [46] | 477<br>187 | Use of HF in synthesis<br>Use of N,N-Dimethylformamide (DMF) in synthesis |
| MIL-100-Fe | MO<br>MB<br>Malachite green (MG)<br>Naproxen<br>Bisphenol A | [47]<br><br>[48]<br>[36]<br>[40] | 1045.2<br>645<br>141<br>104<br>26 | Adsorption didn't work for trace amounts<br>No studies for desorption or recyclability were conducted |
| MIL-100-Cr | MO<br>MB | [47] | 211.8<br>645.3 | Chromium is toxic, especially in its hexavalent state<br>Selective adsorption of MB from MO–MB solutions [47] |
| NH-MIL-101-Al<br><br>NH$_2$-MIL-101-Al | p-Nitrophenol<br><br><br>MB<br>MO | [49]<br><br><br>[50] | 192<br><br><br>762<br>188 | Functionalization and post synthetic steps are highly demanding<br>Use of DMF in synthesis |
| UiO-66<br><br><br>NH$_2$-UiO-66 | Phthalic acid<br>Sulfachloropyradazine (SCP)<br>Arsenic<br>Phthalic acid | [51]<br>[52]<br>[53]<br>[51] | 187<br>417<br>303<br>224 | Use of DMF and HCl in synthesis [53]<br>Optimal pH is highly acidic (pH=2) [53]<br>Functionalization and post synthetic steps are highly demanding |
| HKUST-1 | Benzothiophene (BT)<br>Dibenzothiophene (DBT)<br>Dimethyldibenzothiophene (DMDBT)<br>MO<br><br>Pb (II)<br>Cd (II) | <br>[54]<br><br><br>[55]<br><br>[56] | 25<br>45<br>16<br>4.7<br><br>98.17<br>32.45<br>38.25 | Removal from isooctane matrix not water [54]<br>Copper is toxic, being a catalyst of processes generating reactive oxygen intermediates and |

| | | | | |
|---|---|---|---|---|
| | Cr (III) | | | thus causes cell damage when present in high concentration [57,58] No adsorption of $Hg^{2+}$ and heavy metals under the same experimental conditions [56] |
| UMCM-150 | BT DBT DMDBT | [54] | 40 83 41 | Removal from isooctane matrix and not water [54] |
| MOF-505 | BT DBT DMDBT | [54] | 51 39 27 | |
| PCN-222-Fe | Brilliant green (BG) Crystal violet (CV) Acid red Acid blue | [59] | 854 812 371 417 | Limited to dyes |
| MIL-101-SH UiO-66-SH | Hg (II) | [60] | 250 110 | Functionalization and post synthetic steps are highly demanding |
| MOF-808 | Arsenic | [61] | 24.83 | Synthesis necessities microwave irradiation or using solvothermal method under high temperatures (150 °C) and long reaction times (3–7days) Solvents used in synthesis are DMF and formic acid Crystals exhibit high superacidity Specific to Arsenic |
| MIL-53-Fe | Arsenic | [62] | 21 | Synthesis require DMF Adsorption was suggested to be due to lewis acid-base |

| | | | | interaction between the anionic $H_2AsO_4^-$ species and the MOF node which makes it applicable only for a selective range of adsorbents |
|---|---|---|---|---|
| MIL-53-Al | Arsenic | [63] | 106 | Synthesis needs DMF Adsorption was attributed the hydrogen bonding occurring between the MOF and the adsorbent |
| MOF-5-Zn | Pb (II) | [64] | 658.5 | Synthesis using DMF solvent |

Other than adsorption, MOFs, mostly Fe-based MOFs, were proved to have an effective photocatalytic activity for the removal of organic contaminants. Such activity can be direct through transforming energy from the MOF into the compound or indirect through a homogeneous mediator such as PS. Du et al. studied the photocatalytic decolorization of MB on MIL-53-Fe under 500 W Xe lamp irradiation [65]. MIL-53-Fe concentration used in the study was 10 mg L$^{-1}$, knowing that at higher concentrations, total adsorption of MB dye occurred. Slight photo-degradation was initiated under UV–Vis light irradiation in the absence of MIL-53-Fe and was slightly enhanced in the presence of MIL-53-Fe. Such low efficiency was promoted by introducing a mediator such as hydrogen peroxide, potassium bromate and ammonium persulfate. Considerable degradation occurred under light irradiation in the absence of MIL-53-Fe indicating that light alone was sufficient for

activating the mediators. The degradation was enhanced, under irradiation, in the presence of both MIL-53-Fe and mediators.

Hu et al. studied MIL-101-Fe effect on the photo activation of persulfate for the degradation of organophosphorus flame retardant, tris(2-chloroethyl) phosphate (TCEP) [66]. As proposed in their study, as well as other studies utilizing iron-based MOFs, the mechanism of photo-catalysis reaction is based on the transformation of Fe(III) to Fe(II) (eq. 5), which further transform PS into sulfate radicals (eq. 6) allowing the degradation process to occur by radical oxidation as shown in the following reactions [66].

$$\equiv Fe^{3+} \xrightarrow{irradiation} \equiv Fe^{2+} \tag{5}$$

$$S_2O_8^{2-} + Fe^{2+} \rightarrow SO_4^{2-} + SO_4^{-\bullet} + Fe^{3+} \tag{6}$$

$$SO_4^{-\bullet} + \text{conaminant} \rightarrow \text{byproducts} \tag{7}$$

Lv et al. conducted their study on degrading MB by heterogeneous Fenton process using MIL-100-Fe [67]. In their study, it was shown that the electrostatic attraction influenced MB adsorption over different MOFs and that MIL-100-Fe(II) exhibited highest Fenton catalytic ability compared to MIL-100-Fe. Moreover, some studies developed modified iron-based MOFs to increase their efficiency. For example, Duan et al. applied cobalt and copper doping on MIL-101-Fe [68]. Tang and Wang synthesized graphene oxide-MIL-101-Fe to enhance the electron transfer process for efficient Fenton degradation of MO [69]. All of the above mentioned iron-based MOFs are synthesized using DMF, a carcinogenic organic solvent. Therefore, it was essential to consider an iron-based MOF that can be synthesized using a greener environmentally friendly method. For the best of our knowledge, MIL-88-A is the

only MOF found in literature that can be easily synthesized using water and no organic solvent. For this reason, MIL-88-A was used in several studies for the photocatalytic activation of persulfate [70–72]. However, the existing studies were conducted using relatively high concentration of MOF, 300 mg L$^{-1}$ [71] and ranging from 100 to 1500 mg L$^{-1}$ [72] and were all performed only for the degradation of dyes. Due to the fact that dyes already have high susceptibility to adsorption on MOFs [66], and that the degradation mechanism and byproducts in these studies were unclear, this research is conducted on the degradation of naproxen using a MIL-88-A/persulfate system with an evaluation of the effect of different parameters on the performance of the system.

## 2. Materials and methods

### 2.1. Chemicals

Naproxen sodium ($C_{14}H_{14}NaO_3$), sodium persulfate (PS) ($Na_2S_2O_8$, $\geq 99.0\%$), hydrogen peroxide ($H_2O_2$, 30% w/w), phosphate buffer (monobasic and dibasic), and potassium iodide (KI) (puriss, 99.0-100.5%) were purchased from Sigma-Aldrich (China, France, and Germany, respectively). Iron (III) chloride ($FeCl_3$) (reagent grade>97%) and fumaric acid ($C_4H_4O$) were acquired from Sigma-Aldrich (France and Switzerland respectively). Ethanol (absolute) was purchased from Scharlau (Spain). Formic acid and acetonitrile used for the HPLC mobile phase were purchased from Loba Chemie (India) and Honeywell (Germany) respectively. Millipore deionized water (DI) was used in the preparation of all solutions. To assess the matrix effect, sodium chloride (NaCl) and sodium bicarbonate (NaHCO$_3$) were purchased from Fluka (Netherlands).

25

## 2.2. Synthesis of MIL-88-A

Hydrothermal synthesis was performed in accordance with previously reported procedures [71–73], where 1,949 mg of fumaric acid and 4,544 mg of ferric chloride were added to a beaker filled with 84 mL of DI water. The solution was then stirred for an hour using a magnetic stirrer at 300 rpm to homogenize. It was later transferred into a 100 mL PTFE-lined stainless steel autoclave bomb and heated in an oven at 85°C for a period of 24 hours. After removing the autoclave bomb from the oven, it was passively left to cool to room temperature. The formed solids were then decanted, collected, washed three times with 1:1 ratio of ethanol and DI and two times with DI. This washing process was optimized to remove all the extra unreacted fumaric acid and metal. The precipitate was recovered each time by centrifugation at 4000 rpm (G-force = 2200) for 10 minutes. The obtained precipitate was then dried in a vacuum oven at 100 °C for no less than 10 hours yielding $2,350 \pm 220$ mg of pure MIL-88-A powder.

## 2.3. Characterization of MIL88-A

The powder X-ray diffraction pattern of MIL-88-A was determined by a D8 Advance (Bruker) X-ray diffractometer (XRD), equipped with copper anode material (40 mA, 40 kV). MIL-88-A powder was placed on a zero-background holder and was scanned from $5°$ to $15°$ ($2\Theta$) at a scan speed of 1 step of $0.02°$ per second. The morphology of the synthesized material was determined using a scanning electron microscope (SEM), Tescan, Mira III. Specific surface area of MIL-88-A were obtained using a BET surface area analyzer (Micromeritics, 3 flex surface characterization). Thermogravimetric analysis (TGA) of MIL-88-A was performed under nitrogen

atmosphere with a heating rate of 5 °C min$^{-1}$ and a temperature ranging from 30 to 900 °C using a TG 209 F1 Iris (Netzsch, Germany).

## 2.4. Experimental procedures and conditions

All solutions were prepared on daily basis using DI water. NAP stock solution (100 ppm) was prepared under dark by dissolving 109.5 mg of naproxen sodium salt in 1 L volumetric flask and kept stirring using a magnetic stirrer overnight. NAP physical properties are summarized in Table 2S. PS stock solution (100 mM) was prepared by dissolving 2,381 mg of sodium persulfate in a 100 mL volumetric flask. For each experiment, a specific volume of the NAP stock solution was added along with a corresponding amount of DI water and MIL-88-A to a 200 mL reactor and left stirring for a period of 1 hour to reach adsorption equilibrium according to the conducted adsorption isotherms in section 3.2. After which, the reaction is initiated by spiking with the required volume of PS stock solution. Continuous stirring was maintained to ensure uniform mixing and suspension of MIL-88-A particles. Samples of 2 mL were collected 30 sec before and after the addition of MIL-88-A as well as before and after the addition of PS and every 10 min for the next 40 min to reach a total reaction time of 100 min, the last sample was taken at t = 120 min. All samples were filtered using a 0.45 µm PTFE 13 mm disc filters (Jaytee Biosciences Ltd., UK) and stored in amber HPLC vials at 4°C prior to analysis. Sample withdrawal timing was varied according to specific experimental requirements. Control experiments were performed either in the absence of PS and/or MIL-88-A. All NAP degradation experiments were done in triplicates and each sample was analyzed twice for uncertainty determination.

### 2.5. Reaction setup

For experiments in which UV was not used, reactions took place in 250 mL Erlenmeyer flasks placed on a solid state magnetic stirrer of capacity equal to six flasks (Fig. 1).
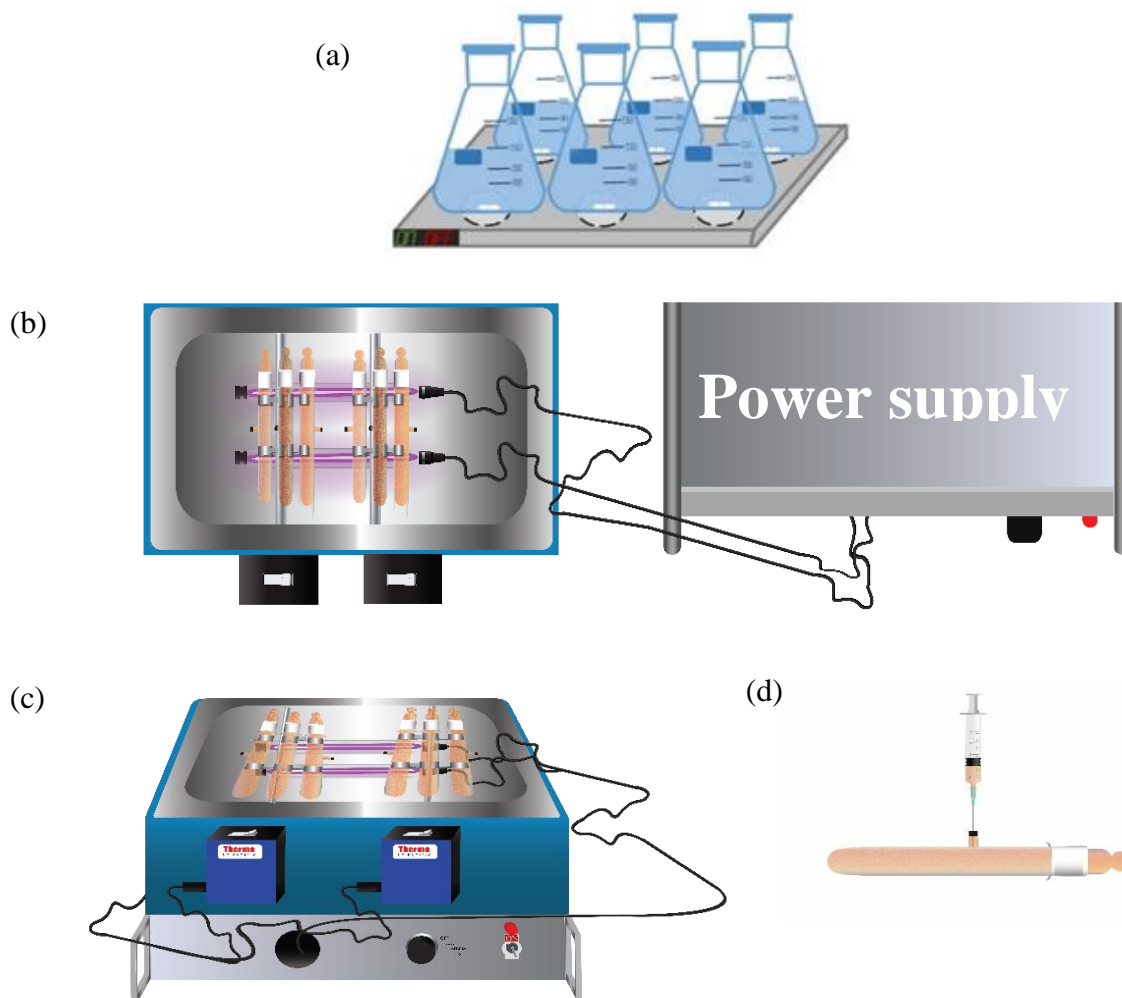


Fig. 1. Illustrations of experimental setups (a) reactors used when no UV was present (b) top view of experimental setup of experiments done under UV irradiation (c) side view of experimental setup of experiments done under UV irradiation (d) single reactor with the syringe showing the sample collecting process

For the experiments conducted under UV irradiation, 8 homemade watertight 110 mL borosilicate reactors were attached radially to a labquake shaker rotisserie of speed 8 revolutions/min. This mixing setup was developed to maintain MIL-88-A in suspension during irradiation. The reactors were placed in a stainless steel reflector with 2 commercial T5 8 watts near-ultraviolet (UV-A) fluorescent lamps, of dosage 450 uW/cm$^2$ and 180 uW/cm$^2$ on the nearest and farthest point to the system respectively, obtained from insects light traps. emission spectrum of the lamps presented in Fig. 2 was obtained using a modified spectrophotometer [74]. This spectrum shows main emission between 350 and 400 nm lying in the UV-A-Vis range.
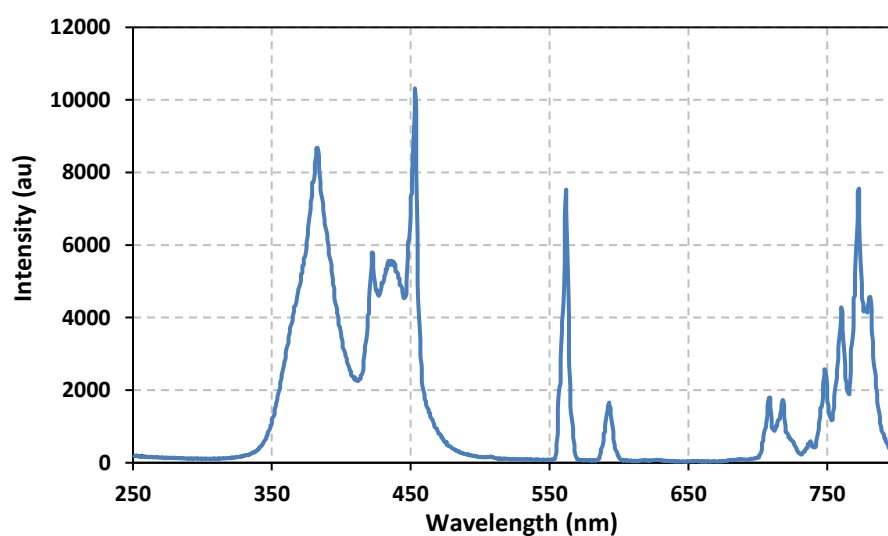


Fig. 2. Emission spectrum of the UV-A lamp

## 2.6. Chemical analysis

Quantifying NAP was performed on an HPLC equipped with a quaternary pump, a vacuum degasser, an auto sampler unit with cooling maintained at 4°C, and a thermally controlled column compartment set at 30°C. A C-18 reverse phase column (5 µm; 4.6 mm internal diameter x 250 mm in length) was used in addition to a security guard column HS C-18 (5 µm; 4.0 mm internal diameter 20 mm long) for the separation of NAP and its byproducts. The HPLC was equipped with a DAD detector (228 nm for NAP). The mobile phase consisted of acetonitrile: 0.1 % formic acid solution of (55:45) (v/v) and was kept under constant flow rate of 1 mL min$^{-1}$. The injection volume was set to 100 µL. Under these conditions, NAP was eluted at a retention time of 6.9 min. The linear dynamic range (LDR) obtained was between 0.1 and 100 mg L$^{-1}$ with limit of detection = 0.0009 mg L$^{-1}$ (Fig. 3).

(a)
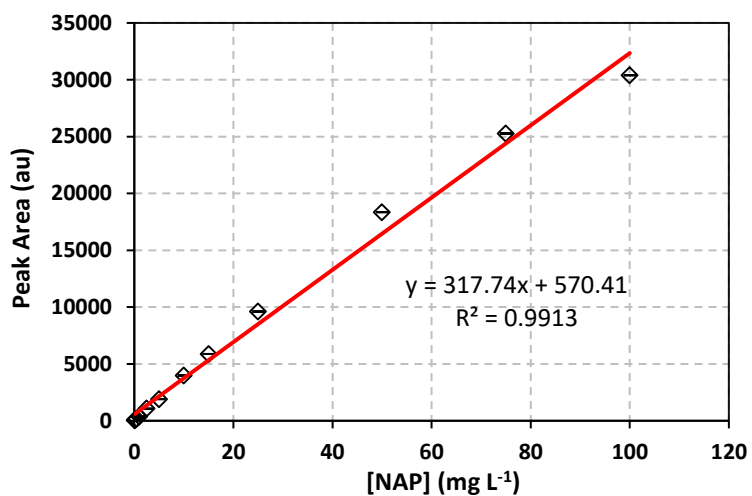


(b)

| Linest Output NAP | | | |
|---|---|---|---|
| y = mx+b | | | |
| m | 317.74 | 570.41 | b |
| Sm | 9.4254 | 376.11 | Sb |
| R² | 0.9913 | 1048.3 | Sy |

Fig. 3. (a) Calibration curve of NAP. The error bars are calculated at 95% confidence level. Absorbance = $A_{(mean)} \pm ts/(n)^{1/2}$ where t is the student value (t = 2.447 for 6 degrees of freedom at 95% confidence level) and s the standard deviation of 7 replicates. (b) The LINEST output calculated through Excel provided the slope, y intercept, the regression coefficient and all statistical data including standard deviations on variables.

Persulfate and $H_2O_2$ concentrations were quantified using a novel flow injection/spectroscopy analytical technique according to the methods developed by Baalbaki et al. [75] and Tantawi et al. [76] respectively . The LDR of the used PS quantification method ranges between 0.1 and 50 mM with a limit of detection 0.0066 mM and that of $H_2O_2$ ranges between 0.01–150 mM with a limit of detection 0.00276 mM.

## 3. Results and discussion

### 3.1. Characterization of MIL-88-A:

The XRD diffraction pattern (Fig. 4b) shows strong peaks at $2\theta$ positions 7.7, 8.7, 10.4 and 11 ensuring the crystalline nature of MIL-88-A synthesized. SEM images (Fig. 4a) showed that MIL-88-A crystals exhibit hexagonal rod-like morphology in the nanometer-scale, with sizes ranging from 100 to 800 nm typical to what is reported in literature [71,72]. BET analysis allowed to calculate the surface area of MIL-88-A which was found to be around $41.4408 \pm 1.7570$ $m^2/g$ complying with that published [71]. TGA analysis (Fig. 4c) illustrates a 20 % weight loss occurring below 100 $^{o}$C attributed to the evaporation of moisture and desorption of other gases from the MIL-88-A sample. After which, the thermogravimetric stability remained constant till approximately 200 $^{o}$C. Thereafter, a major weight loss was observed probably due to the decomposition of fumaric acid.
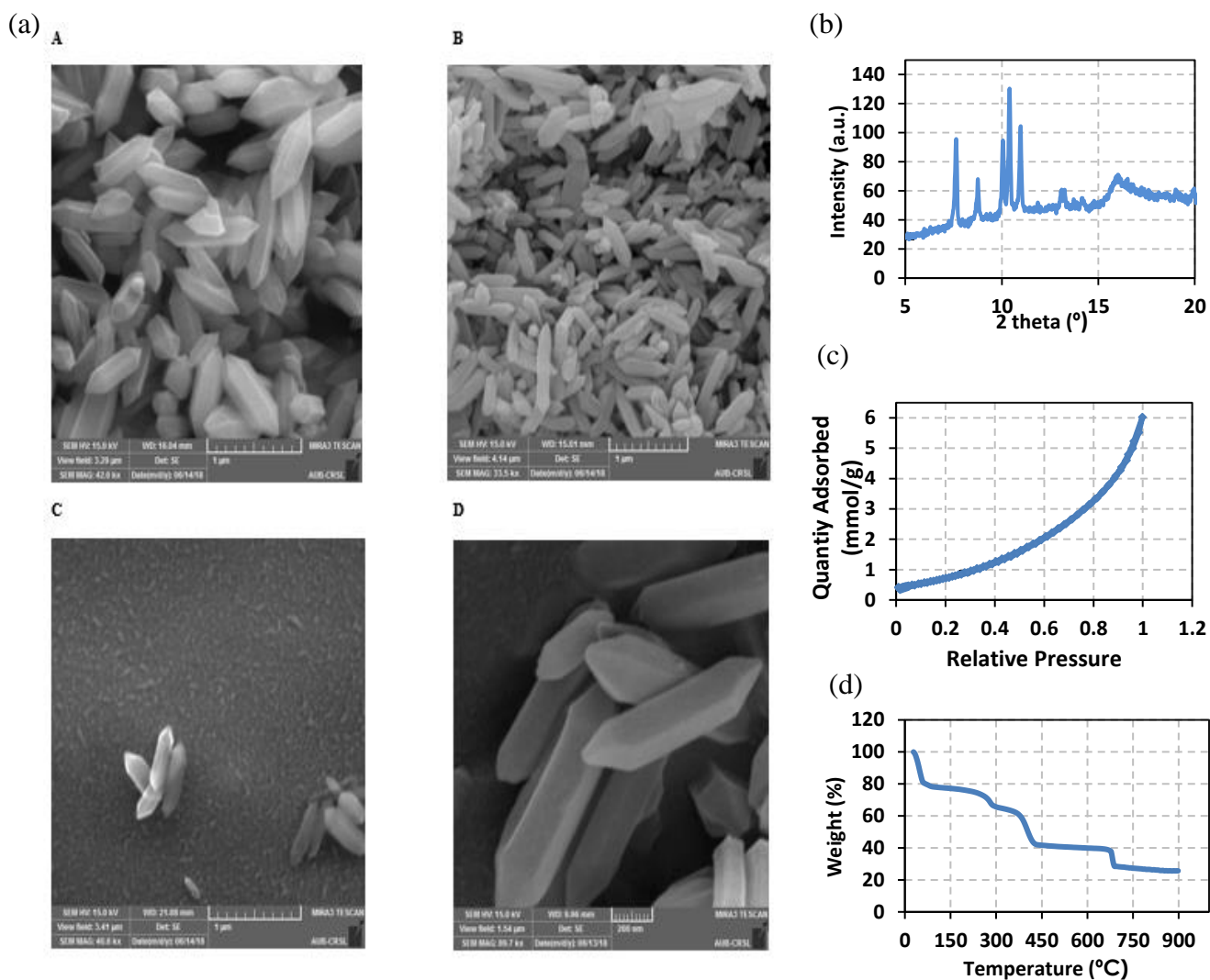
Fig. 4. Characterization of synthesized MIL-88-A (a) SEM of crystals at different magnifications (b) XRD diffraction pattern (c) BET adsorption/desorption isotherms (d) TGA analysis.

## 3.2. Adsorption experiments

A series of adsorption experiments were performed. Quantity of adsorbed NAP was found to be directly proportional to MIL-88-A dose (Fig. 5). When the amount of MIL-

33

88-A increased from 5 to 50 mg in 200 mL reaction volume, NAP adsorption increased from ~ 5 % to ~ 50 % indicating a constant adsorption capacity equal to 500 mg NAP /g of MIL-88-A. Adsorption equilibrium was achieved after one hour from the addition of MIL-88-A.

To eliminate the possibility of interference on the adsorption process due to ionic strength added from the PS and its byproduct, sulfate, the system was either spiked with 2 mM of sodium persulfate or 4 mM of sodium sulfate for control. Sodium sulfate was considered since it is the byproduct of PS oxidation. Each sodium persulfate molecule produces two sulfate ions; accordingly, the spiked concentration of sulfate was double that of PS. Results showed that increasing ionic strength: sulfate and PS ions caused partial desorption of the adsorbed NAP (Fig. 6) where ~ 35 % = 5.25 mg of NAP desorbed upon spiking with 4 mM sodium sulfate.
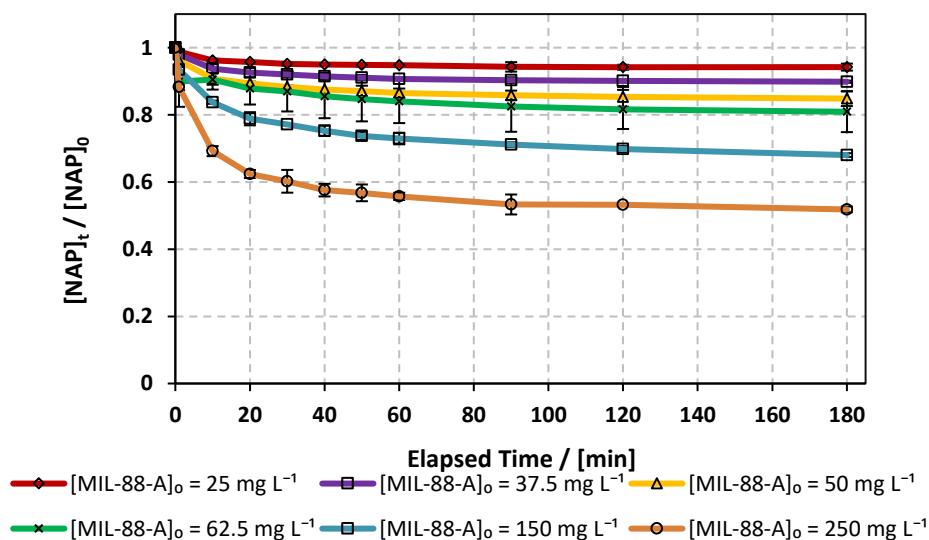


Fig. 5. Adsorption of NAP vs $[MIL\text{-}88\text{-}A]_0$. $[NAP]_0 = 50$ mg L$^{-1}$. Error bars are calculated as $\frac{ts}{\sqrt{n}}$, where absent bars fall within the symbols.

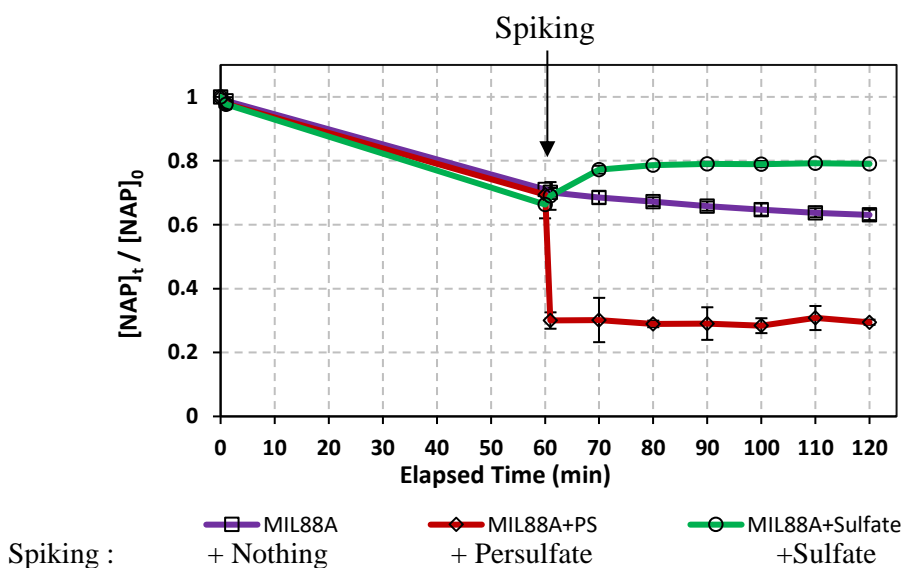Fig. 6. Effect of ionic strength on the adsorption of NAP. $[NAP]_0 = 50$ mg L$^{-1}$.[MIL-88-A]$_0 = 250$ mg L$^{-1}$. $[PS]_0 = 2$ mM. $[Sulfate]_0 = 4$ mM. Error bars are calculated as $\frac{ts}{\sqrt{n}}$, where absent bars fall within the symbols.

### 3.3. PS/MIL-88-A system degradation experiments and optimization

To determine the optimal concentration of PS, spiked $[PS]_0$ was varied between 0.25, 1 and 5 mM. The strongest instantaneous drop occurred at the highest $[PS]_0$ used $= 5$ mM (Fig. 7) . The rebound observed between spiking at t = 60 min and t = 90 min in Fig. 7 is attributed to desorption due to the sudden increase in ionic strength after the addition of PS, the rebound effect is also noticed in all other experiments after the addition of $[PS]_0$.
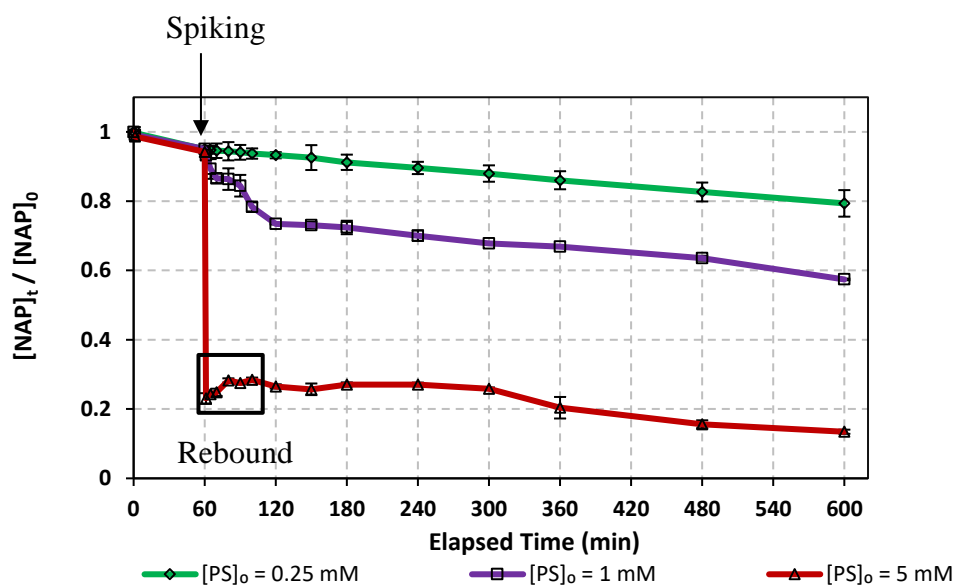
Fig. 7. Effect of $[PS]_0$ on the degradation of NAP. $[NAP]_0 = 50$ mg $L^{-1}$. [ MIL-88-A]$_0 = 25$ mg $L^{-1}$ . Error bars are calculated as $\frac{ts}{\sqrt{n}}$, where absent bars fall within the symbols.

To determine the optimal $[MIL\text{-}88\text{-}A]_0$, it was varied between 25 and 250 mg $L^{-1}$ using a fixed $[PS]_0 = 2$ mM (Fig. 8). High $[MIL\text{-}88\text{-}A]_0$ showed limited NAP degradation enhancement, thus 25 mg $L^{-1}$ was chosen as the best $[MIL\text{-}88\text{-}A]_0$ for cost optimization purposes. Since our objective is to degrade MIL-88-A and not to adsorb it, then a lower $[MIL\text{-}88\text{-}A]_0$ better suits our purpose. 25 mg $L^{-1}$ MIL-88-A was the lowest amount that could be added without sacrificing practicality in experimental procedure. PS was tested as successively spiked vs one time addition where a single spike with high concentration, up to 5 mM, showed the best results in the system proposed Fig. 9. Thus $[MIL\text{-}88\text{-}A]_0 = 5$ mg $L^{-1}$ and $[PS]_0 = 5$ mM were adopted to study the matrix effect.
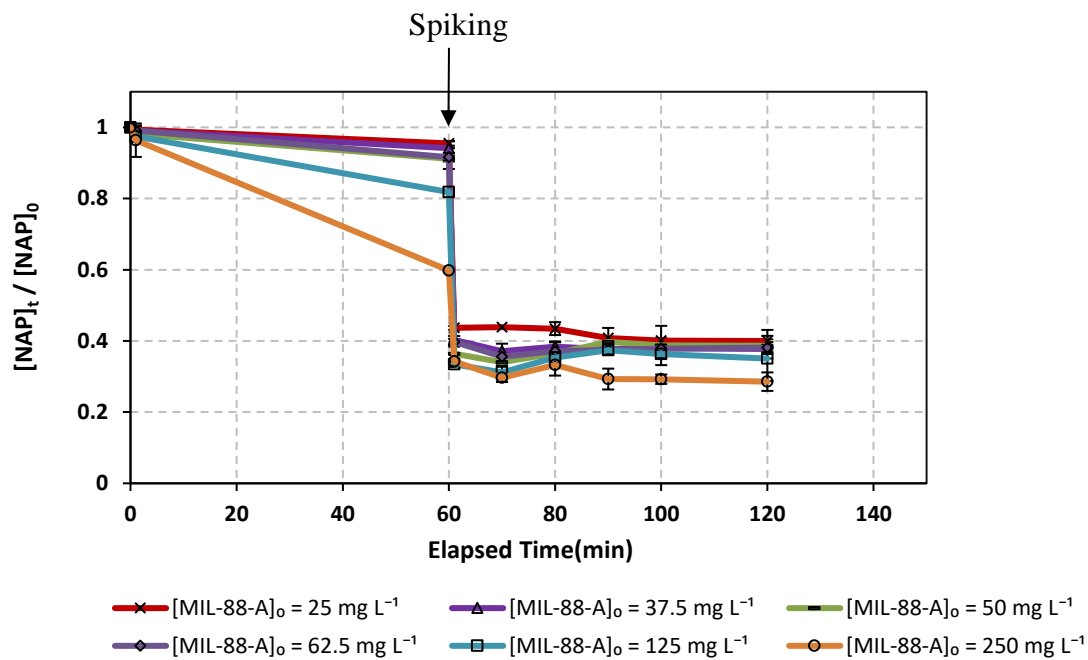
Fig. 8. Effect of [MIL-88-A]$_0$ on NAP degradation. [NAP]$_0$ = 50 ppm. PS spike at t = 60 min with [PS]$_0$ = 2 mM. Error bars representing standard deviation are calculated at 95% confidence level. Error bars are calculated as $\frac{ts}{\sqrt{n}}$, where absent bars fall within the symbols.
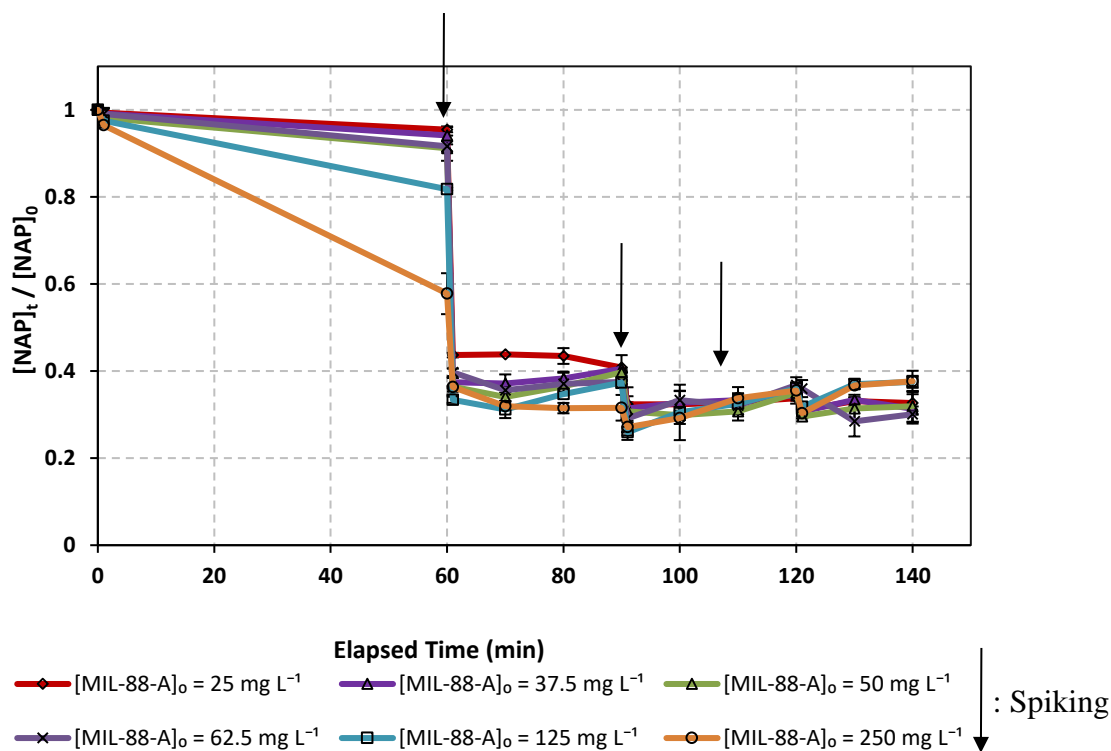
Fig. 9. Effect of [MIL-88-A]$_0$ dosage in on NAP degradation upon spiking with [PS]$_0$ = 2 mM at t = 60 min and [PS]$_0$ = 1 mM at t = 90, and 120 min. [NAP]$_0$ = 50 mg L$^{-1}$. Error bars are calculated as $\frac{ts}{\sqrt{n}}$, where absent bars fall within the symbols.

### 3.4. Recyclability

Recyclability is an essential parameter when studying heterogeneous catalysis applications since the catalyst can be recovered and reused. An experiment was conducted by which the MIL-88-A was recycled in four successive cycles. The recovery process included separation using centrifugation and drying via a vacuum oven at 90$^O$C. Recovered MIL-88-A decreases after each cycle due to the fact that lower amounts of MOF are always harder to collect. After the first cycle, 80% of MIL-88-A was

recovered. This percentage decreased to 53 and 47% after second and third cycles

respectively. The adsorption of NAP on MIL-88-A was reduced in each cycle due to the

decrease in the amount of MIL-88-A added to the solution (Fig. 10). The final

concentration of NAP that is still available in the solution increased from 16 to 30 mg L$^{-1}$ (Fig. 10). A decrease in efficiency was observed after the second cycle and may be

attributed to the full occupation of all the activation sites of MIL-88-A. SEM of MIL-

88-A after recycling showed that the crystals maintained rod-like morphology; however,

lost homogeneity and changed in size, becoming thinner and more elongated (Fig. 11a).

On the other hand, XRD diffraction pattern overlaps that of the initially synthesized

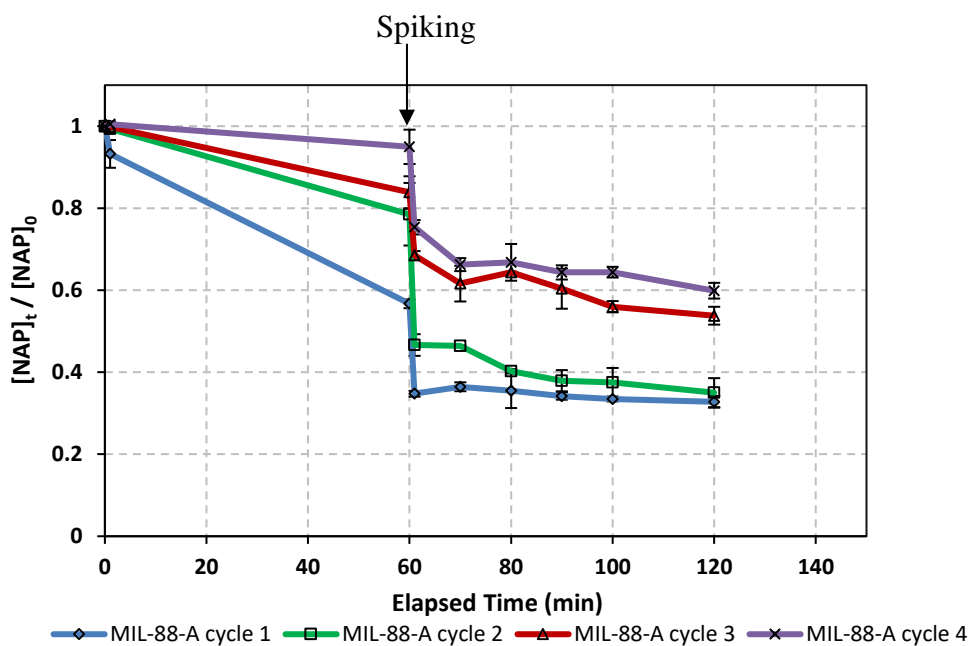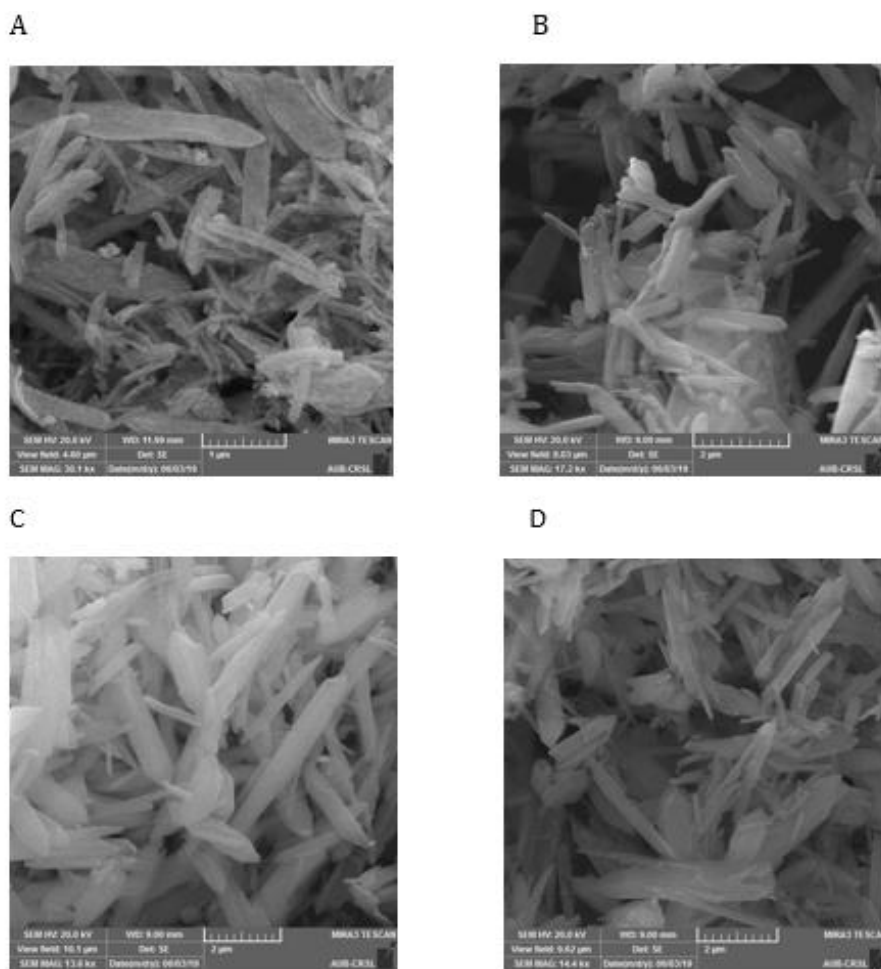MIL-88-A with differences in the intensity of the peaks (Fig. 11b).



Fig. 10. Recyclability experiments. $[NAP]_0 = 50$ mg L$^{-1}$. $[PS]_0 = 5$ mM. Error bars are

calculated as $\frac{ts}{\sqrt{n}}$, where absent bars fall within the symbols.
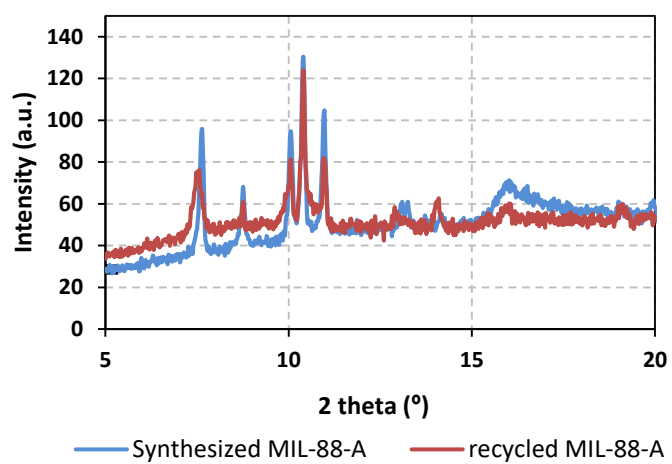
(a)



(b)



Fig. 11. Characterization of recycled MIL-88-A (a) SEM images (b) XRD diffraction

pattern

### 3.5. Matrix effect

#### 3.5.1. Case of Chlorides

The effect of common anions found in natural water samples on NAP degradation was examined. In order to mimic natural water conditions, three different concentrations of chloride ions [77] corresponding to freshwater ($[NaCl] = 200$ mg L$^{-1}$), brackish water ($[NaCl] = 2,000$ mg L$^{-1}$), and saline water ($[NaCl] = 20,000$ mg L$^{-1}$) were tested. The effect of chloride ions in its different concentrations had no significance on the degradation of NAP (Fig. 12). The effect of the increase in ionic strength on adsorption was not expressed clearly due to the low $[MIL\text{-}88\text{-}A]_0$ used (25 mg L$^{-1}$).



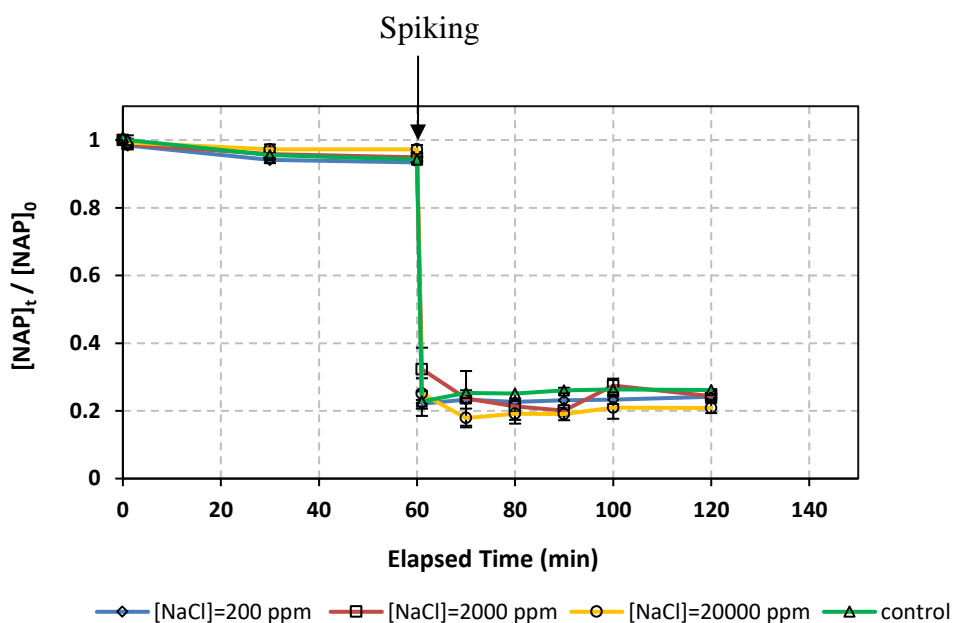Fig. 12. Effect of chloride concentration on the degradation of NAP. $[NAP]_0 = 50$ mg L$^{-1}$. $[PS]_0 = 5$ mM. $[MIL\text{-}88\text{-}A] = 25$ mg L$^{-1}$. Error bars are calculated as $\frac{ts}{\sqrt{n}}$, where absent bars fall within the symbols.

### 3.5.2. Case of phosphates

The effect of phosphate concentration on the degradation of NAP was studied for two main reasons. First of all, to account for phosphate residues escaped from conventional water treatment processes [78]. Moreover, for the aim of choosing a buffer solution to study the effect of pH of the reaction system on the degradation of NAP. Therefore, a study on the effect of phosphate buffer was conducted at three different concentrations: 1, 5, and 10 mM, of phosphate buffer (pH = 4), simulating the pH of the system with DI. The results shows that there was no significant effect of phosphate on NAP degradation (Fig. 13).
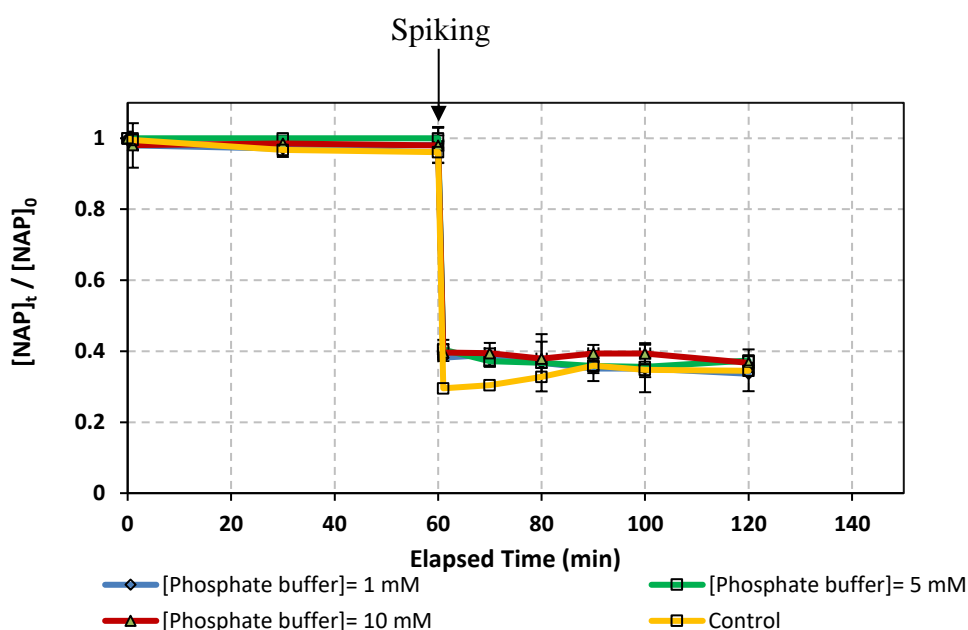


Fig. 13. Effect of phosphate concentration on the degradation of NAP. $[NAP]_0 = 50$ mg $L^{-1}$. $[PS]_0 = 5$ mM. $[MIL-88-A]_0 = 25$ mg $L^{-1}$. Error bars are calculated as $\frac{ts}{\sqrt{n}}$, where absent bars fall within the symbols.

### 3.5.3. pH effect

One major influence factor affecting NAP degradation is the pH value of the system. A study on the pH effect on the degradation of NAP in the MIL-88-A/ PS system was conducted in 10 mM phosphate buffered solutions of different pH values imitating acidic, basic, and neutral conditions (Fig. 14). The results showed that optimum degradation was perceived in acidic conditions (pH = 4) similar to that encountered in the control using DI where pH initial and final falls within the range of acidic conditions tested (Fig. 14). Neutral and basic pH equally inhibited the degradation by 90 %. This can be explained by the fact that fumaric acid, the linker, becomes neutral in acidic conditions, since it has a pka1 value of 3.03 and pka2 = 4.44. This induces a positive charge on the surface of MIL-88-A. Thus more attraction occurs between induced positive charged MIL-88-A and PS anions leading to better activation and thus higher degradation of NAP.
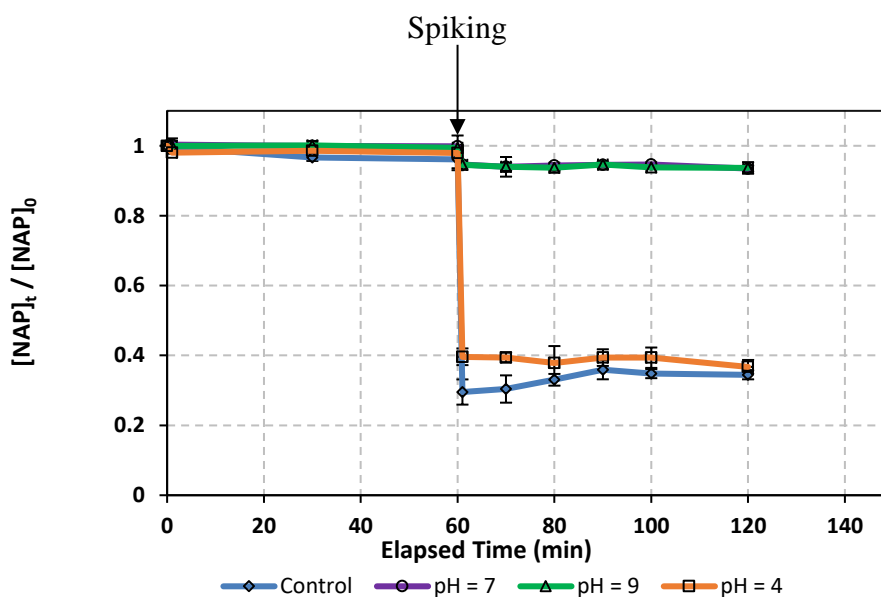
Fig. 14. Effect of pH value on the degradation of NAP. $[NAP]_0 = 50$ mg $L^{-1}$. $[PS]_0 = 5$ mM $[MIL-88-A]_0 = 25$ mg $L^{-1}$. Error bars are calculated as $\frac{ts}{\sqrt{n}}$, where absent bars fall within the symbols.

### 3.5.4. Case of bicarbonates

The effect of bicarbonate in the reaction matrix was also examined. Bicarbonate presence led to a noticeable inhibition to the degradation of NAP (Fig. 15). At $[NaHCO_3] = 1$ mM, the drop of $[NAP]$ after 60 mins from spiking with PS decreased from 75 % to 30 %. The extent of decrease became more significant to reach 20 % and 15 % at $[NaHCO_3] = 50$ and 100 mM respectively. The inhibitory effect of $HCO_3^-$ could be attributed to the reaction between sulfate radicals and $HCO_3^-$ (Eq. 8) yielding $CO_3^{\bullet-}$ (E $^{\circ} = 1.59$ V) [79] which has moderate oxidative properties compared to sulfate radicals towards NAP.

$$SO_4^{-\bullet} + HCO_3^- \rightarrow SO_4^{2-} + CO_3^{-\bullet} + H^+ \tag{8}$$

Also, in case of NAP, an increase in the pH of the solution is noticed with increasing $HCO_3^-$ (Table 2). The buffering at a basic pH induced by the addition of bicarbonate to the system is directly related to the inhibitory effect on the degradation of NAP as discussed in the study on the effect of pH above.

**Table 2**

pH values in the reaction systems at different times during the experiment

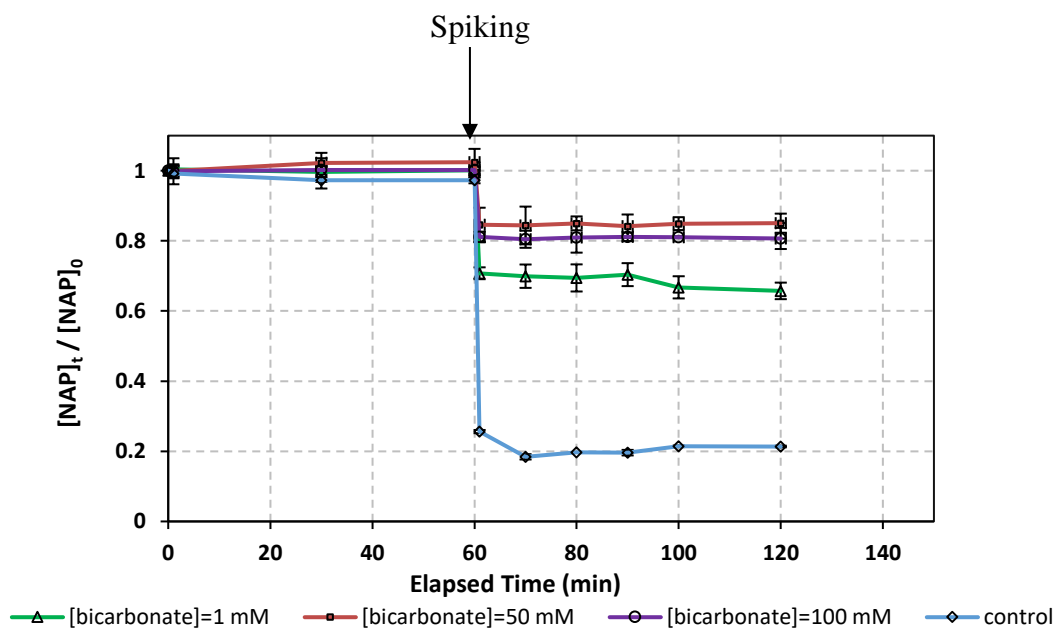|  | pH initial | pH at 60 min | pH at 120 min |
|---|---|---|---|
| Control | 5.21 | 4.96 | 3.95 |
| $[HCO_3^-] = 1$ mM | 7.98 | 7.31 | 5.20 |
| $[HCO_3^-] = 50$ mM | 8.51 | 8.50 | 8.34 |
| $[HCO_3^-] = 100$ mM | 8.54 | 8.52 | 8.44 |



Fig. 15. Effect of bicarbonates concentration on the degradation of NAP. $[NAP]_0= 50$ mg L$^{-1}$. $[PS]_0 = 5$ mM. $[MIL-88-A]_0= 25$ mg L$^{-1}$. Error bars are calculated as $\frac{ts}{\sqrt{n}}$, where absent bars fall within the symbols.

45

### 3.6. MIL-88-A/PS versus MIL-88-A/$H_2O_2$ system

To test for the applicability of MIL-88-A on other oxidants, a common oxidant, $H_2O_2$, was used. The experimental conditions for MIL-88-A/PS system were mimicked for the sake of comparison. $[H_2O_2]_0 = 2$ and 5 mM were used for spiking at t = 60 min. Results showed that $H_2O_2$ had minimal effect on the degradation of NAP compared to that of PS (Fig. 16), which indicates that MIL-88-A in not an efficient activator of $H_2O_2$. The addition of $H_2O_2$ caused an insignificant drop in the pH value compared to that caused by the addition of PS (Table 3). Knowing that the activation of $H_2O_2$ in the presence of $Fe^{3+}$ is optimal at acidic conditions (pH = 3-4) [80,81], the difference in degradation between $H_2O_2$ and PS could be partially attributed to the pH of the solution. Further investigation revealed that $[H_2O_2]$ decreased by about 25% upon spiking at t = 60 min (Fig. 1S) similar to the trend followed by PS (Fig. 2S) indicating that both oxidants are either adsorbed and/or activated; however, only PS is affective for NAP removal.
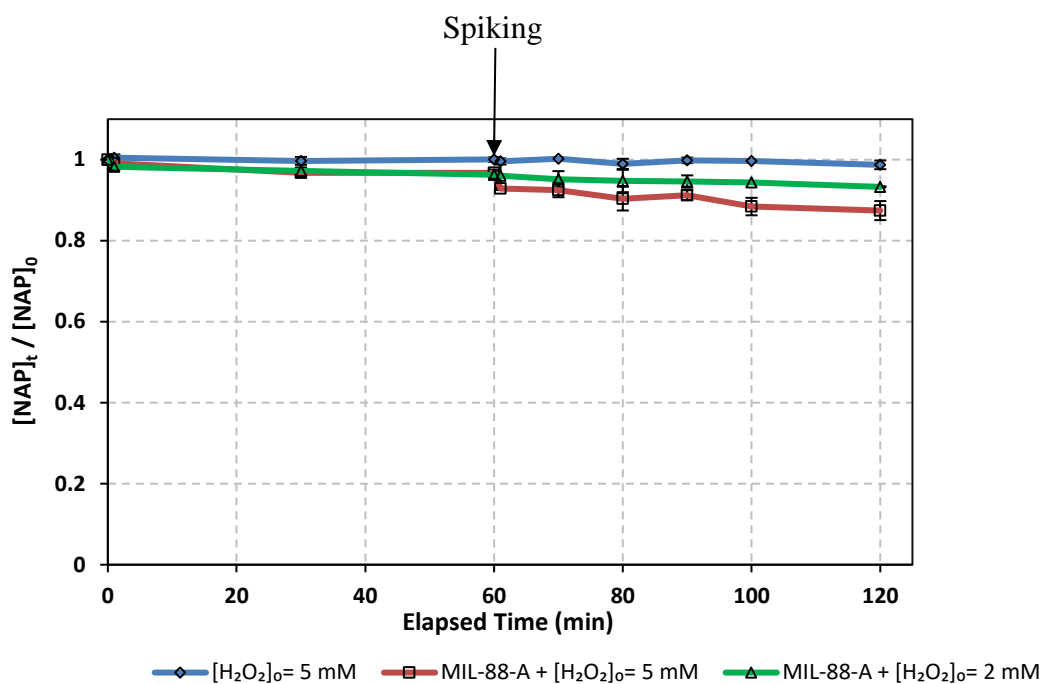
Fig. 16. Effect of $[H_2O_2]_0$ on the degradation of NAP. $[NAP]_0 = 50$ mg $L^{-1}$.[MIL-88-A]$_0 = 25$ mg $L^{-1}$. Error bars are calculated as$\frac{ts}{\sqrt{n}}$, where absent bars fall within the symbols.

**Table 3**

pH values in the reaction systems at different times during the experiment with $H_2O_2$

|  | pH initial | pH at 60 min | pH at 120 min |
|---|---|---|---|
| $[H_2O_2] = 5$ mM | 6.48 | 6.30 | 6.08 |
| $[H_2O_2] = 5$ mM + MIL-88-A | 6.47 | 5.85 | 5.31 |
| $[H_2O_2] = 2$ mM + MIL-88-A | 6.48 | 5.84 | 5.48 |
| $[PS] = 5$ mM + MIL-88-A | 6.44 | 5.62 | 3.03 |

### 3.7. UV-A effect

A study on the effect of UV-A on the proposed system was conducted. NAP has been

proven to be resistant to UV-A irradiation in the absence of MIL-88-A. In the presence

of MIL-88-A, no degradation was observed and only adsorption took place (Fig. 17).

On the other hand, in the UV-A/PS system, in the absence of MIL-88-A, irradiation was

sufficient for minor activation of PS and leading to a 20% drop in the [NAP] from 50 to

40 mg L-1 monitored upon spiking with PS (Fig. 17). This activation was significantly

enhanced when MIL-88-A was added leading to the complete removal of NAP within

60 min of PS addition (Fig. 17).
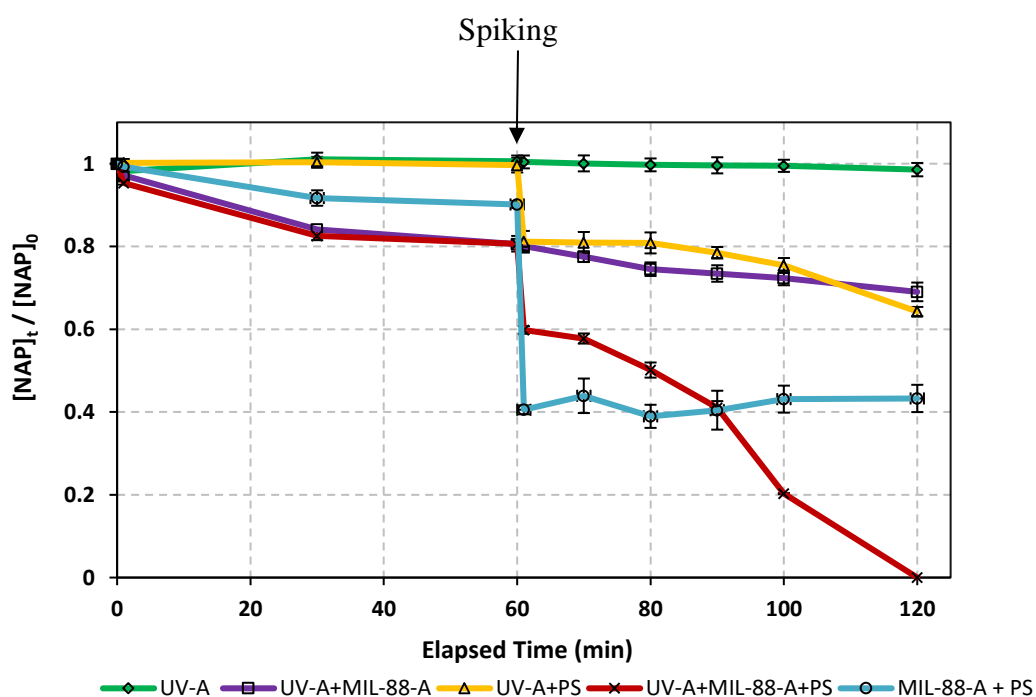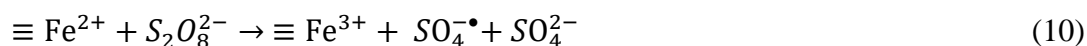


Fig. 17. UV-A effect on NAP degradation. $[NAP]_0 = 50$ mg L$^{-1}$. $[MIL-88-A]_0 = 100$ mg

L$^{-1}$ . $[PS]_0 = 5$ mM. Error bars are calculated as $\frac{ts}{\sqrt{n}}$, where absent bars fall within the

symbols.

### 3.8. Proposed mechanism

To determine the mode of action of MIL-88-A/PS on NAP degradation, the results of several experiments were analyzed as follows. The variation in the initial [MIL-88-A] shown in Fig. 5 showed that the extent of degradation of NAP is independent of MI-88-A dose. However, manipulation of $[PS]_0$ at a fixed $[MIL-88-A]_0$ (Fig. 6) showed a direct relationship between [PS] spiked and the drop of [NAP]. The drop followed the trend of zero-order kinetics with an instantaneous decrease upon spiking with PS noticed by the value of [NAP] taken after 30 seconds of the spike with no further significant decrease obtained afterwards, even with further PS spikes (Fig. 9). This phenomena proposes that the sulfate ions introduced to the reaction medium are adsorbed immediately on the activation sites on MIL-88-A blocking other species. Sulfates also contribute to the global ionic strength of the solution, and thus lowering the adsorption affinity of MIL-88-A to persulfate ions. The presence of active sites within MIL-88-A was reported by the study of Lin et al. on the decolorization of RB in a MIL-88-A/ PS system [72].

On the molecular level, Fe species in MIL-88-A are trivalent; by which, PS activation can be initiated via one-electron reduction mechanism (eq. 9 and 10) [72,82].

$$\equiv Fe^{3+} + S_2O_8^{2-} \rightarrow \equiv Fe^{2+} + S_2O_8^{-\bullet} \tag{9}$$

$$\equiv Fe^{2+} + S_2O_8^{2-} \rightarrow \equiv Fe^{3+} + SO_4^{-\bullet} + SO_4^{2-} \tag{10}$$

$\equiv Fe^{2+}$ is produced upon the reduction of $\equiv Fe^{3+}$ producing persulfate radicals. $\equiv Fe^{2+}$ then returns to its original state, $\equiv Fe^{3+}$, generating sulfate radicals which are responsible for the oxidation/ degradation of NAP molecules in the mixture.

In presence of UV-A, adsorption was enhanced by 10 %, followed by a 20 % inhibition in the instantaneous drop in [NAP] upon spiking with PS. However, the degradation process continued to reach full elimination of NAP at t = 120 min (Fig. 17). After the initial drop of NAP (t = 61 min), the decline process consisted of two stages: a slow followed by a rapid decreasing stage. The first stage lasts till t = 80 min and is reported in literature as the induction period in other Fe-based catalysis [66,83]. The second stage in which the rapid decrease is monitored is where the radical oxidation dominates and the continuous degradation is attributed to the fast regeneration of $\equiv Fe^{2+}$ caused by UV activation (eq. 5).
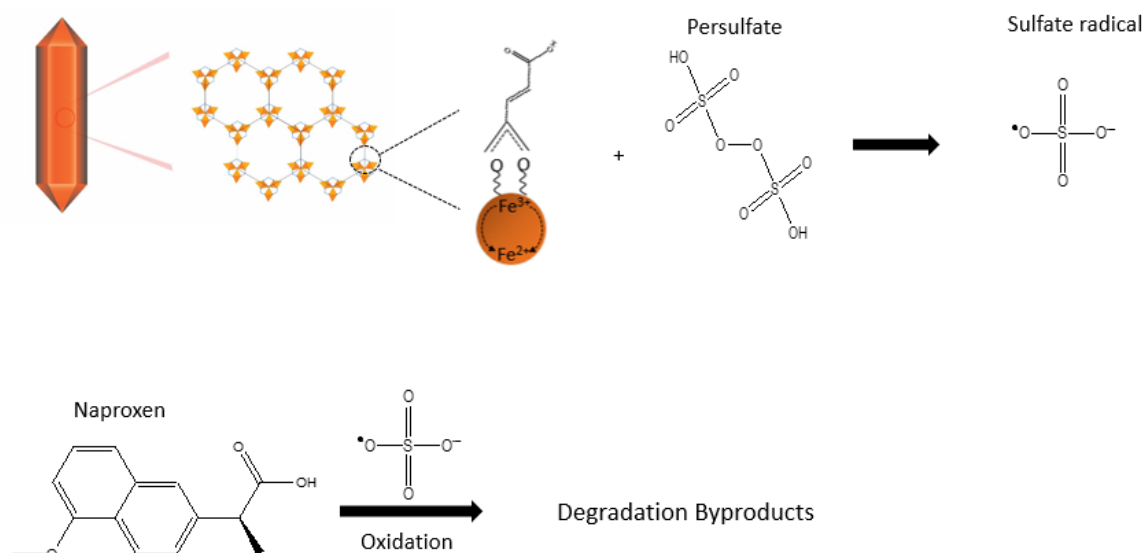
## 4. Conclusion

In this study, MIL-88-A was prepared with the advantage of using an easy, low-cost, and organic solvent free synthesis process. The material was then characterized and applied for the elimination of naproxen from water simulating the waste water effluent of a pharmaceutical production facility through AOPs. MIL-88-A proved to be an effective activator of PS even in absence of photo irradiation. Several parameters were assessed to reach a higher efficiency for the treatment process. $[MIL-88-A]_0$ used in the system was optimized and set at 25 mg $L^{-1}$ and $[PS]_0$ at 5 mM. It was found that MIL-88-A can be used for multiple-cycle activation of persulfate with no need for any regeneration steps to be done. UV-A effect on the activation process was studied and full degradation was achieved within two hours in the MIL-88-A/PS/UV-A activated system proving MIL-88-A to be a promising heterogeneous catalyst that can be used for PS activation for water treatment purposes.

## 5. Acknowledgments

## References

[1]  J.-L. Liu, M.-H. Wong, Pharmaceuticals and personal care products (PPCPs): a review on environmental contamination in China, Environ. Int. 59 (2013) 208–224.

[2]  J.L. Tambosi, L.Y. Yamanaka, H.J. JosÃ\copyright, R. de F.P.M. Moreira, H.F. SchrÃ\Pder, Recent research data on the removal of pharmaceuticals from sewage treatment plants (STP), QuÃ\-Mica Nov. 33 (2010) 411–420.

[3]  T. Heberer, Occurrence, fate, and removal of pharmaceutical residues in the aquatic environment: A review of recent research data, Toxicol. Lett. (2002). doi:10.1016/S0378-4274(02)00041-3.

[4]  K.E. Arnold, A.R. Brown, G.T. Ankley, J.P. Sumpter, Medicating the environment: assessing risks of pharmaceuticals to wildlife and ecosystems, Philos. Trans. R. Soc. B Biol. Sci. 369 (2014).

[5]  C.G. Daughton, T.A. Ternes, Pharmaceuticals and personal care products in the environment: Agents of subtle change?, Environ. Health Perspect. (1999). doi:10.1007/s11113-013-9316-3.

[6]  J. Rivera-Utrilla, M. Sánchez-Polo, M.Á. Ferro-García, G. Prados-Joya, R. Ocampo-Pérez, Pharmaceuticals as emerging contaminants and their removal from water. A review, Chemosphere. 93 (2013) 1268–1287. doi:http://dx.doi.org/10.1016/j.chemosphere.2013.07.059.

[7]  G.R. Boyd, J.M. Palmeri, S. Zhang, D.A. Grimm, Pharmaceuticals and personal

care products (PPCPs) and endocrine disrupting chemicals (EDCs) in stormwater canals and Bayou St. John in New Orleans, Louisiana, USA, Sci. Total Environ. (2004). doi:10.1016/j.scitotenv.2004.03.018.

[8]     D. Ashton, M. Hilton, K. V. Thomas, Investigating the environmental transport of human pharmaceuticals to streams in the United Kingdom, Sci. Total Environ. (2004). doi:10.1016/j.scitotenv.2004.04.062.

[9]     M. Carballa, F. Omil, J.M. Lema, M. Llompart, C. García-Jares, I. Rodríguez, M. Gómez, T. Ternes, Behavior of pharmaceuticals, cosmetics and hormones in a sewage treatment plant, Water Res. (2004). doi:10.1016/j.watres.2004.03.029.

[10]    N. Lindqvist, T. Tuhkanen, L. Kronberg, Occurrence of acidic pharmaceuticals in raw and treated sewages and in receiving waters, Water Res. (2005). doi:10.1016/j.watres.2005.04.003.

[11]    N. Nakada, T. Tanishima, H. Shinohara, K. Kiri, H. Takada, Pharmaceutical chemicals and endocrine disrupters in municipal wastewater in Tokyo and their removal during activated sludge treatment, Water Res. (2006). doi:10.1016/j.watres.2006.06.039.

[12]    T.A. Ternes, M. Meisenheimer, D. McDowell, F. Sacher, H.J. Brauch, B. Haist-Gulde, G. Preuss, U. Wilme, N. Zulei-Seibert, Removal of pharmaceuticals during drinking water treatment, Environ. Sci. Technol. (2002). doi:10.1021/es015757k.

[13]    P.R. Gogate, A.B. Pandit, A review of imperative technologies for wastewater treatment I: oxidation technologies at ambient conditions, Adv. Environ. Res. 8

(2004) 501–551. doi:http://dx.doi.org/10.1016/S1093-0191(03)00032-7.

[14]    C. Wei, F. Zhang, Y. Hu, C. Feng, H. Wu, Ozonation in water treatment: The generation, basic properties of ozone and its practical application, Rev. Chem. Eng. (2017). doi:10.1515/revce-2016-0008.

[15]    S.O. Ganiyu, M. Zhou, C.A. Martínez-Huitle, Heterogeneous electro-Fenton and photoelectro-Fenton processes: A critical review of fundamental principles and application for water/wastewater treatment, Appl. Catal. B Environ. (2018). doi:10.1016/j.apcatb.2018.04.044.

[16]    B.A. Wols, C.H.M. Hofman-Caris, Review of photochemical reaction constants of organic micropollutants required for UV advanced oxidation processes in water, Water Res. (2012). doi:10.1016/j.watres.2012.03.036.

[17]    L.W. Matzek, K.E. Carter, Activated persulfate for organic chemical degradation: A review, Chemosphere. (2016). doi:10.1016/j.chemosphere.2016.02.055.

[18]    W. Da Oh, Z. Dong, T.T. Lim, Generation of sulfate radical through heterogeneous catalysis for organic contaminants removal: Current development, challenges and prospects, Appl. Catal. B Environ. (2016). doi:10.1016/j.apcatb.2016.04.003.

[19]    S. Luo, Z. Wei, D.D. Dionysiou, R. Spinney, W.P. Hu, L. Chai, Z. Yang, T. Ye, R. Xiao, Mechanistic insight into reactivity of sulfate radical with aromatic contaminants through single-electron transfer pathway, Chem. Eng. J. (2017). doi:10.1016/j.cej.2017.06.179.

[20] N.A. Khan, Z. Hasan, S.H. Jhung, Adsorptive removal of hazardous materials using metal-organic frameworks (MOFs): A review, J. Hazard. Mater. (2013). doi:10.1016/j.jhazmat.2012.11.011.

[21] D. Britt, D. Tranchemontagne, O.M. Yaghi, Metal-organic frameworks with high capacity and selectivity for harmful gases, Proc. Natl. Acad. Sci. (2008). doi:10.1073/pnas.0804900105.

[22] J.R. Li, Y. Ma, M.C. McCarthy, J. Sculley, J. Yu, H.K. Jeong, P.B. Balbuena, H.C. Zhou, Carbon dioxide capture-related gas adsorption and separation in metal-organic frameworks, Coord. Chem. Rev. (2011). doi:10.1016/j.ccr.2011.02.012.

[23] K. Sumida, D.L. Rogow, J.A. Mason, T.M. McDonald, E.D. Bloch, Z.R. Herm, T.H. Bae, J.R. Long, Carbon dioxide capture in metal-organic frameworks, Chem. Rev. (2012). doi:10.1021/cr2003272.

[24] L.J. Murray, M. Dincă, J.R. Long, Hydrogen storage in metal–organic frameworks, Chem. Soc. Rev. (2009). doi:10.1109/JPHOTOV.2018.2868021.

[25] H. Wu, Q. Gong, D.H. Olson, J. Li, Commensurate adsorption of hydrocarbons and alcohols in microporous metal organic frameworks, Chem. Rev. (2012). doi:10.1021/cr200216x.

[26] H. Jasuja, J. Zang, D.S. Sholl, K.S. Walton, Rational tuning of water vapor and $CO_2$ adsorption in highly stable Zr-based MOFs, J. Phys. Chem. C. (2012). doi:10.1021/jp308657x.

[27]    P. Horcajada, R. Gref, T. Baati, P.K. Allan, G. Maurin, P. Couvreur, G. Férey, R.E. Morris, C. Serre, Metal-organic frameworks in biomedicine, Chem. Rev. (2012). doi:10.1021/cr200256v.

[28]    A.C. McKinlay, R.E. Morris, P. Horcajada, G. Férey, R. Gref, P. Couvreur, C. Serre, BioMOFs: Metal-organic frameworks for biological and medical applications, Angew. Chemie - Int. Ed. (2010). doi:10.1002/anie.201000048.

[29]    M. Kurmoo, Magnetic metal-organic frameworks, Chem. Soc. Rev. (2009). doi:10.1039/b804757j.

[30]    T. Uemura, N. Yanai, S. Kitagawa, Polymerization reactions in porous coordination polymers, Chem. Soc. Rev. (2009). doi:10.1039/b802583p.

[31]    J. Lee, O.K. Farha, J. Roberts, K.A. Scheidt, S.T. Nguyen, J.T. Hupp, Metal-organic framework materials as catalysts, Chem. Soc. Rev. (2009). doi:10.1039/b807080f.

[32]    S. Yuan, L. Feng, K. Wang, J. Pang, M. Bosch, C. Lollar, Y. Sun, J. Qin, X. Yang, P. Zhang, Q. Wang, L. Zou, Y. Zhang, L. Zhang, Y. Fang, J. Li, H.C. Zhou, Stable Metal–Organic Frameworks: Design, Synthesis, and Applications, Adv. Mater. (2018). doi:10.1002/adma.201704303.

[33]    E. Haque, J.E. Lee, I.T. Jang, Y.K. Hwang, J.S. Chang, J. Jegal, S.H. Jhung, Adsorptive removal of methyl orange from aqueous solution with metal-organic frameworks, porous chromium-benzenedicarboxylates, J. Hazard. Mater. (2010). doi:10.1016/j.jhazmat.2010.05.047.

[34] F. Leng, W. Wang, X.J. Zhao, X.L. Hu, Y.F. Li, Adsorption interaction between a metal-organic framework of chromium-benzenedicarboxylates and uranine in aqueous solution, Colloids Surfaces A Physicochem. Eng. Asp. (2014). doi:10.1016/j.colsurfa.2013.08.074.

[35] C. Chen, M. Zhang, Q. Guan, W. Li, Kinetic and thermodynamic studies on the adsorption of xylenol orange onto MIL-101(Cr), Chem. Eng. J. (2012). doi:10.1016/j.cej.2011.12.021.

[36] Z. Hasan, J. Jeon, S.H. Jhung, Adsorptive removal of naproxen and clofibric acid from water using metal-organic frameworks, J. Hazard. Mater. (2012). doi:10.1016/j.jhazmat.2012.01.005.

[37] E.Y. Park, Z. Hasan, N.A. Khan, S.H. Jhung, Adsorptive removal of bisphenol-A from water with a metal-organic framework, a porous chromium-benzenedicarboxylate., J. Nanosci. Nanotechnol. (2013).

[38] E.T. Kimura, D.M. Ebert, P.W. Dodge, Acute toxicity and limits of solvent residue for sixteen organic solvents, Toxicol. Appl. Pharmacol. (1971). doi:10.1016/0041-008X(71)90301-2.

[39] A. Gałuszka, Z. Migaszewski, J. Namieśnik, The 12 principles of green analytical chemistry and the SIGNIFICANCE mnemonic of green analytical practices, TrAC - Trends Anal. Chem. (2013). doi:10.1016/j.trac.2013.04.010.

[40] F.X. Qin, S.Y. Jia, Y. Liu, H.Y. Li, S.H. Wu, Adsorptive removal of bisphenol A from aqueous solution using metal-organic frameworks, Desalin. Water Treat. (2015). doi:10.1080/19443994.2014.883331.

[41] Z. Hasan, E.J. Choi, S.H. Jhung, Adsorption of naproxen and clofibric acid over a metal–organic framework MIL-101 functionalized with acidic and basic groups, Chem. Eng. J. (2013). doi:10.1016/j.cej.2013.01.002.

[42] X. Luo, T. Shen, L. Ding, W. Zhong, J. Luo, S. Luo, Novel thymine-functionalized MIL-101 prepared by post-synthesis and enhanced removal of Hg 2+ from water, J. Hazard. Mater. (2016). doi:10.1016/j.jhazmat.2015.12.034.

[43] T.L. Litovitz, W. Klein-Schwartz, E.M. Caravati, J. Youniss, B. Crouch, S. Lee, 1998 Annual Report of the American Association of Poison Control Centers Toxic Exposure Surveillance System, Am. J. Emerg. Med. (1999). doi:10.1016/S0735-6757(99)90254-1.

[44] M. Özcan, A. Allahbeickaraghi, M. Dündar, Possible hazardous effects of hydrofluoric acid and recommendations for treatment approach: A review, Clin. Oral Investig. (2012). doi:10.1007/s00784-011-0636-6.

[45] A.D. Paine, A. J., Dayan, Mechanisms of chromium toxicity, carcinogenicity and allergenicity: Review of the literature from 1985 to 2000, Hum. Exp. Toxicol. (2001). doi:10.1191/096032701682693062.

[46] E. Haque, J.W. Jun, S.H. Jhung, Adsorptive removal of methyl orange and methylene blue from aqueous solution with a metal-organic framework material, iron terephthalate (MOF-235), J. Hazard. Mater. (2011). doi:10.1016/j.jhazmat.2010.09.035.

[47] M. Tong, D. Liu, Q. Yang, S. Devautour-Vinot, G. Maurin, C. Zhong, Influence of framework metal ions on the dye capture behavior of MIL-100 (Fe, Cr) MOF

type solids, J. Mater. Chem. A. (2013). doi:10.1039/c3ta11807j.

[48]    S.H. Huo, X.P. Yan, Metal-organic framework MIL-100(Fe) for the adsorption of malachite green from aqueous solution, J. Mater. Chem. (2012). doi:10.1039/c2jm16513a.

[49]    B. Liu, F. Yang, Y. Zou, Y. Peng, Adsorption of phenol and p -nitrophenol from aqueous solutions on metal-organic frameworks: Effect of hydrogen bonding, J. Chem. Eng. Data. (2014). doi:10.1021/je4010239.

[50]    E. Haque, V. Lo, A.I. Minett, A.T. Harris, T.L. Church, Dichotomous adsorption behaviour of dyes on an amino-functionalised metal-organic framework, amino-MIL-101(Al), J. Mater. Chem. A. (2014). doi:10.1039/c3ta13589f.

[51]    N.A. Khan, B.K. Jung, Z. Hasan, S.H. Jhung, Adsorption and removal of phthalic acid and diethyl phthalate from water with zeolitic imidazolate and metal-organic frameworks, J. Hazard. Mater. (2015). doi:10.1016/j.jhazmat.2014.03.047.

[52]    M.R. Azhar, H.R. Abid, V. Periasamy, H. Sun, M.O. Tade, S. Wang, Adsorptive removal of antibiotic sulfonamide by UiO-66 and ZIF-67 for wastewater treatment, J. Colloid Interface Sci. (2017). doi:10.1016/j.jcis.2017.04.001.

[53]    C.O. Audu, H.G.T. Nguyen, C.-Y. Chang, M.J. Katz, L. Mao, O. Farha, J.T. Hupp, S. Nguyen, Electronic Supplementary Material (ESI) for The dual capture of As V and As III by UiO-66 and analogues, Chem. Sci. (2016). doi:10.1039/C6SC00490C.

[54]    K.A. Cychosz, A.G. Wong-Foy, A.J. Matzger, Liquid phase adsorption by

microporous coordination polymers: Removal of organosulfur compounds, J. Am. Chem. Soc. (2008). doi:10.1021/ja802121u.

[55] S. Lin, Z. Song, G. Che, A. Ren, P. Li, C. Liu, J. Zhang, Adsorption behavior of metal-organic frameworks for methylene blue from aqueous solution, Microporous Mesoporous Mater. (2014). doi:10.1016/j.micromeso.2014.03.004.

[56] F. Zou, R. Yu, R. Li, W. Li, Microwave-assisted synthesis of HKUST-1 and functionalized HKUST-1-@H 3PW12O40: Selective adsorption of heavy metal ions in water analyzed with synchrotron radiation, ChemPhysChem. (2013). doi:10.1002/cphc.201300215.

[57] G.F. Nordberg, B.A. Fowler, M. Nordberg, L.T. Friberg, Handbook on the Toxicology of Metals, 2007. doi:10.1016/B978-0-12-369413-3.X5052-6.

[58] N.S. Aston, N. Watt, I.E. Morton, M.S. Tanner, G.S. Evans, Copper toxicity affects proliferation and viability of human hepatoma cells (HepG2 line), Hum. Exp. Toxicol. (2003). doi:10.1191/0960327006788159963.

[59] M. Sarker, S. Shin, J.H. Jeong, S.H. Jhung, Mesoporous metal-organic framework PCN-222(Fe): Promising adsorbent for removal of big anionic and cationic dyes from water, Chem. Eng. J. 371 (2019) 252–259. doi:10.1016/J.CEJ.2019.04.039.

[60] F. Liu, W. Xiong, X. Feng, G. Cheng, L. Shi, D. Chen, Y. Zhang, Highly recyclable cysteamine-modified acid-resistant MOFs for enhancing Hg (II) removal from water, Environ. Technol. (United Kingdom). (2019). doi:10.1080/09593330.2019.1598504.

[61]  Z.Q. Li, J.C. Yang, K.W. Sui, N. Yin, Facile synthesis of metal-organic framework MOF-808 for arsenic removal, Mater. Lett. (2015). doi:10.1016/j.matlet.2015.08.004.

[62]  T.A. Vu, G.H. Le, C.D. Dao, L.Q. Dang, K.T. Nguyen, Q.K. Nguyen, P.T. Dang, H.T.K. Tran, Q.T. Duong, T. V. Nguyen, G.D. Lee, Arsenic removal from aqueous solutions by adsorption using novel MIL-53(Fe) as a highly efficient adsorbent, RSC Adv. (2015). doi:10.1039/c4ra12326c.

[63]  J. Li, Y.N. Wu, Z. Li, M. Zhu, F. Li, Characteristics of arsenate removal from water by metal-organic frameworks (MOFs), Water Sci. Technol. (2014). doi:10.2166/wst.2014.390.

[64]  J.M. Rivera, S. Rincón, C. Ben Youssef, A. Zepeda, Highly Efficient Adsorption of Aqueous Pb(II) with Mesoporous Metal-Organic Framework-5: An Equilibrium and Kinetic Study, J. Nanomater. (2016). doi:10.1155/2016/8095737.

[65]  J.J. Du, Y.P. Yuan, J.X. Sun, F.M. Peng, X. Jiang, L.G. Qiu, A.J. Xie, Y.H. Shen, J.F. Zhu, New photocatalysts based on MIL-53 metal-organic frameworks for the decolorization of methylene blue dye, J. Hazard. Mater. (2011). doi:10.1016/j.jhazmat.2011.04.029.

[66]  H. Hu, H. Zhang, Y. Chen, Y. Chen, L. Zhuang, H. Ou, Enhanced photocatalysis degradation of organophosphorus flame retardant using MIL-101(Fe)/persulfate: Effect of irradiation wavelength and real water matrixes, Chem. Eng. J. 368 (2019) 273–284. doi:10.1016/j.cej.2019.02.190.

[67]  H. Lv, H. Zhao, T. Cao, L. Qian, Y. Wang, G. Zhao, Efficient degradation of high concentration azo-dye wastewater by heterogeneous Fenton process with iron-based metal-organic framework, J. Mol. Catal. A Chem. (2015). doi:10.1016/j.molcata.2015.02.007.

[68]  M.J. Duan, Z. yu Guan, Y.W. Ma, J.Q. Wan, Y. Wang, Y.F. Qu, A novel catalyst of MIL-101(Fe) doped with Co and Cu as persulfate activator: synthesis, characterization, and catalytic performance, Chem. Pap. (2018). doi:10.1007/s11696-017-0276-7.

[69]  J. Tang, J. Wang, Fe-based metal organic framework/graphene oxide composite as an efficient catalyst for Fenton-like degradation of methyl orange, RSC Adv. (2017). doi:10.1039/c7ra10145g.

[70]  K.Y.A. Lin, F.K. Hsu, Magnetic iron/carbon nanorods derived from a metal organic framework as an efficient heterogeneous catalyst for the chemical oxidation process in water, RSC Adv. (2015). doi:10.1039/c5ra06043e.

[71]  J. Wang, J. Wan, Y. Ma, Y. Wang, M. Pu, Z. Guan, Metal-organic frameworks MIL-88A with suitable synthesis conditions and optimal dosage for effective catalytic degradation of Orange G through persulfate activation, RSC Adv. (2016). doi:10.1039/C6RA24429G.

[72]  K.Y. Andrew Lin, H.A. Chang, C.J. Hsu, Iron-based metal organic framework, MIL-88A, as a heterogeneous persulfate catalyst for decolorization of Rhodamine B in water, RSC Adv. (2015). doi:10.1039/c5ra01447f.

[73]  T. Chalati, P. Horcajada, R. Gref, P. Couvreur, C. Serre, Optimisation of the

synthesis of MOF nanoparticles made of flexible porous iron fumarate MIL-88A, J. Mater. Chem. (2011). doi:10.1039/c0jm03563g.

[74]  A. Ghauch, A. Ammouri, Smart anti-counterfeiting optical system (sacos) for the detection of fraud using advanced spectroscopy-based technique, (2015). https://patents.google.com/patent/EP3216012A2/nl (accessed June 12, 2019).

[75]  A. Baalbaki, N. Zein Eddine, S. Jaber, M. Amasha, A. Ghauch, Rapid quantification of persulfate in aqueous systems using a modified HPLC unit, Talanta. 178 (2018) 237–245. doi:10.1016/j.talanta.2017.09.036.

[76]  O. Tantawi, A. Baalbaki, R. El Asmar, A. Ghauch, A rapid and economical method for the quantification of hydrogen peroxide (H 2 O 2 ) using a modified HPLC apparatus, Sci. Total Environ. (2019). doi:10.1016/j.scitotenv.2018.10.372.

[77]  H. A. Gorrell (2), Classification of Formation Waters Based on Sodium Chloride Content: GEOLOGICAL NOTES, Am. Assoc. Pet. Geol. Bull. (2003). doi:10.1306/0bda5be8-16bd-11d7-8645000102c1865d.

[78]  L. Zhao, Y. Ji, D. Kong, J. Lu, Q. Zhou, X. Yin, Simultaneous removal of bisphenol A and phosphate in zero-valent iron activated persulfate oxidation process, Chem. Eng. J. (2016). doi:10.1016/j.cej.2016.06.016.

[79]  V. Shafirovich, A. Dourandin, W. Huang, N.E. Geacintov, The Carbonate Radical Is a Site-selective Oxidizing Agent of Guanine in Double-stranded Oligonucleotides, J. Biol. Chem. (2001). doi:10.1074/jbc.M101131200.

[80]   J. Fernandez, J. Bandara, A. Lopez, P. Buffat, J. Kiwi, Photoassisted Fenton Degradation of Nonbiodegradable Azo Dye (Orange II) in Fe-Free Solutions Mediated by Cation Transfer Membranes, Langmuir. (2002). doi:10.1021/la980382a.

[81]   M.E. El Haddad, A. Regti, M.R. Laamari, R. Mamouni, N. Saffaj, Use of fenton reagent as advanced oxidative process for removing textile dyes from aqueous solutions, J. Mater. Environ. Sci. (2014).

[82]   H. Liu, T.A. Bruton, F.M. Doyle, D.L. Sedlak, In situ chemical oxidation of contaminated groundwater by persulfate: Decomposition by Fe(III)- and Mn(IV)-containing oxides and aquifer materials, Environ. Sci. Technol. (2014). doi:10.1021/es502056d.

[83]   J.G. Carriazo, E. Guelou, J. Barrault, J.M. Tatibouët, S. Moreno, Catalytic wet peroxide oxidation of phenol over Al-Cu or Al-Fe modified clays, Appl. Clay Sci. (2003). doi:10.1016/S0169-1317(03)00124-8.

**B. Supporting Information: Iron-Based Metal Organic Framework MIL-88-A**

**for the Degradation of Naproxen in Water through Persulfate Activation**

**Rime El Asmar, Abbas Baalbaki, Zahraa Abou Khalil, Antoine Ghauch**
American University of Beirut | Faculty of Arts and Sciences | Department of Chemistry
P.O. Box 11-0236 Riad El Solh – 1107-2020 Beirut – Lebanon

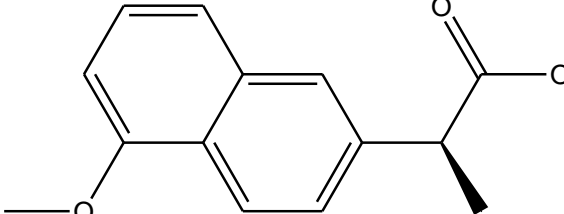**July 12, 2019**
3Pages, 2 Figures, 2Tables

**Table 1S**

**Table 2S** [1]

The 12 principles of green chemistry

| Principle 1 | It is better to prevent waste than to treat or clean up waste after it is formed |
|---|---|
| Principle 2 | Synthetic methods should be designed to maximize the incorporation of all materials used in the process into the final product. |
| Principle 3 | Wherever practicable, synthetic methodologies should be designed to use and generate substances that possess little or no toxicity to human health and the environment |
| Principle 4 | Chemical products should be designed to preserve efficacy of function while reducing toxicity |
| Principle 5 | The use of auxiliary substances (solvents, separation agents, etc.), should be made unnecessary whenever possible and innocuous when used |
| Principle 6 | Energy requirements should be recognized for their environmental and economic impacts and should be minimized |
| Principle 7 | A raw material feedstock should be renewable rather than depleting whenever technically and economically practical. |
| Principle 8 | Unnecessary derivatization (blocking group, protection/deprotection, temporary modification of physical/chemical processes) should be avoided whenever possible |
| Principle 9 | Catalytic reagents (as selective as possible) are superior to stoichiometric reagents |
| Principle 10 | Chemical products should be designed so that at the end of their function they do not persist in the environment and ultimately break down into innocuous degradation products. |
| Principle 11 | Analytical methodologies need to be further developed to allow for real-time in-process monitoring and control prior to the formation of hazardous substances |
| Principle 12 | Substances and the form of a substance used in a chemical process should be chosen so as to minimize the potential for chemical accidents, including releases, explosions and fires |

**Table 2S [1]**

Physical properties of naproxen (NAP)

| Chemical Formula | Chemical structure | Molecular Weight (g.mol-1) | Water solubility | pKa | in water $\lambda$max | Log Kow |
|---|---|---|---|---|---|---|
| $C_{14}H_{14}O_3$ | | 230.26 | 15.9 mg/L (at 25 °C) | 4.15 | 228 | 3.18 |
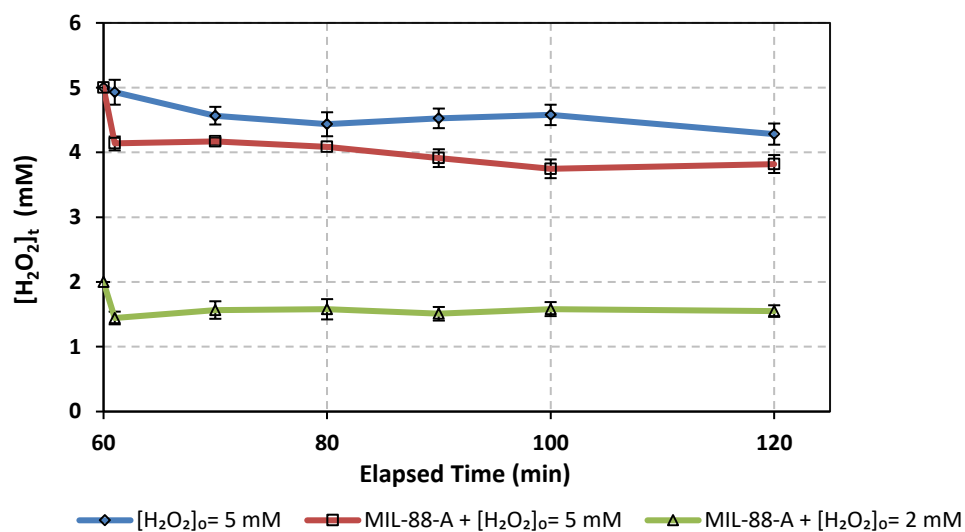


Fig. 1S. [$H_2O_2$] during the reaction time. [NAP]$_0$= 50 mg L$^{-1}$ . [MIL-88-A]$_0$ = 25 mg L$^{-1}$.Error bars are calculated as $\frac{ts}{\sqrt{n}}$, where absent bars fall within the symbols.
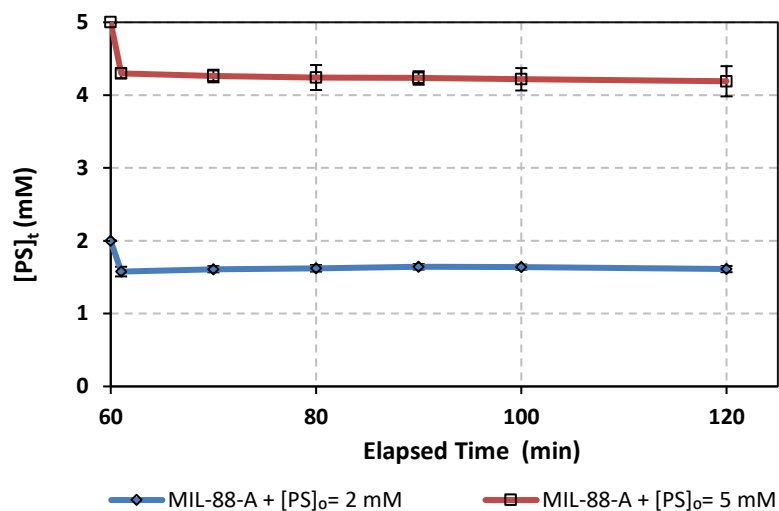
Fig. 2S. [PS] during the reaction time. $[NAP]_0 = 50$ mg $L^{-1}$ . $[MIL\text{-}88\text{-}A]_0 = 25$ mg $L^{-1}$. Error bars are calculated as $\frac{ts}{\sqrt{n}}$, where absent bars fall within the symbols.

References:

[1]    A. Gałuszka, Z. Migaszewski, J. Namieśnik, The 12 principles of green

analytical chemistry and the SIGNIFICANCE mnemonic of green analytical practices,

TrAC - Trends Anal. Chem. (2013). doi:10.1016/j.trac.2013.04.010.

# CHAPTER III

PROJECT 2

## A. A rapid and economical method for the quantification of hydrogen peroxide ($H_2O_2$) using a modified HPLC apparatus

As mentioned in project 1, MIL-88-A was tested for its ability to activate $H_2O_2$ and a comparison between the two systems, MIL-88-A/$H_2O_2$ and MIL-88-A/ PS, was conducted. For this aim, it was crucial to monitor the level of oxidants during the reaction. Most of $H_2O_2$ quantification methods found in literature are time and labor demanding in terms of extensive sample preparation and unautomated measurement taking. Available methods also require expensive catalysts, hazardous reagents, and dedicated devices that are not readily available. Therefore, a rapid and economical novel method for $H_2O_2$ quantification was developed. It is based on using an HPLC-DAD setup on which simple modifications are applied. Such setup is always available in most of the analytical chemistry laboratories and is used in many cases for quantification of organic contaminants in AOPs studies, such as our study. Thus the same sample can be taken and tested for the contaminant and the oxidant minimizing time, labor and material demand.

After applying simple modifications on the instrument configuration, LOQ, LOD, LDR, and cost efficiency of the developed method were evaluated. The method was validated using a well-known titrimetric method tested against several matrices.

The results of this project are presented in the form of a paper published in Science of the Total Environment journal.

Contents lists available at ScienceDirect

# Science of the Total Environment

# A rapid and economical method for the quantification of hydrogen peroxide ($H_2O_2$) using a modified HPLC apparatus

Omar Tantawi, Abbas Baalbaki, Rime El Asmar, Antoine Ghauch *

American University of Beirut, Faculty of Arts and Sciences, Department of Chemistry, P.O. Box 11-0236, Riad El Solh, 1107-2020 Beirut, Lebanon

## HIGHLIGHTS

- An innovative HPLC method is applied for $H_2O_2$ quantification.
- $H_2O_2$ can be automatically determined in aqueous solution.
- The quantification method is very easy, rapid, accurate and reproducible.
- The LOD and LOQ are within oxidant concentration needed for AOP applications.
- Absence of significant interferences is obtained in natural matrices.

## GRAPHICAL ABSTRACT
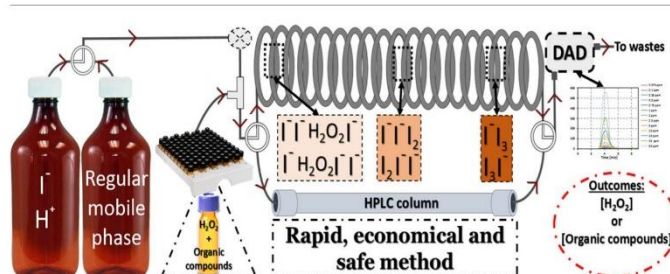


## ARTICLE INFO

## ABSTRACT

$H_2O_2$ is one of the most commonly used oxidants for the degradation of recalcitrant organic contaminants in advanced oxidation processes (AOPs). However, most research aiming to optimize AOPs is missing the monitoring of the remaining $H_2O_2$, an important parameter to assess the efficiency of the process. In this work, a novel method for [$H_2O_2$] quantification was developed using simple modifications of an HPLC-DAD setup that is available in most analytical chemistry laboratories. The modifications include the use of acidified potassium iodide solution as mobile phase and replacing the reverse phase column with a series of capillary columns. This instrument configuration allowed also the quantification of organic contaminants using the same $H_2O_2$ containing sample. The method's LOD and LOQ were calculated to be as low as $8.29 \times 10^{-4}$ mM and $2.76 \times 10^{-3}$ mM, respectively with an LDR range of 0.01–150 mM. The cost per analysis ranged between 0.8 and 1.8 USD cents depending on the concentration tested. This analytical method was validated by a statistical comparison to a well-known titrimetric method that is commonly used for $H_2O_2$ quantification. It was also tested using standards prepared in natural matrices such as spring and seawater, and in media containing high concentration of several spectator species such as chlorides, bicarbonates, humic acids, fumaric acids and micro pollutants. The method showed excellent robustness by maintaining high regression coefficient and excellent sensitivity in all calibration curves regardless of the matrix content.

© 2018 Elsevier B.V. All rights reserved.

# 1. Introduction

## 1.1. Hydrogen peroxide ($H_2O_2$)

$H_2O_2$ is a widely used reducing and oxidizing agent (Huling and Pivetz, 2006). In addition, it is commonly used as an oxidant in the industry and research since its final byproduct is water (Sheldon, 1994). $H_2O_2$ has a relatively high oxidation/reduction potential (ORP) of 1.8 V (Huling and Pivetz, 2006). Several radicals are produced upon $H_2O_2$ activation, of which hydroxyl radicals (HRs), (OH•), are the most prominent (Buxton et al., 1988; Chen et al., 2015; Collivignarelli et al., 2017; Wang and Xu, 2012). HRs' ORP is pH dependent and is higher in acidic media (2.7 V) than in neutral ones (1.8 V) (Buxton et al., 1988). Therefore, HRs are excellent oxidizers for almost all organic contaminants and thus $H_2O_2$ is widely used in AOPs (Passananti et al., 2014; Wang and Xu, 2012). For the abovementioned reasons, it is very important to find innovative and affordable methods for the quantification of $H_2O_2$ in a laboratory or industrial environment.

## 1.2. Overview on $H_2O_2$ quantification methods

Most $H_2O_2$ quantification methods mentioned in literature are either labor demanding and/or require advanced analytical setups. Table 1 summarizes [$H_2O_2$] quantification techniques available in the literature, presenting the advantages and drawbacks in comparison to the proposed method.

All of the abovementioned techniques require extensive sample preparation, expensive catalysts, hazardous reagents and dedicated measurement devices that are not readily available and most importantly not connected to an autosampler. In this work, the use of a simple modification to an HPLC apparatus with environmentally non-hazardous chemicals to quantify $H_2O_2$ at relevant concentrations was accomplished in compliance to 9 of the 12 green chemistry principles (Table 1S) (Gałuszka et al., 2013); therefore minimizing time, labor, and material demand.

# 2. Materials and methods

## 2.1. Reagents

$H_2O_2$ standards were prepared from a 30% (w/w) stabilized analytical grade reagent (Sigma-Aldrich, Germany). The HPLC mobile phase was made using potassium iodide (KI) (99.0–100.5%), 85% (w/w) orthophosphoric acid ($H_3PO_4$), and sodium bicarbonate (NaHCO$_3$) (Sigma Aldrich, Germany). Sodium hydroxide (NaOH) (Himedia, India), sodium phosphate monobasic (NaH$_2$PO$_4$), sodium phosphate dibasic (Na$_2$HPO$_4$), and phosphoric acid ($H_3PO_4$) (Sigma Aldrich, Germany) were used to adjust the pH whenever needed. Sodium chloride (NaCl) (Fisher Chemical, UK), technical grade humic acid sodium salt, sodium bicarbonate (NaHCO$_3$) (Sigma Aldrich, Germany) and fumaric acid (Sigma Aldrich, Switzerland) were used to study spectator species effect. Analytical grade starch, sodium thiosulfate, sodium bicarbonate, ammonium molybdate, and sulfuric acid were used to validate the method (Sigma Aldrich, USA). Analytical grade (≥99.00% assay) ketoprofen ($C_{16}H_{14}O_3$), chloramphenicol ($C_{11}H_{12}Cl_2N_2O_5$) (Sigma Aldrich, China), theophylline ($C_7H_8N_4O_2$) and ferrous chloride tetrahydrate (Fluka, Switzerland) were all used to study AOPs application. All water used was of a Millipore DI grade.

## 2.2. Detection setup

For the quantification of $H_2O_2$, an HPLC: Agilent 1100 series was used. The latter is equipped with a quaternary pump, a vacuum degasser, an autosampler compartment maintained at 4 °C, capillary columns connected in series kept at room temperature (20–25 °C) and a DAD (Fig. 1, Fig. 2S and Table 9S).

## 2.3. Standards and mobile phase preparation

To prepare the HPLC mobile phase, 5 g of NaHCO$_3$ were first dissolved in 1000 mL of DI water to remove dissolved oxygen. 6.64 g of potassium iodide and 5 mL of phosphoric acid were then added to 500 mL of the above solution and stirred until complete dissolution. The remaining 500 mL were later added to reach a total volume of 1 L. Afterwards, this solution was ultrasonicated for 60 min. The solution's pH was then measured and adjusted to a value between 3 and 4 by adding few drops of phosphoric acid. The prepared mobile phase was stored in an airtight amber bottle to prevent the light-catalyzed oxidation of I$^-$ into I$_2$ and was always discarded after a maximum period of one week from the preparation date.

To prepare the $H_2O_2$ standards, the stock solution was diluted using calibrated and certified micropipettes; 10 mL of each standard were prepared out of which 2 mL were transferred into an HPLC vial. Standards were discarded after a maximum period of three days.

## 2.4. Theory and method concept

In this paper, a novel analytical technique was developed using an HPLC coupled to bypass capillary columns and a DAD in resemblance to flow injection/spectroscopy to quantify $H_2O_2$ in water. The mobile phase used is concentrated acidified potassium iodide solution (pH ≈ 3 to 4, [KI] = 40 mM) that acts on rapidly reducing the $H_2O_2$ present in the sample. I$_2$ suspension is produced in the capillary columns as a result of a reaction between $H_2O_2$ and I$^-$. I$_2$ then reacts with I$^-$ present in excess in the medium to yield Triiodide anion (I$_3^-$), which has a $\lambda_{max}$ of 352 nm, a wavelength at which most common emerging organic pollutants don't absorb. This work is based on a study previously done by our research group for the quantification of another oxidant, sodium persulfate (Baalbaki et al., 2018). The method was amended accordingly in order to achieve optimum conditions for $H_2O_2$ quantification. The main modifications were acidifying the mobile phase using orthophosphoric acid and reconfiguring the capillary columns as shown in Fig. 1.

## 2.5. Mobile phase optimization

NaHCO$_3$ solution was first added to the mobile phase to remove dissolved oxygen since the presence of oxygen in water results in I$^-$ oxidation into I$_2$ leading to higher background intensity.

KI was then added and chosen as the main component of the mobile phase due to its properties: it is affordable, highly soluble in water, and characterized by its low toxicity that is limited to irritation by direct skin contact, ingestion or inhalation (MSDS, 2013b). KI is also highly compatible and non-corrosive to HPLC components' material; stainless steel 316 (MSDS, 2013b).

Phosphoric acid was finally added to the mobile phase since $H_2O_2$ ORP is highly dependent on the solution's pH, thus it is necessary to lower the originally neutral pH (6–8) of the KI/NaHCO$_3$ solution. Kessi-rabia et al. (1995) discussed two oxidation pathways according to the following reactions in Eqs. (1) and (2):

$$H_2O_2 + 3I^- \rightarrow I_3^- + 2OH^- \tag{1}$$

$$H_2O_2 + HO_2^- \rightarrow O_2 + OH^- + H_2O \tag{2}$$

The reactions presented in Eqs. (1) and (2) have similar kinetics. However, in acidic conditions (pH = 3–4), Eq. (1) is favored over Eq. (2) which results in maximizing the amount of I$_3^-$ produced; while, the occurrence of Eq. (2) becomes more significant at higher pHs (Kessi-Rabia et al., 1995). This explains the low sensitivity under high pH conditions. Furthermore, HO$_2^-$ which is the basic form of

**Table 1**
Summary of [$H_2O_2$] quantification techniques available in the literature, presenting the advantages and drawbacks in comparison to the proposed method.

| Authors | Analytical technique | Description | Advantages | Drawbacks |
|---|---|---|---|---|
| Hurdis and Romeyn, 1954 | | $H_2O_2$ is titrated with ceric sulfate (cerium (IV) sulfate) | | |
| Huckaba and Keyes, 1948 | Titrimetric | $H_2O_2$ is titrated with potassium permanganate ($KMnO_4$) | Accuracy | – Excessive reagent and labor requirements |
| Graves Group, n.d. | | Iodide is oxidized to iodine by $H_2O_2$ in the presence of an acid and molybdate as a catalyst. Thiosulfate is titrated against Iodide. | | |
| Zhou et al., 2006 | | Monitoring the red-colored product from the reaction between 4-aminoantipyrine and phenol in the presence of peroxidase | | |
| Pick and Keisari, 1980 | | Monitoring the product of the oxidation of phenol red by $H_2O_2$ at its absorbance wavelength (610 nm) | | – Toxicity of organic dyes (phenol) |
| Eisenberg, 1943 | | Monitoring pertitanic acid, yellow in color, produced from the reaction of titanium sulfonate with $H_2O_2$ | | – Expensive; the use of catalysts adds an extra cost |
| Fossati et al., 1983; Fossati and Prencipe, 1982 | Colorimetric | Monitoring quinone-monoimine dye measured at 510 nm upon the reaction of $H_2O_2$ with 3,5-dichloro-2-hydroxybenzenesulfonic acid and 4-aminophenazone Catalyzed by horseradish peroxidase and occurs between $H_2O_2$ | Sensitivity | – Not readily automated; which means that the analysis has to be harmonically timed, when testing large number of samples, otherwise adding significant error to the measurement. |
| Domínguez-Henao et al., 2018 | | Oxidation of iodide by PAA and $H_2O_2$ catalyzed by ammonium molybdate generate colored by-products that can be selectively measured by spectrophotometry | | |
| Lu et al., 2006 | Chemiluminescence | Reactive oxygen species can generate electronically excited products, which emit the weak CL during their decay to the ground state. | Sensitivity over a wide LDR can be coupled to flow injection | – Compounds such as luminol, lucigenin, and peroxylate used for amplifying the CL signal are very expensive and toxic (MSDS, 2013a) – Requires special apparatus |
| Welch et al., 2005 | Electrochemical | Using an edge-plane pyrolytic-graphite electrode (EPPG), a glassy carbon (GC) electrode, and a silver nanoparticle-modified GC electrode | Low LOD | – Requires the use of platinum electrodes which are expensive, easily poisoned, and necessitate regular cleaning via an expensive pre-treatment process |
| Sánchez et al., 1990 | Electrochemical flow injection | Using a horseradish peroxidase-modified amperometric electrode | Can be coupled to flow injection | – Slow electrode kinetics using common electrode materials – Low signal to noise ratio proportional to the flow – Requires high over-potentials reaching a potential wave in the same region as that of other compounds like paracetamol, ascorbate, and urate, and thus causing lower sensitivity and signal interference |
| Albers et al., 2006 | Ratiometric FRET | Changes in [$H_2O_2$] can be detected by measuring the ratio of blue (absence of $H_2O_2$) to green (in presence of $H_2O_2$) fluorescence intensities. | Adaptable for biological and biomedical research | – Complex: requires specialized apparatus and expertise |
| Gimeno et al., 2015 | | Oxidation of triphenylphosphine (TPP) into triphenylphosphine oxide (TPPO) and by $H_2O_2$ for 2 h | Adapted to bleaching and disinfection kits | – High LOD (30 mg L$^{-1}$) – Time consuming |
| Pinkernell et al., 1997 | | | | – Costly – TPP has low water solubility and is toxic to aquatic life – Requires reverse phase chromatography |
| Steinberg, 2013 | HPLC colorimetric | Reaction of $H_2O_2$ with I$^-$ for 30 min in the presence of ammonium molybdate and vanillic acid at 50 °C to produce iodovanillic acid before running on the HPLC | Acceptable LOD ~ 0.1 μM and strong selectivity | – Converting $H_2O_2$ into an equivalent quantity of acid before using HPLC, is similar to using UV-VIS spectrophotometer in terms of time and labor demand |
| Liu et al., 2003 | | $H_2O_2$ activated by ferrous ions to oxidize sodium salicylate and produce dihydroxybenzoic acids that are separated and detected using HPLC-UV | Adapted for atmospheric quantification of $H_2O_2$ | – Requires reverse phase chromatography |
| Deadman et al., 2017 | | HPLC used to selectively quantify different oxidants. Upon the reaction of $H_2O_2$ with titanium(IV) oxysulfate (TiOSO$_4$), it produces a yellow titanic acid detected using HPLC-DAD at 407 nm | Rapid and selective | – Not automated – HPLC setup isn't sufficient for the reaction to effectively take place – Method is still in development |

73

**Table 1** (*continued*)

| Authors | Analytical technique | Description | Advantages | Drawbacks |
|---|---|---|---|---|
| Huang et al., 2003 | HPLC electrochemical | Electro chemical detection coupled to regular reverse phase chromatography, the sample is dissolved in the mobile phase and injected into the HPLC. | Rapid peak elution | – Yue et al. applied this method on other pharmaceutical product samples and discovered an unidentified peak in the sample matrix co-eluting with the $H_2O_2$ |
| Yue et al., 2009 | HPLC coulometric | Effluent elutes the column into the coulometric detector equipped with palladium reference electrodes and an array of eight porous graphite working electrodes | Adapted for the quantification of $H_2O_2$ in a pharmaceutical excipient cross linked polyvinyl N-pyrrolidone, or PVP | – Complexity of the detector<br>– Extraction procedure had to be developed and followed before the analysis since the initial separation conditions did not sufficiently retain $H_2O_2$ on the column, creating interference from the sample's matrix and low sensitivity due to excessive dilution |
| Tarvin et al., 2010 | HPLC fluorescence electrochemical | $H_2O_2$ participates in the hemin-catalyzed oxidation of *p*-hydroxyphenylacetic acid to yield the fluorescent dimer.<br>$H_2O_2$ also detected based upon its oxidation at a gold working electrode | Trace level quantification | – Not adequate for AOPs, industrial or environmental analysis<br>– Requires a specialized Ion chromatography column |
| Owen et al., 1996 | HPLC colorimetric fluorescence | HPLC configuration with tetrabutylammonium hydroxide as a mobile phase. Degradation of mobile phase by $H_2O_2$ into 2,5-dihydroxybenzoic acid and 2,3-dihydroxybenzoic acid monitored using a complex chromatographic technique | Adapted to microbiology research | – Requires reverse phase chromatography and is complicated to use in the presence of other organic molecules in the sample matrix due to interference and peak overlapping |
| Hamano et al., 1987 | | Fluorescence detection after HPLC separation involving the enzymatic conversion of $H_2O_2$ into formaldehyde by catalase-methanol, followed by the derivatization of formaldehyde with 4-amino-3-penten-2-one | Adapted for beverages | Requires:<br>– Extensive sample preparation<br>– Expensive catalysts<br>– Hazardous reagents<br>– Specialized columns |
| Takahashi et al., 1999 | HPLC electrochemical ion exchange | Electrochemical detector (ECD) for $H_2O_2$ detection by HPLC with a cation-exchange resin gel column | Adapted for food | |
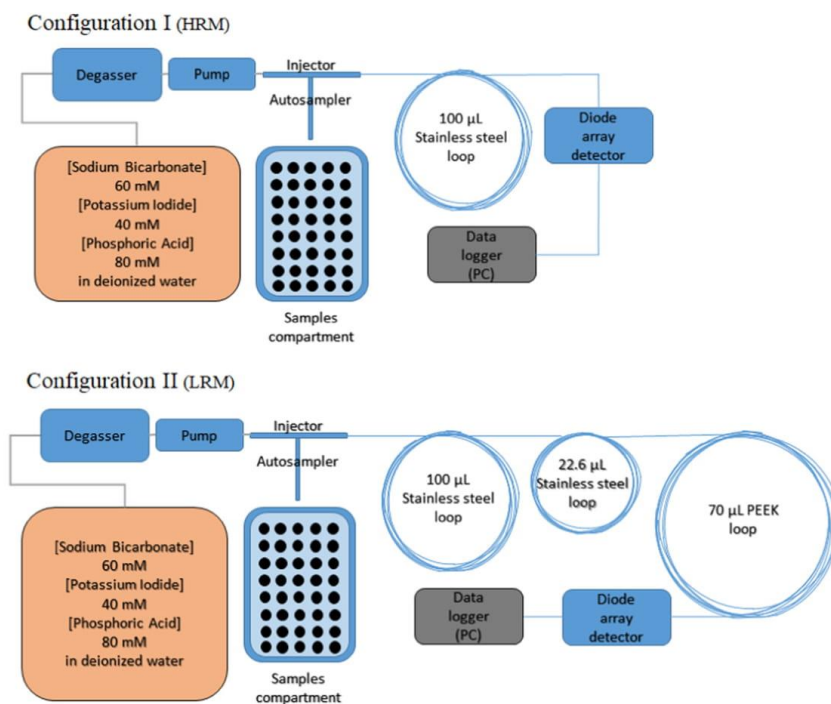


**Fig. 1.** Schematic diagram of the detection setup used for the rapid and automated quantification of $H_2O_2$ in aqueous samples for both high (HRM 0.1–150 mM) and low (LRM 0.01–1.0 mM) concentration ranges.
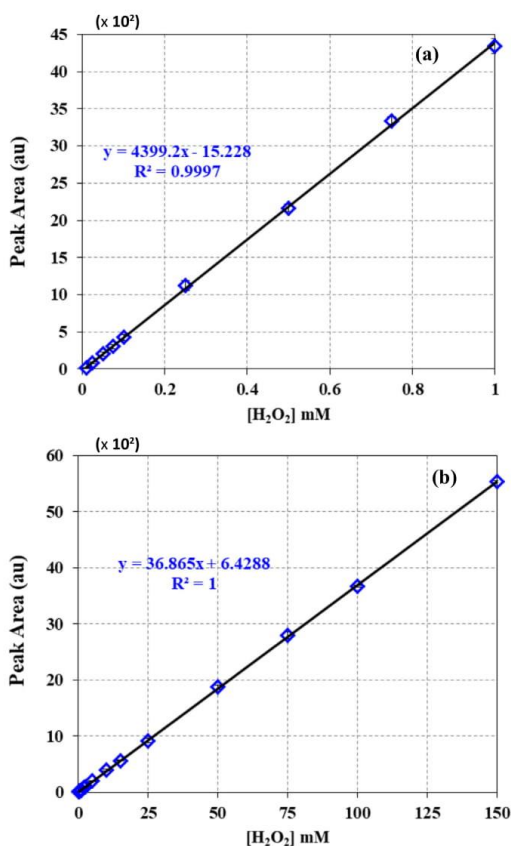
Fig. 2. $H_2O_2$ calibration curves for the repeatability tests in (a) LRM and (b) HRM calibration methods. Vertical bars represent the error on the mean of three injections calculated at 95% confidence interval ($U = K\frac{SD}{\sqrt{n}}$); absent bars fall within symbols.

$H_2O_2$ at pH = 8, reduces $I_2$ to $I^-$ according to Eq. (3):

$$I_2 + HO_2^- \rightarrow O_2 + 2I^- + H^+ \qquad (3)$$

To decrease the pH value, a maximum of 1 wt% phosphoric acid was used which is much lower than the HPLC's materials compatibility. According to Lizlovs (1969), 316 stainless steel has good corrosion resistance to 25 wt% boiling phosphoric acid. To confirm that lower pH will give better results, two experiments were conducted using neutral (pH 6–8) and acidic (pH 3–4) mobile phases. The obtained results showed very poor linearity when using neutral mobile phase $R^2 = 0.766$ and 0.2514 for low range method (LRM) and high range method (HRM) methods, respectively (Fig. 1S). However, using acidic (pH 3–4) mobile phase, the outcomes were much better with $R^2 = 0.9990$ and 0.9997 for LRM and HRM calibration methods, respectively (Fig. 1S).

### 2.6. Method development and optimization

The development of this method was conceptualized after applying the same technique on persulfate oxidant (Baalbaki et al., 2018). Similar method development and optimization approach was adopted. Four different HPLC pump flow rates (0.1, 0.25, 0.5, and 1 mL min$^{-1}$), and injection volumes (5, 20, 50 and 100 μL) were combined to cover the technical capability range of the instrument available and to produce 16 different HPLC methods as listed with their parameters in Tables 2S and 3S. These methods were applied using two different capillary column configurations (Fig. 1). The first consisted of only one column that has a relatively wide diameter and large volume allowing in theory for effective and complete reaction between $H_2O_2$ and KI; the second configuration consisted of the same column connected to two other columns with different diameters and lengths/volumes to allow for better mixing and longer reaction time (Fig. 1 and Table 9S). The first configuration showed better adaptability for the HRM calibration method while the second configuration exhibited higher quality results for the LRM calibration method (Tables 2S and 3S).
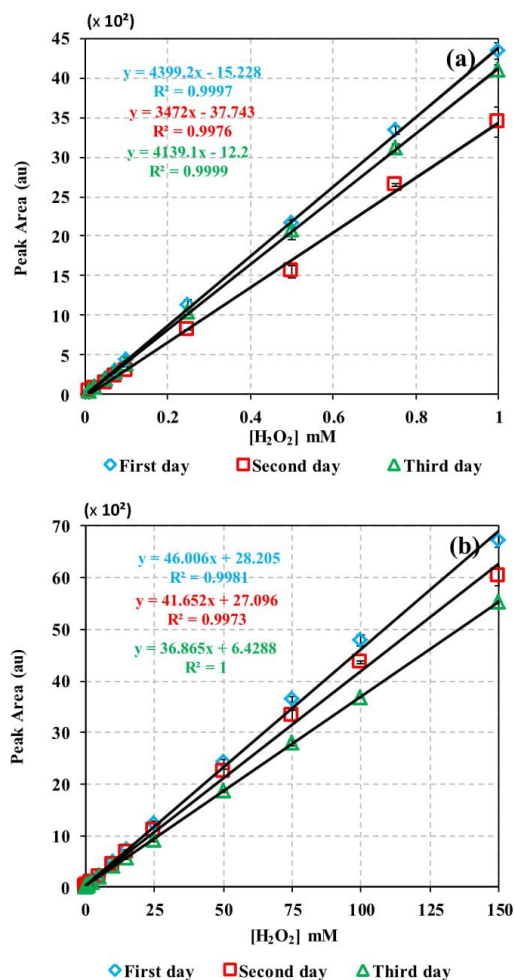


Fig. 3. $H_2O_2$ calibration curves for reproducibility tests in (a) LRM and (b) HRM calibration methods. Vertical bars represent the error on the mean of three injections calculated at 95% confidence interval ($U = K\frac{SD}{\sqrt{n}}$); absent bars fall within symbols.

The results showed that LRM applied to low [$H_2O_2$] requires longer spatial and temporal mixing for high reaction yield which can be achieved by low flow rate and multiple columns configuration. Additionally, an injection volume of 20 μL showed an optimal signal using the second column configuration. Higher injection volumes exhibited peak splitting indicating improper mixing with the mobile phase. On the other hand, HRM calibration method required higher flow rate and shorter column to yield the best results. This can be explained by the less time and space required for the complete mixing and reaction to take place when [$H_2O_2$] is high. The lowest injection volume tested (5 μL) gave the best results since higher volumes led to peak splitting. After each set of analysis, DI was used to flush the system at 1 mL min$^{-1}$ for 15 min in order to clean the HPLC tubes and compartments.

### 2.7. Experimental procedures and conditions

To ensure the robustness of the proposed method, its repeatability, reproducibility, LOD and LOQ were first tested using $H_2O_2$ standards prepared in DI water. The experiments applied and their results are further discussed in Section 3.1. The matrix effect was then investigated in which $H_2O_2$ standards were prepared and tested using solutions that have the following characteristics:

- pH values of 2, 7 and 11 using 10 mM phosphate buffer to investigate the pH effect.
- [NaCl] = 20,000 mg L$^{-1}$
- [HCO$_3^-$] = 150 mg L$^{-1}$
- [Humic acids] = [Fumaric acid] = [Theophylline] = [Chloramphenicol] = [Ketoprofen] = 10 mg L$^{-1}$

The obtained results are further discussed in Sections 3.2 and 3.3. $H_2O_2$ standards were also prepared and tested using natural water

matrices: (sea, spring and waste water) of which their tested water quality parameters and corresponding sampling geographical coordinates are listed in Table 8S.

In order to validate the proposed analytical method, the procedure stated in the eighth edition of the adopted textbook reference in analytical chemistry entitled: *Quantitative Chemical Analysis* (Chapter 4 section 4-3; Comparison of Means with Student's *t*) (Harris, 2010) was adopted. Standards were prepared and tested using LRM, HRM and iodometric titration method which is a common analytical technique for $H_2O_2$ quantification (Graves Group, n.d.; Held et al., 1978; Payne et al., 1961).

## 3. Results and discussion

### 3.1. Quality assurance and method validation

In order to assess $H_2O_2$ quantification procedure under the present testing conditions, method validation and quality assurance methodology was adopted as it is taught in *Quantitative Chemical Analysis* textbook by Harris (2010, chapter 5). Specificity was assured by only accepting capillary column configurations that showed peaks of good quality. Linearity was assured by R$^2$ value ≥ 0.98 (Tables 2S and 3S). Accuracy was assessed by testing certified reference material in the repeatability experiments. Precision (reproducibility), range, limit of detection, limit of quantitation, and robustness were all determined using the procedures described in their subsequent sections.

### 3.1.1. Repeatability

According to the practical guide to analytical method validation by González and Herrador (2007), repeatability test requires testing three different triplicates of each standard on the same day by a single researcher using one HPLC. Thus, three different triplicates of each standard were prepared and tested. The average calibration

**Table 2**
Comparison of LRM and HRM calibration methods results with the iodometric titration method.

| Sample number | Comparison of $H_2O_2$ quantification methods | | | | | |
|---|---|---|---|---|---|---|
| | Theoretical concentration of the sample (mM) | Obtained concentration (mM) | | | Difference ($d_i$) | |
| | | Iodometric titration | LRM | HRM | LRM | HRM |
| 1 | 0.01 | 0.01 | 0.0218 | – | 0.0118 | – |
| 2 | 0.025 | 0.028 | 0.0244 | – | −0.0035 | – |
| 3 | 0.05 | 0.052 | 0.0419 | – | −0.0100 | – |
| 4 | 0.075 | 0.07 | 0.0703 | – | 0.0003 | – |
| 5 | 0.1 | 0.095 | 0.0961 | 0.0814 | 0.0011 | −0.0135 |
| 6 | 0.25 | 0.23 | 0.2562 | 0.2409 | 0.0262 | 0.0109 |
| 7 | 0.5 | 0.43 | 0.5081 | 0.4994 | 0.0781 | 0.0694 |
| 8 | 0.75 | 0.78 | 0.7180 | 0.8599 | −0.0619 | 0.0799 |
| 9 | 1 | 1.1 | 0.9938 | 1.0162 | −0.1061 | −0.0837 |
| 10 | 2 | 1.9 | – | 1.9605 | – | 0.0605 |
| 11 | 2.5 | 2.7 | – | 2.5156 | – | −0.1843 |
| 12 | 5 | 5.1 | – | 5.0296 | – | −0.0703 |
| 13 | 10 | 10.3 | – | 10.3902 | – | 0.0902 |
| 14 | 15 | 15.2 | – | 13.9737 | – | −1.2263 |
| 15 | 25 | 25.1 | – | 25.4776 | – | 0.3776 |
| 16 | 50 | 49.8 | – | 49.5937 | – | −0.2062 |
| 17 | 75 | 74.6 | – | 72.4348 | – | −2.1651 |
| 18 | 100 | 99.2 | – | 97.4534 | – | −1.7465 |
| 19 | 150 | 148.9 | – | 152.635 | – | 3.7350 |

| Statistical parameters | Mean ($\bar{d}$) | Std Dev ($S_d$)* | $t_{calculated}$ | Degrees of freedom (n) | Student value at 95% confidence interval |
|---|---|---|---|---|---|
| LRM | −0.007097848 | 0.052077045 | 0.408885 | 8 | 2.306 |
| HRM | −0.084827223 | 1.29115044 | 0.254451 | 14 | 2.131 |

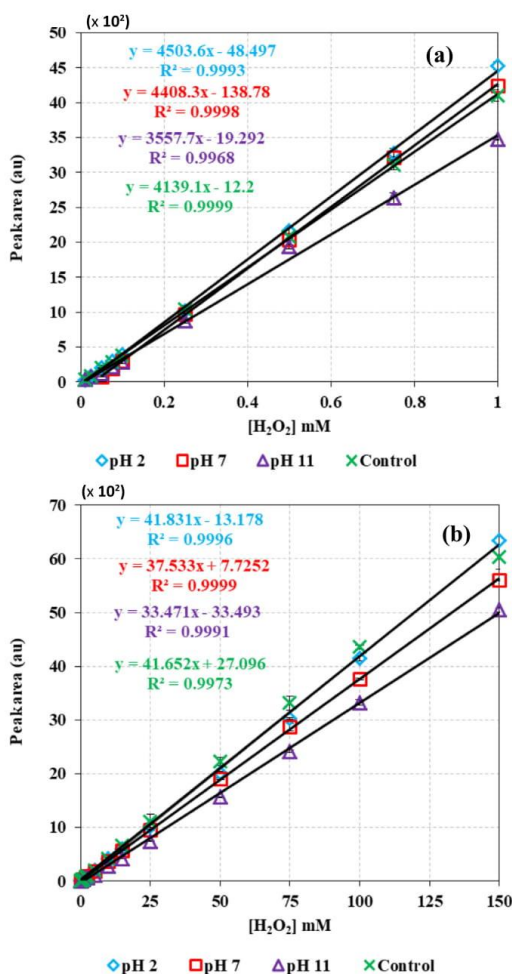$$S_d = \sqrt{\frac{\sum (d_i - \bar{d})^2}{n-1}}.$$

* Standard deviation.

**Fig. 4.** The effect of sample's pH on (a) LRM and (b) HRM calibration methods, $[PB]_0 =$ 10 mmol L$^{-1}$. Vertical bars represent the error on the mean of three injections calculated at 95% confidence interval ($U = K \frac{SD}{\sqrt{n}}$); absent bars fall within symbols.

curves are presented in Fig. 2 with their corresponding error bars. Error bars in all parts of this research paper represent expanded uncertainty and are calculated based on the review paper by Konieczka and Namieśnik (2010). To calculate expanded uncertainty, an uncertainty budget was constructed which only included the major contributing factor: the repeatability of determinations for a true sample, calculated using Eq. (4).

$$U = K \frac{SD}{\sqrt{n}} \qquad (4)$$

where SD is the standard deviation of the triplicates, K is the coverage factor for 95% confidence interval (K = 2) and n is the number of replicates (Konieczka and Namieśnik, 2010). The obtained results showed insignificant variation in the slope while maintaining high regression coefficient ($R^2$). Using Microsoft Excel, the LINEST

function was applied to calculate the slope, the y-intercept, and $R^2$ with all the corresponding statistical parameters including standard deviations on variables as reported in Table 4S. The insignificant values of error bars validate that both, LRM and HRM calibration methods are repeatable (Fig. 2).

### 3.1.2. Reproducibility

Over three days, reproducibility tests were conducted for both LRM and HRM calibration methods covering their corresponding LDR. Each day, fresh mobile phase and standards were prepared, after which three replicates of each standard were analyzed using the same HPLC. Although it is recommended to use a different HPLC instrument each day as recommended by Harris (2010), only one HPLC instrument was available. Calibration curves with their corresponding error bars, calculated using Eq. (4), are presented in Fig. 3. Both LRM and HRM calibration methods showed deviation from day to day. The slope changed from 4399.20 to 4139.10 and from 46.00 to 36.86 for LRM and HRM calibration methods respectively, while maintaining a very good $R^2 > 0.99$ (Table 4S). Thus, it is highly recommended to prepare fresh standards and obtain a new calibration curve whenever using this method since it showed low reproducibility.

### 3.1.3. Limit of detection and quantification

The limit of detection (LOD) and limit of quantification (LOQ) for LRM and HRM calibration methods were determined following the guidelines recommended by Harris (Harris, 2010). The lowest detectable standards in LRM and HRM calibration methods were measured seven times to obtain their average peak area and its corresponding standard deviation. The LOD and LOQ were calculated using Eqs. (5) and (6) to be $8.29 \times 10^{-4}$ mM and $2.76 \times 10^{-3}$ mM for LRM calibration method and $1.62 \times 10^{-2}$ mM and $5.39 \times 10^{-2}$ mM for HRM calibration method, respectively (Table 5S).

$$LOD = \frac{3 \times \text{Standard Deviation}}{\text{Slope}} \qquad (5)$$

$$LOQ = \frac{10 \times \text{Standard Deviation}}{\text{Slope}} \qquad (6)$$

### 3.1.4. Method validation

Method validation was conducted according to the procedure stated in Harris textbook (Chapter 4 section 4-3; Comparison of Means with Student's $t$) (Harris, 2010). Standards were prepared and tested using LRM, HRM and iodometric titration method which is a common analytical technique for $H_2O_2$ quantification (Graves Group, n.d.; Held et al., 1978; Payne et al., 1961). Single measurement of each standard was performed, and the obtained results are presented in Table 2. The collected data was treated, and paired $t$-test was used to compare the results. The difference between the acquired concentrations in LRM and HRM calibration methods versus iodometric titration technique was calculated. Standard deviation, mean and calculated student value of the differences was obtained for both LRM and HRM calibration methods (Table 2).

The calculated Student values ($t_{calculated}$) using Eq. (7) (Harris, 2010) were 0.136 and 0.254 for LRM and HRM calibration methods respectively, both lower than the student value 2.306 (LRM) and 2.131 (HRM) for 8 and 14 degrees of freedom at 95% confidence interval, respectively. Therefore, it can be concluded that the null hypothesis, stating that the results of the tested methods are not significantly different at 95% confidence interval is true. Consequently, there is a 95% confidence that the results obtained from LRM and HRM calibration methods are the true values within the experimental error. This proves that LRM and HRM calibration methods

**Table 3**
LINEST function output for spectator species effect, natural water matrix effect, and pH effect experiments.

| | Experiment | Matrix | m | b | $s_m$ | $s_b$ | $s_y$ | $R^2$ |
|---|---|---|---|---|---|---|---|---|
| LRM | Spectator species effect (ppm or mg L$^{-1}$) | [NaCl] = 20,000 | 3636.15 | −71.79 | 48.19 | 22.10 | 49.32 | 0.9988 |
| | | [HCO$_3^-$] = 150 | 3906.82 | −35.86 | 40.21 | 18.44 | 41.15 | 0.9988 |
| | | [HA] = 10 | 4322.21 | −68.00 | 0.18 | 9.74 | 68.04 | 0.9983 |
| | | [FA] = 10 | 4376.38 | −63.01 | 45.13 | 20.70 | 46.19 | 0.9993 |
| | | [KTP] = 10 | 4257.43 | −54.79 | 35.30 | 16.20 | 36.13 | 0.9995 |
| | | [Theo] = 10 | 4016.68 | −62.01 | 21.16 | 9.71 | 21.66 | 0.9998 |
| | | [CAP] = 10 | 3856.24 | −62.49 | 27.94 | 12.82 | 28.60 | 0.9996 |
| | Natural water matrix effect | Spring water | 3219.74 | −11.52 | 81.83 | 37.54 | 83.75 | 0.9955 |
| | | Sea water | 4015.76 | −25.19 | 42.67 | 19.57 | 43.67 | 0.9992 |
| | pH effect at [PB] = 10 mM | pH = 2 | 4503.64 | −48.50 | 45.94 | 21.07 | 47.02 | 0.9993 |
| | | pH = 7 | 4408.32 | −138.78 | 31.05 | 16.15 | 28.33 | 0.9998 |
| | | pH = 11 | 3557.69 | −19.29 | 75.61 | 34.68 | 77.38 | 0.9968 |
| HRM | Spectator species effect (ppm or mg L$^{-1}$) | [NaCl] = 20,000 | 42.00 | 38.22 | 0.51 | 26.71 | 86.18 | 0.9981 |
| | | [HCO$_3^-$] = 150 | 40.17 | 21.55 | 0.34 | 18.05 | 58.25 | 0.9991 |
| | | [HA] = 10 | 38.77 | 4.12 | 0.18 | 9.74 | 31.42 | 0.9997 |
| | | [FA] = 10 | 38.30 | 7.62 | 0.19 | 10.09 | 32.56 | 0.9997 |
| | | [KTP] = 10 | 41.39 | 21.79 | 0.46 | 24.39 | 78.69 | 0.9984 |
| | | [Theo] = 10 | 39.90 | −1.10 | 0.40 | 21.30 | 68.72 | 0.9987 |
| | | [CAP] = 10 | 40.97 | 25.58 | 0.95 | 49.89 | 160.95 | 0.9931 |
| | Natural water matrix effect | Spring water | 37.08 | 59.47 | 0.83 | 43.72 | 141.06 | 0.9935 |
| | | Sea water | 37.08 | 37.05 | 0.36 | 20.24 | 58.72 | 0.9990 |
| | | Waste water | 18.58 | 11.09 | 0.26 | 1.03 | 2.40 | 0.9986 |
| | pH effect at [PB] = 10 mM | pH = 2 | 41.83 | −13.18 | 0.24 | 12.60 | 40.66 | 0.9996 |
| | | pH = 7 | 37.53 | 7.73 | 0.11 | 5.82 | 18.79 | 0.9999 |
| | | pH = 11 | 33.47 | −33.49 | 0.27 | 14.29 | 46.10 | 0.9991 |

m: slope; b: intercept; $s_m$: standard deviation on slope; $s_b$: standard deviation on intercept; $s_y$: standard deviation on y-axis.

are statistically valid in comparison to a commonly used method.

$$t_{calculated} = \frac{\text{Mean} \times n^{1/2}}{\text{Standard Deviation}} \quad (7)$$

Time, labor, and chemicals requirement for LRM and HRM calibration methods were significantly lower than that of the iodometric titration technique. The average time of preparation and analysis per sample was 27 min using the iodometric titration technique while it was only 7.5 min using LRM and HRM calibration methods. Furthermore, LRM and HRM calibration methods allow testing large number of samples without any experimental work (labor) since HPLC instruments are usually equipped with an automated sampler. Additionally, iodometric titration technique requires extra chemicals such as the very hazardous ammonium molybdate (MSDS, 2013c) and sulfuric acid (MSDS, 2013d). Finally, the cost per sample was calculated to be 0.8 and 1.8 USD cents for LRM and HRM calibration methods, respectively which is 600 to 1,300 times cheaper than the cost using the iodometric titration method (around 11 USD per analysis, the detailed cost is further elaborated in Table 6S).

### 3.2. pH effect

As mentioned in section (2.5), H$_2$O$_2$/I$^-$ reaction is highly pH dependent and requires acidic pH. Thus, it is highly important to investigate the effect of the presence of a buffered sample matrix. For this purpose, standards were prepared in a matrix containing 10 mM phosphate buffer (PB) for three designated pH values of 2, 7 and 11 (Fig. 4). The values were chosen to cover a wide range of the matrix's alkalinity/acidity under significant buffer strength. Basic pH matrix showed a slight negative effect on the sensitivity of LRM and HRM calibration methods which is negligible compared to the relatively high signal intensity. Good linearity (R$^2$ > 0.99) was observed for all of the buffered matrices' calibration curves; a slight decrease in the slope was observed as the pH increased indicating lower sensitivity and vice versa. The slopes of the calibration curves increased at pH = 2 by 8.8% and 0.4% and decreased at pH = 11 by 14% and 19.6% for LRM and HRM calibration methods, respectively (Fig. 4 and Table 3). As it can be noticed, the proposed

method is highly resistant to changes in pH and is capable of testing samples having a basic pH although the main reaction in LRM and HRM calibration methods is pH sensitive. This resistance is caused by the high acidity of the mobile phase and the small injection volume. Therefore, the developed method is capable of quantifying H$_2$O$_2$ under a wide range of pHs and buffer strengths. Regardless, it is recommended to prepare the standards in a matrix having a pH value similar to that of the samples to be tested.

### 3.3. The effect of spectator species

It is important to consider the effect of common ions, organic and inorganic compounds in the matrix of samples tested. For this purpose, standards were prepared in aqueous matrices having high concentration of spectator species to ensure that there is no interference due to the presence of naturally encountered species; which usually exist at much lower concentrations. Additives tested were chlorides (Cl$^-$), bicarbonates (HCO$_3^-$), humic acids (HA), fumaric acid (FA), and organic contaminants (OCs). The results showed minimal effect on the linearity and slopes of their respective calibration curves (Fig. 5, Tables 3 and 7S). The standards' variation from the control calibration curve is within the experimental error of the reproducibility tests (Fig. 5). The choice of species tested and their concentrations is discussed thereafter.

The effect of NaCl, which is known to boost the decomposition of H$_2$O$_2$ was tested (De Laat et al., 2004; Liao et al., 2001). The standards were prepared in a matrix having [NaCl] = 20,000 mg L$^{-1}$, which is classified as highly saline water according to the Food and Agriculture Organization of the United Nations (FAO) (Rhoades et al., 1992). Additionally, it was important to investigate the effect of HCO$_3^-$ since Richardson et al. (2000) reported that it could work as an activator of H$_2$O$_2$ tested on sulfides degradation. Moreover, [HCO$_3^-$], which is the dissolved form of carbon dioxide in water, is present in most water matrices from atmospheric CO$_2$. Therefore, [HCO$_3^-$] = 150 mg L$^{-1}$ was used in the standards' matrices which was later tested using LRM and HRM calibration methods. Furthermore, HA and FA are organic substances that originate from decaying organic matter and are present in many natural water matrices (Stevenson, 1994). For this reason, H$_2$O$_2$ standards containing 10 mg L$^{-1}$ of [HA] or [FA] were prepared and
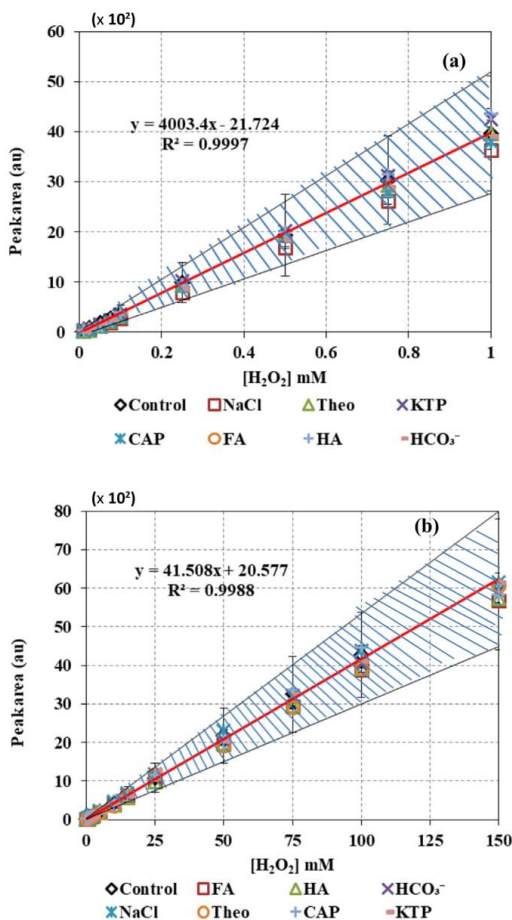
**Fig. 5.** The effect of spectator species on (a) LRM and (b) HRM calibration methods. Vertical bars represent the error on the mean of three injections calculated at 95% confidence interval ($U = K\frac{SD}{\sqrt{n}}$); absent bars fall within symbols. The shaded area reflects the experimental error of the reproducibility tests. (Experimental conditions: [FA], [HA], [Theo], [CAP], [KTP] = 10 mg L$^{-1}$; [NaCl] = 20,000 mg L$^{-1}$, and [HCO$_3^-$] = 150 mg L$^{-1}$).

tested. Finally, more chemically complex OCs that could also be present in the samples were tested such as micro-contaminants that are especially present in water subjected to AOPs treatment. For this purpose, three sets of standards were prepared in matrices each containing 10 mg L$^{-1}$ of three pharmaceutical active ingredients: Chloramphenicol (CAP), Ketoprofen (KTP) or Theophylline (Theo). As mentioned above, no significant effect was observed by all of the aforementioned additives (Fig. 5 and Table 3).

### 3.4. Application of LRM and HRM calibration methods to natural water matrices

To prove the tolerance of LRM and HRM calibration methods to natural water matrices, H$_2$O$_2$ standards were prepared in sea, spring and waste water. The water quality parameters of the used natural water samples are listed in Table 8S with their corresponding sampling geographical coordinates. The obtained results showed that sea and spring water matrices slightly reduced the signal intensity (slope) by 22% and

3%, respectively for LRM and by 11% for HRM without any effect on the linearity coefficient R$^2$ (Fig. 6). On the other hand, peak splitting was observed in LRM when wastewater was used which can be attributed to the reactivity of H$_2$O$_2$ towards organic contaminants present in waste water (COD = 1106 mg L$^{-1}$) (Fig. 6a). When waste water matrix was tested using HRM calibration method, acceptable linearity (R$^2$ > 0.99) was obtained only for the range of 0.1–10 mM with significant decrease in the slope by 56%; however, at higher concentrations the quality of the obtained peaks significantly degraded (Fig. 6b).

### 3.5. Application of LRM and HRM calibration methods to AOPs research

H$_2$O$_2$ is one of the most commonly used oxidants in AOPs applications. However, most researches that aim at optimizing their applications are missing the monitoring step of the remaining oxidant (H$_2$O$_2$). Such an important factor requires substantial labor and
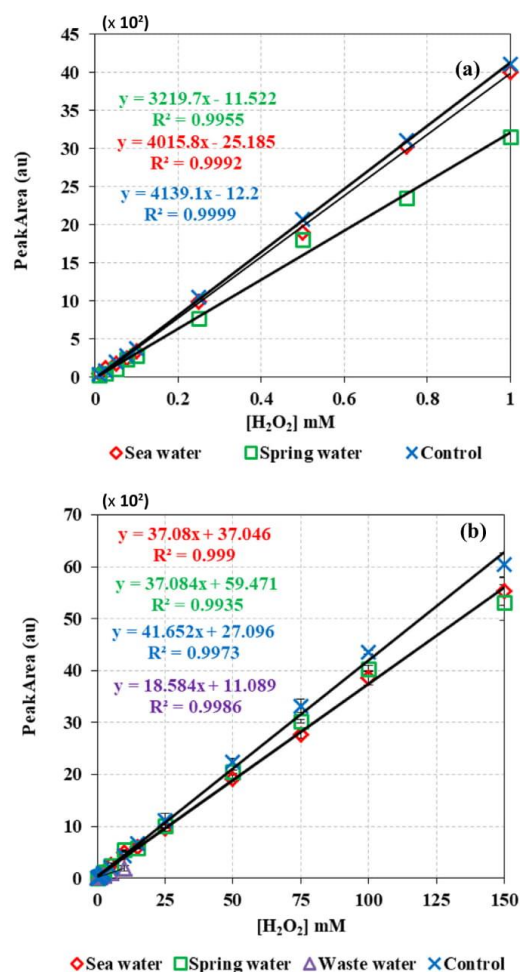


**Fig. 6.** H$_2$O$_2$ calibration curves of natural water matrix effect on (a) LRM and (b) HRM calibration methods. Vertical bars represent the error on the mean of three injections calculated at 95% confidence interval ($U = K\frac{SD}{\sqrt{n}}$); absent bars fall within symbols. (In waste water matrix, HRM was the only applicable method showing an LDR 0.1–10 mM).

time if done using the conventional quantification techniques, while the use of advanced techniques is costly. This also limits the ability of researchers to calculate the percent reaction stoichiometric efficiency (% RSE) and thus determining the sustainability of the oxidant in the reaction medium. For instance, 27 min per sample was the time required by an experienced researcher in our laboratory to quantify $H_2O_2$ using the common iodometric titration method as reported by Prof. David Graves (Graves Group, n.d.). Faster methods require special electrodes or apparatus, not easily automated and expensive. HPLC devices with autosamplers are fundamental for most AOPs applications and are available in most laboratories conducting this type of research. As a part of the research conducted in our laboratory on the sustainability of $H_2O_2$ for the degradation of several organic probes using different activation techniques, LRM and HRM calibration methods were used. Both methods exhibited the desired capacity to quantify the remaining $[H_2O_2]$.

Different $[H_2O_2]_0$ (0.25, 0.5, 1 and 40 mM) were tested on various OCs such as Theo, CAP and KTP. The aim of the aforementioned experiments was to optimize the degradation process of the OCs using UV-254 nm and $Fe^{2+}$ activated $H_2O_2$. LRM and HRM calibration methods were used to determine the remaining $[H_2O_2]$ and to calculate the % RSE which is defined by Eq. (8) (Ghauch et al., 2017).

$$\% \, RSE = \left( \frac{[Probe \, degraded]}{[Oxidant \, consumed]} \right) \times 100 \qquad (8)$$

The obtained results are presented in Fig. S3. The experiments conducted clearly show different patterns in $H_2O_2$ consumption; for instance, in the case of CAP and KTP, $H_2O_2$ consumption persisted even after the complete disappearance of the probe. This indicates that $H_2O_2$ is effective towards the mineralization of the formed degradation byproducts (Fig. 3Sb, 3Sc and 3Sd). On the other hand, a very small amount of $H_2O_2$ was consumed for the complete degradation of Theo in the UV activated system indicating that the degradation process is UV-driven (Fig. 3Sa). Another important factor is the % RSE calculated using LRM and HRM calibration methods which demonstrates a high efficiency in the case of Theo (% RSE = 423%) which is mainly due to the high contribution of the UV radiation through direct photolysis and the low % RSE in the case of CAP and KTP (% RSE = 49, 11 and 3%) caused by the high affinity of $H_2O_2$ towards the degradation byproducts formed in the oxidative reactive medium. Such outcomes will enable us to recommend further investigation on the role of UV in the case of Theo and on the monitoring of the degradation byproducts in the case of CAP and KTP so that to optimize the applied AOP. It is important to report that special technique was improvised to be able to monitor the chemically activated $H_2O_2$. Such monitoring especially in an $Fe^{2+}/H_2O_2$ system is almost impossible using non-automated methods since the activation of $H_2O_2$ will continue even after sampling is done. The improvised technique overcomes this hurdle by directly testing the sample. The technique was applied in the system of $KTP/H_2O_2/Fe^{2+}$ where a sample was periodically withdrawn and injected without delay into the HPLC quantifying almost instantaneously the remaining $[H_2O_2]$ in solution. During the injection process the sample was mixed with large volume of the mobile phase inhibiting any further reaction between the OCs (probe and degradation byproducts) and $H_2O_2$. Another sample was withdrawn at the same time and quenched with large amount of methanol to prevent the further degradation of the OCs caused by the continuous generation of hydroxyl radicals. The [OCs] was later determined using the same HPLC but with a different chromatographic configuration (Fig. 2S).

## 4. Conclusion

$H_2O_2$ is one of the most commonly used oxidants in AOPs and ISCO applications. Several methods have been developed to quantify $H_2O_2$. Even though these methods showed very low LOD and very good adaptability to biological samples, each of these methods exhibits its own drawbacks associated with cost, labor and time requirements. Thus, it is important to have an efficient and effective method for $H_2O_2$ quantification. In this paper a new method is reported helping researchers and industries to accurately quantify $[H_2O_2]$ using an easy, fast, economical and automated way over a wide LDR. This method was also proven to be repeatable, fairly reproducible, and with a great tolerance to naturally occurring spectator species. The method relies on a simple modification of the HPLC instrument available in most analytical chemistry laboratories and uses environmentally nonhazardous chemicals for the quantification of $[H_2O_2]$ in water matrices of environmental interst.

## Appendix A. Supplementary data

Supplementary data to this article can be found online at https://doi.org/10.1016/j.scitotenv.2018.10.372.

## References

Albers, A.E., Okreglak, V.S., Chang, C.J., 2006. A FRET-based approach to ratiometric fluorescence detection of hydrogen peroxide. J. Am. Chem. Soc. 128, 9640–9641. https://doi.org/10.1021/ja063308k.

Baalbaki, A., Zein Eddine, N., Jaber, S., Amasha, M., Ghauch, A., 2018. Rapid quantification of persulfate in aqueous systems using a modified HPLC unit. Talanta 178, 237–245. https://doi.org/10.1016/j.talanta.2017.09.036.

Buxton, G.V., Greenstock, C.L., Helman, W.P., Ross, A.B., 1988. Critical review of rate constants for reactions of hydrated electrons, hydrogen atoms and hydroxyl radicals. J. Phys. Chem. Ref. Data 17, 513–886. https://doi.org/10.1063/1.555805.

Chen, L., Li, X., Zhang, J., Fang, J., Huang, Y., Wang, P., Ma, J., 2015. Production of hydroxyl radical via the activation of hydrogen peroxide by hydroxylamine. Environ. Sci. Technol. 49, 10373–10379. https://doi.org/10.1021/acs.est.5b00483.

Collivignarelli, M.C., Pedrazzani, R., Sorlini, S., Abbà, A., Bertanza, G., 2017. $H_2O_2$-based oxidation processes for the treatment of real high strength aqueous wastes. Sustain 9. https://doi.org/10.3390/su9020244.

De Laat, J., Truong Le, G., Legube, B., 2004. A comparative study of the effects of chloride, sulfate and nitrate ions on the rates of decomposition of $H_2O_2$ and organic compounds by $Fe(II)/H_2O_2$ and $Fe(III)/H_2O_2$. Chemosphere 55, 715–723. https://doi.org/10.1016/j.chemosphere.2003.11.021.

Deadman, B.J., Hellgardt, K., Hii, K.K., 2017. A colorimetric method for rapid and selective quantification of peroxodisulfate, peroxomonosulfate and hydrogen peroxide. React. Chem. Eng. 2, 462–466. https://doi.org/10.1039/C7RE00050B.

Domínguez-Henao, L., Turolla, A., Monticelli, D., Antonelli, M., 2018. Assessment of a colorimetric method for the measurement of low concentrations of peracetic acid and hydrogen peroxide in water. Talanta 183, 209–215. https://doi.org/10.1016/j.talanta.2018.02.078.

Eisenberg, G., 1943. Colorimetric determination of hydrogen peroxide. Ind. Eng. Chem. Anal. Ed. 15, 327–328. https://doi.org/10.1021/i560117a011.

Fossati, P., Prencipe, L., 1982. Serum triglycerides determined colorimetrically with an enzyme that produces hydrogen peroxide. Clin. Chem. 28, 2077–2080.

Fossati, P., Prencipe, L., Berti, G., 1983. Enzymic creatinine assay: a new colorimetric method based on hydrogen peroxide measurement. Clin. Chem. 29, 1494–1496.

Gałuszka, A., Migaszewski, Z., Namieśnik, J., 2013. The 12 principles of green analytical chemistry and the SIGNIFICANCE mnemonic of green analytical practices. TrAC Trends Anal. Chem. 50, 78–84. https://doi.org/10.1016/j.trac.2013.04.010.

Ghauch, A., Baalbaki, A., Amasha, M., El Asmar, R., Tantawi, O., 2017. Contribution of persulfate in UV-254 nm activated systems for complete degradation of chloramphenicol antibiotic in water. Chem. Eng. J. 317, 1012–1025. https://doi.org/10.1016/J.CEJ.2017.02.133.

Gimeno, P., Bousquet, C., Lassu, N., Maggio, A.F., Civade, C., Brenier, C., Lempereur, L., 2015. High-performance liquid chromatography method for the determination of hydrogen peroxide present or released in teeth bleaching kits and hair cosmetic products. J. Pharm. Biomed. Anal. 107, 386–393. https://doi.org/10.1016/j.jpba.2015.01.018.

González, A.G., Herrador, M.Á., 2007. A practical guide to analytical method validation, including measurement uncertainty and accuracy profiles. TrAC Trends Anal. Chem. 26, 227–238. https://doi.org/10.1016/j.trac.2007.01.009.

Graves Group, n.d. Peroxide quantification via iodometric titration — GravesLab [WWW Document]. URL http://www.graveslab.org/lab-resources/procedures/peroxide-quantification-via-iodometric-titration (accessed 1.30.18).

Hamano, T., Mitsuhashi, Y., Yamamoto, S., 1987. Determination of hydrogen peroxide in beverages by high-performance liquid chromatography with fluorescence detection. J. Chromatogr. A 411, 423–429. https://doi.org/10.1016/S0021-9673(00)93994-3.

Harris, D.C., 2010. Quantitative Chemical Analysis. W.H. Freeman & Company https://doi.org/10.1017/CBO9781107415324.004.

Held, A.M., Halko, D.J., Hurst, J.K., 1978. Mechanisms of chlorine oxidation of hydrogen peroxide. J. Am. Chem. Soc. 100, 5732–5740. https://doi.org/10.1021/ja00486a025.

Huang, T., Garceau, M.E., Gao, P., 2003. Liquid chromatographic determination of residual hydrogen peroxide in pharmaceutical excipients using platinum and wired enzyme electrodes. J. Pharm. Biomed. Anal. 31, 1203–1210. https://doi.org/10.1016/S0731-7085(03)00022-0.

Huckaba, C.E., Keyes, F.G., 1948. The accuracy of estimation of hydrogen peroxide by potassium permanganate titration. J. Am. Chem. Soc. 70, 1640–1644. https://doi.org/10.1021/ja01184a098.

Huling, S.G., Pivetz, B.E., 2006. In-situ chemical oxidation. EPA Eng. Issue, 1–60. https://doi.org/epa/600/R-06/072.

Hurdis, E.C., Romeyn, H., 1954. Accuracy of determination of hydrogen peroxide by cerate oxidimetry. Anal. Chem. 26, 320–325. https://doi.org/10.1021/ac60086a016.

Kessi-Rabia, M., Gardès-Albert, M., Julien, R., Ferradini, C., 1995. Effect of pH on the system $I^-/I_3^-/H_2O_2$. Application to iodine hydrolysis. J. Chim. Phys. 92, 1104–1123. https://doi.org/10.1051/jcp/1995921104.

Konieczka, P., Namieśnik, J., 2010. Estimating uncertainty in analytical procedures based on chromatographic techniques. J. Chromatogr. A 1217, 882–891. https://doi.org/10.1016/J.CHROMA.2009.03.078.

Liao, C.-H., Kang, S.-F., Wu, F.-A., 2001. Hydroxyl radical scavenging role of chloride and bicarbonate ions in the $H_2O_2$/UV process. Chemosphere 44, 1193–1200. https://doi.org/10.1016/S0045-6535(00)00278-2.

Liu, J., Steinberg, S.M., Johnson, B.J., 2003. A high performance liquid chromatography method for determination of gas-phase hydrogen peroxide in ambient air using Fenton's chemistry. Chemosphere 52, 815–823. https://doi.org/10.1016/S0045-6535(03)00260-1.

Lizlovs, E.A., 1969. Corrosion behavior of types 304 and 316 stainless steel in hot 85% phosphoric acid. Corrosion 25, 389–393. https://doi.org/10.5006/0010-9312-25.9.389.

Lu, C., Song, G., Lin, J.M., 2006. Reactive oxygen species and their chemiluminescence-detection methods. TrAC — Trends Anal. Chem. 25, 985–995. https://doi.org/10.1016/j.trac.2006.07.007.

MSDS, 2013a. Material Safety Data Sheet Luminol MSDS Section 1: Chemical Product and Company Identification.

MSDS, 2013b. Material Safety Data Sheet Potassium Iodide MSDS Section 1: Chemical Product and Company Identification.

MSDS, 2013c. Material Safety Data Sheet Ammonium Molybdate Tetrahydrate MSDS.

MSDS, 2013d. Material Safety Data Sheet Sulfuric Acid MSDS Section 1: Chemical Product and Company Identification.

Owen, R.W., Wimonwatwatee, T., Spiegelhalder, B., Bartsch, H., 1996. A high performance liquid chromatography system for quantification of hydroxyl radical formation by determination of dihydroxy benzoic acids. Eur. J. Cancer Prev. 5, 233–240. https://doi.org/10.1097/00008469-199608000-00003.

Passananti, M., Temussi, F., Iesce, M.R., Previtera, L., Mailhot, G., Vione, D., Brigante, M., 2014. Photoenhanced transformation of nicotine in aquatic environments:

involvement of naturally occurring radical sources. Water Res. 55, 106–114. https://doi.org/10.1016/j.watres.2014.02.016.

Payne, G.B., Deming, P.H., Williams, P.H., 1961. Reactions of hydrogen peroxide. VII. Alkali-catalyzed epoxidation and oxidation using a nitrile as co-reactant. J. Org. Chem. 26, 659–663. https://doi.org/10.1021/jo01062a004.

Pick, E., Keisari, Y., 1980. A simple colorimetric method for the measurement of hydrogen peroxide produced by cells in culture. J. Immunol. Methods 38, 161–170. https://doi.org/10.1016/0022-1759(80)90340-3.

Pinkernell, U., Effkemann, S., Karst, U., 1997. Simultaneous HPLC determination of peroxyacetic acid and hydrogen peroxide. Anal. Chem. 69, 3623–3627. https://doi.org/10.1021/ac9701750.

Rhoades, J.D., Kandiah, A., Mashali, A.M., 1992. The Use of Saline Waters for Crop Production. Food and Agriculture Organization of the United Nations.

Richardson, D.E., Yao, H., Frank, K.M., Bennett, D.A., 2000. Equilibria, kinetics, and mechanism in the bicarbonate activation of hydrogen peroxide: oxidation of sulfides by peroxymonocarbonate. J. Am. Chem. Soc. 122, 1729–1739. https://doi.org/10.1021/ja9927467.

Sánchez, P.D., Blanco, P.T., Alvarez, J.M.F., Smyth, M.R., O'Kennedy, R., 1990. Flow-injection analysis of hydrogen peroxide using a horseradish peroxidase-modified electrode detection system. Electroanalysis 2, 303–308. https://doi.org/10.1002/elan.1140020407.

Sheldon, R.a., 1994. Catalytic oxidations with hydrogen peroxide as oxidant. Inorg. Chim. Acta https://doi.org/10.1016/0020-1693(93)0378B-E.

Steinberg, S.M., 2013. High-performance liquid chromatography method for determination of hydrogen peroxide in aqueous solution and application to simulated Martian soil and related materials. Environ. Monit. Assess. 185, 3749–3757. https://doi.org/10.1007/s10661-012-2825-4.

Stevenson, F., 1994. Humus chemistry. Genesis. Compos. React. 443. https://doi.org/10.1038/245109a0.

Takahashi, A., Hashimoto, K., Kumazawa, S., Nakayama, T., 1999. Determination of hydrogen peroxide by high-performance liquid chromatography with a cation-exchange resin gel column and electrochemical detector. Anal. Sci. 15 (5), 481–483.

Tarvin, M., McCord, B., Mount, K., Sherlach, K., Miller, M.L., 2010. Optimization of two methods for the analysis of hydrogen peroxide: high performance liquid chromatography with fluorescence detection and high performance liquid chromatography with electrochemical detection in direct current mode. J. Chromatogr. A 1217, 7564–7572. https://doi.org/10.1016/j.chroma.2010.10.022.

Wang, J.L., Xu, L.J., 2012. Advanced oxidation processes for wastewater treatment: formation of hydroxyl radical and application. Crit. Rev. Environ. Sci. Technol. 42, 251–325. https://doi.org/10.1080/10643389.2010.507698.

Welch, C.M., Banks, C.E., Simm, A.O., Compton, R.G., 2005. Silver nanoparticle assemblies supported on glassy-carbon electrodes for the electro-analytical detection of hydrogen peroxide. Anal. Bioanal. Chem. 382, 12–21. https://doi.org/10.1007/s00216-005-3205-5.

Yue, H., Bu, X., Huang, M.H., Young, J., Raglione, T., 2009. Quantitative determination of trace levels of hydrogen peroxide in crospovidone and a pharmaceutical product using high performance liquid chromatography with coulometric detection. Int. J. Pharm., 33–40 https://doi.org/10.1016/j.ijpharm.2009.03.027.

Zhou, B., Wang, J., Guo, Z., Tan, H., Zhu, X., 2006. A simple colorimetric method for determination of hydrogen peroxide in plant tissues. Plant Growth Regul. 49, 113–118. https://doi.org/10.1007/s10725-006-9000-2.

81

**Omar Tantawi, Abbas Baalbaki, Rime El Asmar, Antoine Ghauch***

[1]American University of Beirut | Faculty of Arts and Sciences | Department of Chemistry

P.O. Box 11-0236 Riad El Solh – 1107-2020 Beirut – Lebanon
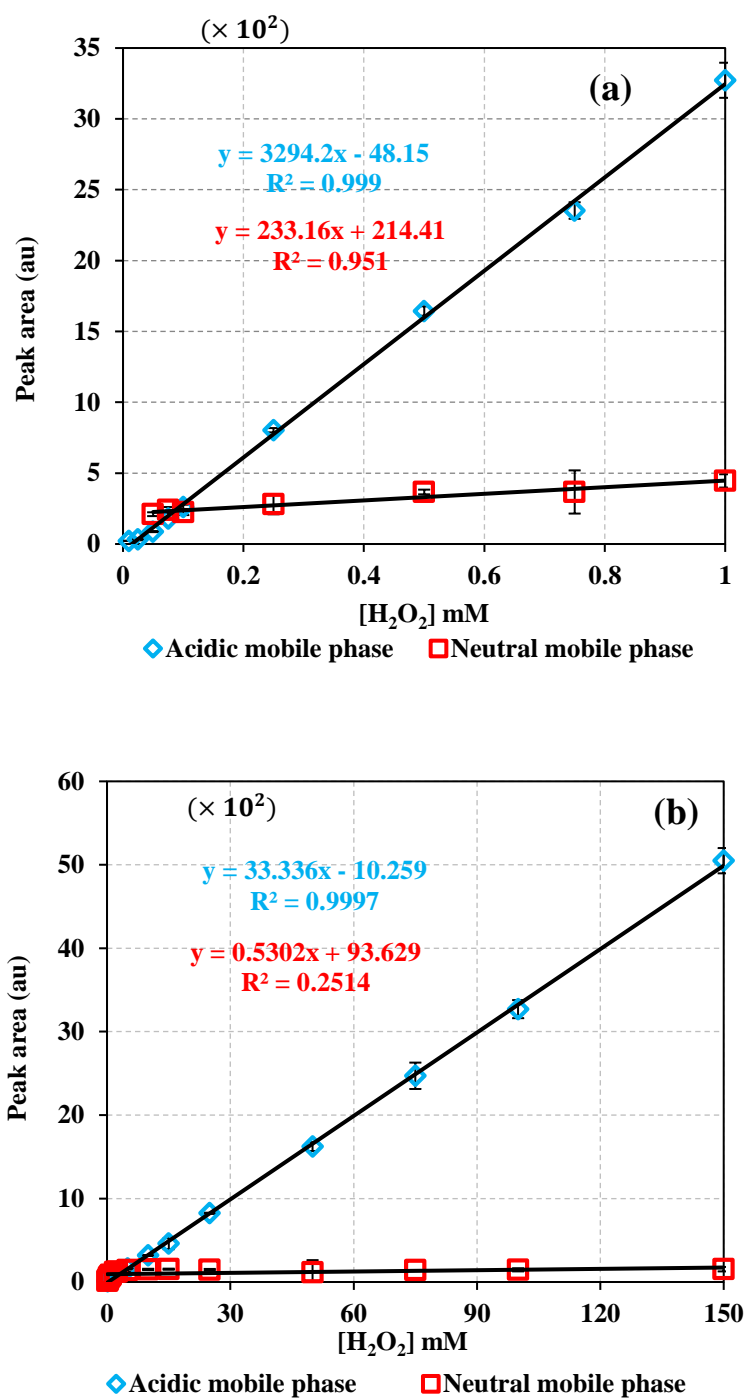
**Fig. 1S.** $H_2O_2$ calibration curves tested using acidic and neutral mobile phases for (a) LRM and (b) HRM calibration methods. Vertical bars represent the expanded uncertainty on the mean of three injections calculated at 95% confidence interval ($U = K\frac{SD}{\sqrt{n}}$); absent bars fall within symbols.

[Sodium Bicarbonate]
60 mM
[Potassium Iodide]
40 mM
[Phosphoric Acid]
80 mM
in deionized water

Mobile phase degasser

Quaternary pump

Sample compartment and injector

Capillary columns

Diode array detector
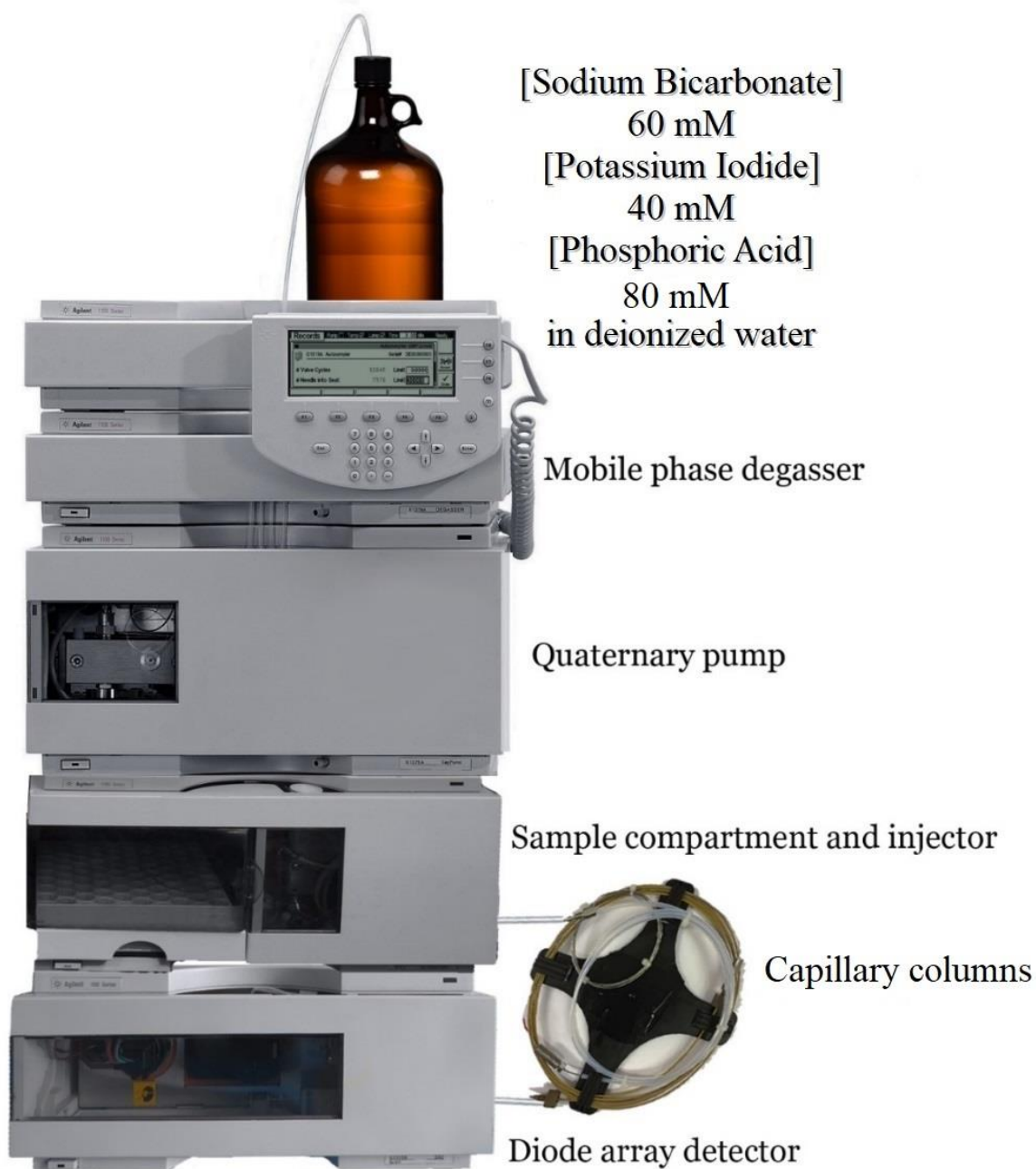
**Fig. 2S.** Modified HPLC setup for $H_2O_2$ quantification
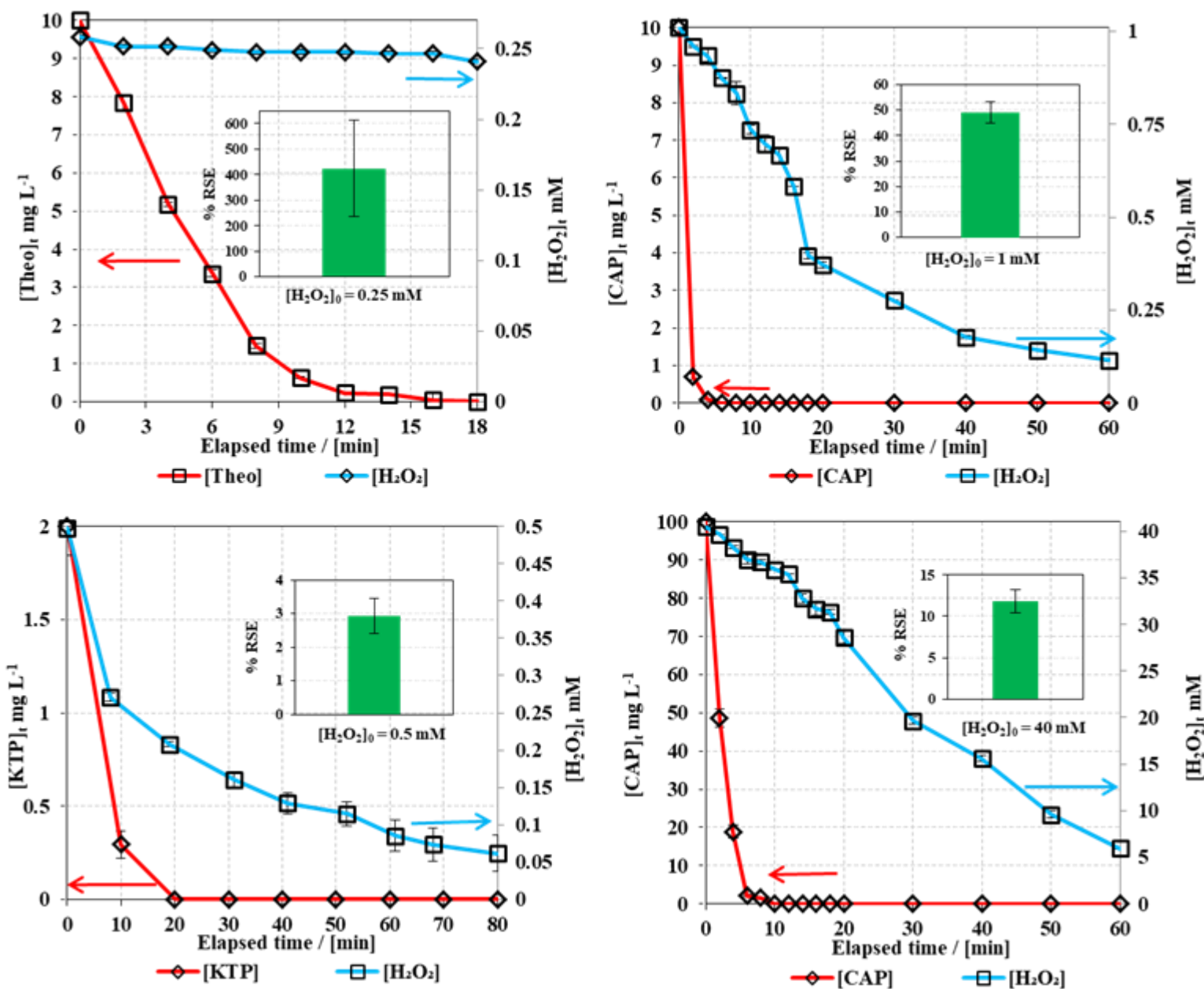
Fig. 3S. Application of LRM (a,b,c) and HRM (d) for $H_2O_2$ quantification in AOPs research. Experimental conditions: (a) $H_2O_2$ $UV_{254}$ activated system, [Theo] = 10 mg L$^{-1}$, [$H_2O_2$] = 0.25 mM; (b) $H_2O_2$ $UV_{254}$ activated system, [CAP] = 10 mg L$^{-1}$, [$H_2O_2$] = 1.0 mM; (c) $H_2O_2$ chemically (Fe$^{2+}$) activated system, [KTP] = 2 mg L$^{-1}$, [$H_2O_2$] = 0.5 mM (d) $H_2O_2$ $UV_{254}$ activated system, [CAP] = 100 mg L$^{-1}$, [$H_2O_2$] = 40 mM

**Table 1S**

The method's compliance to the 12 principles of green analytical chemistry[1].

| Principles | Compliance | Comments on compliance |
|---|---|---|
| Direct analytical techniques should be applied to avoid sample treatment | Yes | No sample treatment required |
| Minimal sample size and minimal number of samples are goals | Yes | The sample volume required for measurement is very low: 5-100 μL |
| In situ measurements should be performed | No | the method can be used for in situ measurement in very limited cases: studying kinetics of a reaction in an HPLC sample vial |
| Integration of analytical processes and operations saves energy and reduces the use of reagents | Yes | Sample storage, treatment, detection, data acquisition and treatment are all done using a single instrument. Energy and reagent use are minimized |
| Automated and miniaturized methods should be selected | Yes | HPLC systems are automated, compact HPLC systems are already available in the market |
| Derivatization should be avoided | Yes | No derivatization is required |
| Generation of a large volume of analytical waste should be avoided and proper management of analytical waste should be provided | Yes | Volume of mobile phase consumed per sample is minimal and ranges between 0.7 and 2 mL, the waste generated has low toxicity and can be recycled. |
| Multi-analyte or multi-parameter methods are preferred versus methods using one analyte at a time | Not applicable | The target analyte of this method is $H_2O_2$ |
| The use of energy should be minimized | Yes | The HPLC used requires a power of 288 Watts @220 V to run, which is similar to the power consumed by incandescent light bulbs |
| Reagents obtained from renewable source should be preferred | No | The reagents obtained are not from a renewable source |
| Toxic reagents should be eliminated or replaced | Yes | The use of toxic catalyst (molybdate) and dyes is eliminated in this method |
| The safety of the operator should be increased | Yes | Safety is increased since the method is highly automated, and the operator interference is minimal |

| Method name | Flow rate (mL min$^{-1}$) | Injection volume (µL) | Retention time* (min) | Data acquisition time (min) | Volume of mobile phase consumed /sample (mL) | LDR (mM) | $R^2$ | Slope | Pressure (bar) |
|---|---|---|---|---|---|---|---|---|---|
| H$_2$O$_2$-1 | 0.1 | 5 | 2.9 / 3.1 | 7 | 0.7 | 0.1-15 | 0.9998 | 1174.4 | 4 |
| H$_2$O$_2$-2 | 0.1 | 20 | 2.9 / 3.1 | 7 | 0.7 | 0.1-5 | 0.9992 | 3294.1 | 4 |
| H$_2$O$_2$-3 | 0.1 | 50 | 2.8 / 3.4 | 7 | 0.7 | 0.1-2.5 | 0.9955 | 1579.3 | 4 |
| H$_2$O$_2$-4 | 0.1 | 100 | 2.8 / 3.9 | 7 | 0.7 | 0.1-2.5 | 0.9973 | 1673.8 | 4 |
| H$_2$O$_2$-5 | 0.25 | 5 | 1.2 / 3.4 | 4.5 | 1.125 | 0.1-25 | 0.9993 | 212.3 | 8 |
| H$_2$O$_2$-6 | 0.25 | 20 | 1.2 / 3.3 | 4.5 | 1.125 | 0.1-25 | 0.9968 | 608.56 | 8 |
| H$_2$O$_2$-7 | 0.25 | 50 | 1.3 | 4.5 | 1.125 | 0.1-25 | 0.9932 | 910.84 | 8 |
| H$_2$O$_2$-8 | 0.25 | 100 | 1.1 / 1.6 | 4.5 | 1.125 | 0.25-25 | 0.9936 | 334.85 | 8 |
| H$_2$O$_2$-9 (HRM) | 0.5 | 5 | 0.5 | 3 | 1.5 | 0.1-150 | 0.9917 | 50.313 | 15 |
| H$_2$O$_2$-10 | 0.5 | 20 | 0.6 | 3 | 1.5 | 0.1-50 | 0.9966 | 169.92 | 15 |
| H$_2$O$_2$-11 | 0.5 | 50 | 0.6 | 3 | 1.5 | 0.1-25 | 0.9993 | 337.43 | 15 |
| H$_2$O$_2$-12 | 0.5 | 100 | 0.5 / 0.7 | 3 | 1.5 | 0.1-15 | 0.9973 | 96.14 | 15 |
| H$_2$O$_2$-13 | 1 | 5 | 2.8 | 2 | 2 | 0.1-15 | 0.9979 | 1160.7 | 30 |
| H$_2$O$_2$-14 | 1 | 20 | 0.28 | 2 | 2 | 0.1-100 | 0.9962 | 49.777 | 30 |
| H$_2$O$_2$-15 | 1 | 50 | 0.3 | 2 | 2 | 0.25-50 | 0.9967 | 105.65 | 30 |
| H$_2$O$_2$-16 | 1 | 100 | 0.3 | 2 | 2 | 0.1-50 | 0.9904 | 150.52 | 30 |

**Table 2S** Properties of different methods using the first configuration (HRM)

*Some methods exhibited peak splitting shown by the two values in the retention time column.

**Table 3S**
Properties of different methods using the second configuration (LRM)

| Method name | Flow rate (mL $min^{-1}$) | Injection volume (μL) | Retention time (min) | Data acquisition time (min) | Volume of mobile phase consumed /sample (mL) | LDR (mM) | $R^2$ | Slope | Pressure (bar) |
|---|---|---|---|---|---|---|---|---|---|
| $H_2O_2$-1 | 0.1 | 5 | 4 | 7 | 0.7 | 0.025-15 | 0.9993 | 1168.4 | 11 |
| $H_2O_2$-2 (LRM) | 0.1 | 20 | 4.9 | 7 | 0.7 | 0.01-1 | 0.9992 | 3947.8 | 11 |
| $H_2O_2$-3 | 0.1 | 50 | 4.56 | 7 | 0.7 | 0.01-1 | 0.9636 | 6404 | 11 |
| $H_2O_2$-4 | 0.1 | 100 | 4 | 7 | 0.7 | 0.05-2 | 0.9994 | 7289.6 | 11 |
| $H_2O_2$-5 | 0.25 | 5 | 2 | 4.5 | 1.125 | 0.075-50 | 0.9996 | 212.48 | 26 |
| $H_2O_2$-6 | 0.25 | 20 | 2.1 | 4.5 | 1.125 | 0.025-25 | 0.9973 | 664.24 | 26 |
| $H_2O_2$-7 | 0.25 | 50 | 2.14 | 4.5 | 1.125 | 0.025-10 | 0.9995 | 1345.3 | 26 |
| $H_2O_2$-8 | 0.25 | 100 | 1.48 | 4.5 | 1.125 | 0.05-10 | 0.9997 | 1875.4 | 26 |
| $H_2O_2$-9 | 0.5 | 5 | 0.8 | 3 | 1.5 | 0.1-25 | 0.9997 | 61.388 | 50 |
| $H_2O_2$-10 | 0.5 | 20 | 0.8 | 3 | 1.5 | 0.05-15 | 0.9995 | 203.31 | 50 |
| $H_2O_2$-11 | 0.5 | 50 | 0.73 | 3 | 1.5 | 0.025-15 | 0.9966 | 381.66 | 50 |
| $H_2O_2$-12 | 0.5 | 100 | 1.23 | 3 | 1.5 | 0.025-25 | 0.996 | 528.18 | 50 |
| $H_2O_2$-13 | 1 | 5 | 0.4 | 2 | 2 | 0.25-100 | 0.999 | 14.88 | 100 |
| $H_2O_2$-14 | 1 | 20 | 0.5 | 2 | 2 | 0.075-100 | 0.9982 | 54.533 | 100 |
| $H_2O_2$-15 | 1 | 50 | 0.45 | 2 | 2 | 0.05-100 | 0.9983 | 115.24 | 100 |
| $H_2O_2$-16 | 1 | 100 | 0.56 | 2 | 2 | 0.05-100 | 0.9943 | 152.18 | 100 |

**Table 4S**
LINEST function output for repeatability and reproducibility experiments

| Calibration method | Experiment | Matrix | m | b | $s_m$ | $s_b$ | $s_y$ | $R^2$ |
|---|---|---|---|---|---|---|---|---|
| **LRM** | Repeatability | | 4399.16 | -15.23 | 30.92 | 14.18 | 31.65 | 0.9997 |
| | Reproducibility | DI | 4003.40 | -21.72 | 27.75 | 12.73 | 28.41 | 0.9997 |
| **HRM** | Repeatability | | 36.86 | 6.43 | 0.07 | 3.72 | 12.01 | 1.0000 |
| | Reproducibility | | 41.51 | 20.58 | 0.39 | 20.62 | 66.54 | 0.9988 |

(m: slope; b: intercept; $s_m$: standard deviation on slope; $s_b$: standard deviation on intercept; $s_y$: standard deviation on y-axis).

**Table 5S**

LOD and LOQ calculations for LRM and HRM

| Trial # | Peak Area (au) | |
| --- | --- | --- |
| | LRM | HRM |
| 1 | 22 | 5.8 |
| 2 | 22.9 | 5.9 |
| 3 | 22.3 | 5.6 |
| 4 | 21.3 | 5.7 |
| 5 | 21.6 | 5.6 |
| 6 | 20.9 | 5.5 |
| 7 | 23.5 | 6 |
| Average | 22.1 | 5.7 |
| Standard deviation | 0.9 | 0.2 |
| Equation | y= 3294.2x-48.15 | y=33.336x-10.26 |
| LOD (mM) | $8.29 \times 10^{-4}$ | $1.62 \times 10^{-2}$ |
| LOQ (mM) | $2.76 \times 10^{-3}$ | $5.39 \times 10^{-2}$ |

**Table 6S**

Average cost per test for the iodometric titration technique compared to LRM and HRM

| Chemicals used | Chemical's price (for 1 gram in USD cents ($\cent$)) | Average cost of chemicals used per test in USD cents ($\cent$) | | |
|---|---|---|---|---|
| | | Iodometric titration | LRM | HRM |
| Potassium iodide | 35 [2] | 36.4 | 0.16 | 0.34 |
| Ammonium molybdate | 1580 [3] | 831.6 | Not applicable | |
| Sulfuric acid | 62 [4] | 30.0 | | |
| Sodium thiosulfate | 24 [5] | 157.9 | | |
| Starch indicator | 44 [6] | 23.4 | | |
| Phosphoric acid | 98 [7] | Not applicable | 0.65 | 1.39 |
| Sodium bicarbonate | 9 [8] | | 0.03 | 0.06 |
| Total average cost | | 1079 | 0.84 | 1.79 |


**Table 7S**

Summary of spectator species effect on LRM and HRM

| Spectator species | % slope difference relative to control* | | $R^2$ | |
|---|---|---|---|---|
| | LRM | HRM | LRM | HRM |
| NaCl | -12.2 | 0.8 | 0.9988 | 0.9981 |
| $HCO_3^-$ | -5.6 | -3.6 | 0.9993 | 0.9991 |
| HA | 10.4 | -12.5 | 0.9992 | 0.9998 |
| FA | 11.8 | -8.1 | 0.9993 | 0.9997 |
| KTP | 2.9 | -0.6 | 0.9995 | 0.9984 |
| Theo | -3.0 | -4.2 | 0.9998 | 0.9987 |
| CAP | -6.8 | -1.6 | 0.9996 | 0.9931 |

*% slope difference of the calibration curves relative to control $= \frac{slope_{(spectator\ speices)} - slope_{(control)}}{slope_{(control)}} \times 100$

**Table 8S**

Water quality parameters of the natural water matrices used.

| Parameters | Units | Spring water | Sea water | Waste water |
|---|---|---|---|---|
| pH | - | 7 | 8 | 8.2 |
| Chemical Oxygen Demand (COD) | ppm | 132 | 970** | 1106 |
| Total Coliforms | CFU | 0 | 76 | TNTC |
| Fecal Coliforms | CFU | 0 | 4 | TNTC |
| Turbidity | NTU | 0.63 | 1 | 95 |
| Total Suspended Solids* (TSS) | ppm | 2 | 88 | 85 |
| Total Dissolved Solids (TDS) | | 350 | 32500 | 4400 |
| Sulfate ($SO_4^{2-}$) | | 16 | 3500 | 420 |
| Nitrates ($NO_3^{2-}$) | | 42.6 | 2525 | 3375 |
| GPS locations | - | 33°44'17.9"N 35°34'12.5"E | 33°54'11.1"N 35°28'44.8"E | 33°54'08.2"N 35°29'05.0"E |

TNTC: Too Numerous To Count

*ppm as NaCl

** Highly polluted sea water

**Table 9S**

Properties of the columns used

| Column order | Column Manufacturer | Part number | Length (mm) | Outer diameter (mm) | Inner diameter (mm) | Capacity (mm$^3$/µL) | Column material | Image |
|---|---|---|---|---|---|---|---|---|
| First | Agilent | 01078-87302 | 1100 | 0.9 | 0.35 | 100 | Stainless steel | |
| Second | Agilent | 5022-2159 | 2000 | 0.6 | 0.12 | 23 | Stainless steel | |
| Third | IDEX Health & Science | 1536L | 3100 | 1.6 | 0.17 | 70 | poly ether ether ketone (PEEK) | |

References:

[1] Gałuszka, A., Migaszewski, Z. and Namieśnik, J., 2013. The 12 principles of green analytical chemistry and the SIGNIFICANCE mnemonic of green analytical practices. TrAC Trends in Analytical Chemistry, 50, pp.78-84. https://doi.org/10.1016/j.trac.2013.04.010

[2] Potassium iodide | Sigma-Aldrich, (n.d.). https://www.sigmaaldrich.com/catalog/search?term=Potassium iodide&interface=All&N=0&lang=en&region=US&focus=product (accessed March 5, 2018).

[3] Ammonium molybdate 99.98% trace metals basis | Sigma-Aldrich, (n.d.). https://www.sigmaaldrich.com/catalog/product/aldrich/277908?lang=en&region= US (accessed March 5, 2018).

[4] Sulfuric acid 99.999% | Sigma-Aldrich, (n.d.). https://www.sigmaaldrich.com/catalog/product/aldrich/339741?lang=en&region= US (accessed March 5, 2018).

[5] Sodium thiosulfate | Sigma-Aldrich, (n.d.). https://www.sigmaaldrich.com/catalog/search?term=sodium+thiosulfate&interfac e=All&N=0&mode=partialmax&lang=en&region=US&focus=product (accessed March 5, 2018).

[6] Starch | Sigma-Aldrich, (n.d.). https://www.sigmaaldrich.com/catalog/search?term=starch&interface=All&N=0 +&mode=partialmax&lang=en&region=US&focus=product (accessed March 5, 2018).

[7] Phosphoric acid | Sigma-Aldrich, (n.d.). https://www.sigmaaldrich.com/catalog/search?term=phosphoric acid&interface=All&N=0&mode=partialmax&lang=en&region=US&focus=prod uct&F=PR&ST=RS&N3=mode matchpartialmax&N5=All (accessed March 5, 2018).

[8] Sodium bicarbonate powder, BioReagent, for molecular biology, suitable for cell culture, suitable for insect cell culture | Sigma-Aldrich, (n.d.). https://www.sigmaaldrich.com/catalog/product/sigma/s5761?lang=en&region=U S (accessed March 5, 2018).

CHAPTER IV

CONCLUSION

This work is a demonstration of a new heterogeneous activator of PS, MIL-88-A. MIL-88-A/PS activated system proved to be effective for the degradation of persistent compounds like the NSAID pharmaceutical: naproxen. The findings of this study showed that a relatively low amount of MIL-88-A ($[\text{MIL-88-A}]_0 = 25$ mg L$^{-1}$) is sufficient for activating PS for the degradation of 65-70% of high concentrations of naproxen ($[\text{NAP}]_0 = 50$ mg L$^{-1}$) within two hours. It also proved MIL-88-A to be a recyclable catalyst that can be used in at least 4 successive cycles. Studying the system in different matrices showed that salinity and phosphate do not affect the activation/degradation process; however, bicarbonates inhibit it. As for the pH effect, it was inferred that the catalyst works better in acidic media (pH = 4). On the other hand, applying the system on another oxidant, evidenced PS to be superior over $H_2O_2$ in MIL-88-A activated systems. The system was finally optimized to reach full degradation of naproxen by introducing UV-A irradiation to the system.

For the sake of comparing the two systems, MIL-88-A/PS and MIL-88-A/ $H_2O_2$, in the first project in this work, a new analytical technique for the quantification of $[H_2O_2]$ was developed. The new method allowed to reach an LOD = $8.29 \times 10^{-4}$ mM and LOQ = $2.76 \times 10^{-4}$ mM with an LDR ranging from 0.01-150 mM. Repeatability, reproducibility, and tolerance to naturally occurring spectator species along with the efficiency on the level of cost, time, labor, and material demand reveals that the developed technique serves as an excellent method for $H_2O_2$ quantification in a wide range of applications especially analytical ones.

95

Extended future work will be focused on testing the proposed activation system, MIL-88-A/PS, on different PPCPs with further understanding to degradation mechanisms and pathways. Investigations towards utilizing solar energy for the enhancement of the system has been also initiated in our laboratory for better and environmentally friendly AOPs applications. Finally, characterization of MIL-88 before and after the oxidation process has been tested using the TOF SIMS (Time-of-Flight secondary ion mass spectrometry) technique where preliminary results are promising and will help better elucidate the degradation process at the surface of the catalyst and/or in the bulk of the solution.